ON SHORT-TERM AND SUSTAINED-LOAD ANALYSIS OF CONCRETE FRAMES

ON SHORT-TERM AND SUSTAINED-LOAD ANALYSIS OF CONCRETE FRAMES

by

K. B. Tan , B.Sc.

A Thesis

Submitted to the Faculty of Graduate Studies

in Partial Fulfillment of the Requirements

for the Degree

Master of Engineering

McMaster University

Hamilton, Ontario

Canada

1972

MASTER OF ENGINEERING (1972)

McMaster University
Hamilton, Ontario
Canada

TITLE : On Short-term and Sustained-load Analysis of Concrete Frames

AUTHOR : Tan King-Bing, B.Sc. (Chung-Hsing University)

SUPERVISOR : Dr. R. G. Drysdale

NUMBER OF PAGES : XI , 169

SCOPE AND CONTENTS :

A Matrix Stiffness-Modification Technique has been proposed for the inelastic analysis of reinforced concrete frames subjected to short term or sustained loads. To check the applicability of the analytical method, two large scale concrete frames were tested under short-term loads and sustained-loads respectively. In addition, data for twenty-two frame tests from other sources has also been compared with the non-linear analysis. Close agreement has been observed for all the frames considered. It was further concluded that a conventional elastic matrix method using stiffnesses based on a cracked transformed section of concrete does not yield accurate results, especially in the case of sustained loading conditions. From the method developed, comments can therefore be made on present column design practice.

ACKNOWLEDGEMENTS

The author would like to express his sincere gratitude to Dr. R. G. Drysdale for his generous guidance and advice during the course of this investigation. Frequent consultation with Dr. Drysdale had been invaluable for this research to reach its conclusions.

The author also takes this opportunity to thank the following :

(1) McMaster University for providing financial support in the form of a teaching assistantship and the National Research Council of Canada for additional support.

(2) The staff of the Applied Dynamics Laboratory of McMaster University for their help in the experimental program.

(3) The Steel Company of Canada for providing the reinforcing steel.

(4) The Cement and Concrete Association (England), and McGill University for providing publications containing their experimental frame test results.

Last, but not least, the author wishes to express his appreciation to his wife, Lee, for her understanding and encouragement.

TABLE OF CONTENTS

PAGE

PAGE

LIST OF TABLES

LIST OF FIGURES

LIST OF SYMBOLS

Any symbols used are generally defined when introduced. The standard symbols are listed below :

A_g	Concrete gross section area
A_s	Total area of longitudinal tensile steel
A'_s	Area of longitudinal compression steel
b	Width of cross-section
d	effective depth or distance of tensile reinforcement from the compression face
d'	Concrete cover measured to the centroid of each bars
E_c	Modulus of elasticity of concrete
E_s	Modulus of elasticity of steel
EA	Equivalent axial stiffness
EI	Equivalent flexural stiffness
f_c	concrete stress
f'_c	concrete cylinder strength at age 28 days
f_s	Stress of steel
f_y	yield strength of steel
I_c	Moment of inertia of cracked transformed section of concrete
I_g	Moment of inertia of gross-section of concrete
Kh/r	Slenderness ratio
L, l	length of individual member
M	Bending moment acting on a cross-section
P	Axial force acting on a cross-section
p	Percentage of steel reinforcement

r	Radius of gyration of concrete section
R_m	Ratio of dead load moment to total moment
t	Thickness of concrete cross-section
w, ϵ	strain
w_1	Strain at extreme compressive fibre of concrete section
w_{axial}	Axial strain of concrete
w_c, ϵ_c	Strain of concrete
w_{creep}	Creep strain in concrete
$w_{effective}$	Effective strain of concrete
$w_{elastic}$	Elastic strain of concrete, same as effective strain
w_s, ϵ_s	Strain of steel
$w_{shrinkage}$	Shrinkage strain of concrete
w_{total}	Total strain of concrete
w_y, ϵ_y	yield strain of steel
ϕ	Curvature

Chapter 1

INTRODUCTION AND LITERATURE REVIEW

(1.1) General :

It is well known that a complete elastic analysis of even a very simple indeterminate structure, for instance, a portal frame, involves a fairly large amount of work by hand computation. The amount of work increases disproportionately with the increase in the degree of indeterminacy in the structure. When a high degree of redundancy is contained in the structure, an exact analysis by hand solution may be rendered impossible. Consequently, when a complicated structural system is encountered, it has been necessary to make simplifying assumptions in the analysis. The result of this simplified analysis frequently reflects an erroneous depiction of the behavior of real structures.

Fortunately, because of the development of high-speed electronic computers, the art and science of Structural Engineering has been greatly advanced. The ease of a computer to perform thousands of digital computation and data processing steps within seconds and with high accuracy has enabled the implementation of matrix methods for systematic structural analysis. More recently, the advancement of the highly versatile finite element methods has facilitated a more accurate evaluation of stress for almost any structural shape.

However, most work done by the matrix approach has been confined to the analysis of elastic systems in which the structures respond linearly to the applied loadings. Relatively little attention had been devoted to the behaviorial study of inelastic concrete structures by matrix methods. The area of sustained load behavior of concrete structures using a generalized matrix approach remains largely unexplored. The reasons may be due to the difficulties in formulating a unique set of stiffnesses for the concrete system. It is known, and will be shown later in this report, that the stiffnesses of a concrete cross-section are influenced by the degree of cracking , the amount of reinforcing steel and the geometric properties of the cross-section. Creep and shrinkage of concrete influence the long-term behavior of structures by causing them to continue to deform in the course of time even under constant applied loads. The implication is that the stiffnesses of the structural system are functions of creep shrinkage and time. All the uncertainties associated with these functions have hindered the development of an efficient and systematic matrix method for the structural analysis of concrete frameworks.

Nevertheless, with the increasing use of computer, researchers have developed an incremental method, termed by the author as the "Numerical Moment-Curvature Method " , for the more exact analysis of concrete structures. The Numerical Moment-Curvature Method will be briefly described in the next section. Several important papers have then been published during the past decade. However, most work done by the previous investigators had been focused on the analysis of single members , especially the column. The reason has been twofold . Firstly, a single member is much easier and simpler to analyse than a structural system with discontinuities and complicated boundary conditions. Secondly, slender columns have been used increasingly in recent building construction for architectural purpose and also due to the use of high strength materials which has resulted in smaller column sections.

Columns, especially those with high slenderness ratio, are compression members which are very sensitive to the time-dependent effect of creep and shrinkage. A column may fail in one of the two modes: Material failure which is the crushing of concrete in reaching its ultimate strength, or buckling failure in which lateral deflection increases without an increase in loads. Creep increases the deflection of a column by decreasing its stiffnesses, which alternately results in a reduction of the proportion of the joint moment which the column must resist . This then means that a redistribution of moments occurs due to the effect of creep of the concrete. The rather complex interactions associated with the behavior of slender columns have been excellent topics for research, and have thus stimulated a great deal of interest in column investigation.

(1.2) Numerical Moment-Curvature Method of Analysis :

From a survey of previous literature concerned with research in the area of behaviorial study of concrete structures, it was found that most investigators employed a fairly similar approach in analysing concrete structures. To avoid repetition in the literature review to be described in the next section, this approach, termed by the author as the Numerical Moment-Curvature Method, is described in this section as follows :

(1) The structure is divided into a number of small discrete elements which in turn are subdivided into a finite number of element strips.

(2) By assuming plane strain distribution over the concrete cross-section, for cases where the stress-strain relation of materials are known, an arbitrary set of strains at the extreme fibres of the cross-section are imposed and the compatible stresses can be evaluated.

(3) The internal axial force and bending moment for the given strain distribution are computed using a numerical integration procedure, and are compared to the externally applied load and bending moment acting at the geometric centroid of the cross-section. If equilibrium does not exist, the assumed strain distribution is changed until external and internal load and moment differ by less than some permissible tolerance.

(4) Member deformations at consecutive division points are then computed by using numerical integration procedures.

(5) The compatibility between deformations and moments at a joint in a structure is then established by another trial and error iterative process.

Several researchers havereported that the numerical moment-curvature method can yield satisfactory predictionsof the behavior of concrete structures. This has then lead to the reasoning that for an inelastic concrete structure, there must exist an equivalent set of stiffnesses which can be obtained after modification of an initially arbitrary assumed set of stiffnesses for the whole structural system. This idea has been the basis for the development of the Matrix Stiffness-Modification Method to be reported in detail in this thesis.

(1.3) Historical Review:

In this section a brief review of recent literatures concerned with the behaviorial studies of inelastic concrete structures for the past ten years has been presented. Previous Reviews (1, 29)** have provided excellent documentation of all but fairly recent publications.

In 1961, Brom and Viest (11) reported that for short columns, the effect of slenderness on deflection and stability of a column was very small but not so for long columns. In CEB (1) recommended practice for slender column design, the effect of slenderness was considered as a complementary moment to be added to the initial eccentricity of the load. The complementary moment was expressed as a function of the geometric slenderness ratio and the end eccentricity ratio.

In 1963, Furlong (28) tested six rectangular frames restrained from lateral sidesway and having single curvature columns. He found that the capacity of the restrained column permitted up to fifteen percent more axial load capacity than would be expected for an equivalent isolated column. He then developed two methods for analysis of columns. In the numerical moment-curvature method, he assumed the deflected shape of the column was in the form of a parabola while for the Elastic method, he used an effective stiffness EI for simplicity of analysis.

** Number in the Parenthesis refers to number in bibliography

Chang(14) in the same year also analysed concentrically loaded long hinged columns employing Von Karman's theory and a numerical intergration procedure for predicting the deflected shape of columns. Separate mathematical equations for column moment and load in term of edge strains were derived and plotted for a rectangular concrete cross-section. He also proposed a method for determining the critical length of long hinged and restrained concrete columns as part of a box frame (15). An analog computer was used to solve the differential equation for predicting the critical length of a column. He concluded that a long reinforced concrete column may buckle laterally as the critical section reached material failure, but the material failure of a column cannot be used as the criteria to determine the critical column length. Plastic hinges may be developed in a frame, but a long column may become unstable without developing plastic hinges.

The use of plastic methods of structural analysis incorporated with the ultimate strength design method have been applied to concrete structures. However, these methods do not always recognize the effects of axial force and creep deformation on the structures. In 1964, Sawyer presented a method based on a bilinear moment-curvature relationship and used a Plasticity Factor to account for the redistribution of moment (3). Later, Adenoit (4) applied the bilinear moment-curvature concept to the analysis of double-bay one-storey frames. He reported that the calculation of the rotation capacity of a plastic hinge by the bilinear moment-curvature method gives an over-estimated capacity.

Cranston (17) tested eight single-bay one-storey frames with fixed end conditions. He concluded that the mechanism method for plastic design can be applied to concrete structures. However, the frames he tested did not have high axial load in the columns. Cranston also presented a computer method for inelastic frame analysis (18). The frame has to be idealized into an arch or a ring, each with three hinges. The numerical moment-curvature method was used to obtain the solution. His method neglected the influence of axial force in the frame and the curvature of the section was assumed to be dependent on the bending moment only. Plastic hinge behavior would be dealt with until the structure had developed into a mechanism.

In 1964, Pfrang (46) studied the effect of creep and shrinkage on the behavior and capacity of reinforced concrete columns. For a column with a slenderness ratio below some critical value, creep will increase its capacity, but when the slenderness is high above the critical value, creep will decrease its capacity significantly. Increasing the ratio of reinforcement reduced the extent to which creep influenced the behavior and capacity of the column. Also increasing the degree of end restraint reduced the detrimental effects due to creep. He used a varying stress-strain relation similar to the Hognestad's curve (32) to approximate creep deformations, and employed the numerical moment-curvature method to predict the behavior of his frames.

In 1966, Green (29) tested 10 unrestrained eccentrically loaded columns subjected to sustained load and having a wide range of axial load intensities applied at varying end eccentricities. A time-dependent stress-strain relationship was used in his numerical moment-curvature approximation. He concluded that for long columns under sustained loading, deformation will increase with increasing duration of loading, and will cause the member to fail in the instability mode. The deformational characteristics of members under sustained loading are greatly affected by the yielding of the compression reinforcement. If yielding of the compression steel had not occurred after one month of sustained loading, the subsequent increases in sectional deformations were small.

In 1967, Manual and MacGregor (38) proposed a method of sustained load analysis of the behavior of concrete columns in frames. They also used a time-dependent stress-strain curve modified from Rusch's (48) relationship to account for the effect of creep of concrete under variable stress.

Drysdale (20) investigated the behavior of slender concrete columns subjected to sustained biaxial bending at the University of Toronto. A creep and shrinkage function was derived for a general concrete member. A modified superposition method for determining creep strain of concrete under varying stress was proposed. The numerical moment-curvature developed for the analysis yielded excellent agreement with test results.

In 1970, MacGregor, Breen and Pfrang published jointly a highly important paper (37) proposing the moment magnifier method for the design of slender columns. They found that the most significant variables which affect the strength and behavior of slender columns were the slenderness ratio, end eccentricity, eccentricity ratio, ratio of the reinforcement ratio to the concrete cylinder strength, degree of end restraint and sustained load. The ACI 1963 Building Code(2) recommended a Reduction Factor method which was investigated and found to be unsafe for use with slenderness ratio Kh/r exceeded 70. In these cases, the Moment Magnifier Method should be used instead of the reduction factor method when a rational second order method of structural analysis is not available. The method suggested that the moment in the slender column section should be increased by a moment magnifier which is a function of the ratio of the ultimate load to the critical load and the ratio of end moments of the column. In addition, Furlong (27) presented a useful moment multiplier graph for design of slender column so that the selection of a column cross-section has been greatly simplified.

(1.4) Work in McMaster University:

Drysdale (20,21) in 1967 has initiated an extensive program in the behaviorial research of the non-linear response of concrete structures in all forms of buildings subjected to short term and sustained loads. The program has been aimed mainly at the evaluation of present design methods, with particular attention to the design of slender columns , and to the modification and development of new methods of structural concrete analysis.

Gray(30) in 1968 developed a method using small elements to predict creep under variable stress.

Danielson (19) started research in the sustained-load behavior of a single-bay one story portal frame. He applied the numerical moment-curvature method in the analysis. By assuming a set of elastic reactions at the left base of the frame, the deflection at the right base of the frame was computed by the numerical moment-curvature method. By a trial and error method, and by use of the slope-deflection equations, the compatibility of deflection in the right base was finally adjusted so that it was satisfied within allowable limits. A word of comment is that his method is not general enough to be applicable to more complicated structures.

Eichler (22) in 1971 developed a practical method for calculating creep under variable stress.

The work undertaken and reported in this thesis is intended to provide the basis for the evaluation of design and analysis methods as applied to real structures. It is hoped that this will contribute especially to the rationalization of column design procedures.

(1.5) Conclusion:

Although several methods have been developed to account for and predict the behavior of inelastic concrete structures, the author discovered that a systematic and efficient method for the analysis of general and complicated concrete structures is still lacking. For the research in the area of slender columns, the reduction factor method has been concluded to be unrealistic and inadequate. However, the newly proposed Moment Magnifier Method and the Comite Europeen Du Beton (CEB) recommended practice for designing a slender column do not properly account for the effect of creep and shrinkage on the capacity of slender columns. This is evident by the fact that the Moment Magnifier method used only a "R_m" factor which is the ratio of the dead load moment to the total moment in the column to account for the effect of creep and shrinkage in the column.

(1.6) Proposal :

It is the purpose of this research to develop a new method for analysing reinforced concrete structures. The Matrix-Stiffness Modification method has been developed. This method incorporates the effect of secondary bending moment and creep and shrinkage of concrete, so that a general frame with short or long columns can be analysed equally well. The computer program is designed to analyse any general multi-storey concrete frames. However, with some modification to the program, it can be applied to deal with general prestressed concrete and composite structures which are not within the scope of this study. To test the applicability of the method, two large scale frames have been tested by the author to provide data for comparison of the experimental and analytical results. In addition, a total of twenty two frame test results from other sources were compared.

Chapter 2

EXPERIMENTAL PROGRAM

(2.1) Introduction:

Two large scale portal frames with fixed bases were built in the Applied Dynamic Laboratory (ADL) of McMaster University. The purpose of these experiments was to provide data to check the applicability of the proposed Matrix Stiffness-Modification Method of Analysis which is described later. This method of analysis is intended to be used to investigate the behavior of indeterminate frames and to provide criteria and information for present engineering practice. This comparison should provide a more exact and comprehensive evaluation of presently recommended methods of design and analysis of inelastic concrete structures.

Frame FS1 was designed for a sustained load test while frame FR1 was intended for a short-term proportional loading test. The fabrication details, instrumentation and testing technique are described in the following sections.

(2.2) Details of the Test Frames:

The frames were designed to have high axial loads on both columns while the beam was loaded slightly off-centre so that a tendency for sidesway was intentionally incorporated. This loading facilitated the study of the distribution and the redistribution of bending moment due to variation of axial and flexural stiffnesses caused by cracking of the concrete and by creep deformations. The dimension of the frames was restricted by the available clear height and size of the temperature and humidity controlled enclosure, the dimension of the adjustable steel formwork and the position of the anchor bolt holes in the test floor of laboratory which were spaced at three foot centres. Hence, the span of the beam was set at nine feet and the height of the columns was ten feet. The beam cross-section was eight inches square with four number six bars. Each bar was located in a corner with one inch cover from the near faces. The column cross-section was eight inches wide by five inches deep with a number four bar in each corner with 3/4 inch cover from the eight inches face and one inch cover from the five inch face. The selection of such a large scale experimental model minimized the error for simulation of a real structure. Figure 2.1 contains a sketch of the frame with slender columns and the details of the cross-sections.

The stirrups for the beams and columns were made from the 0.15 inch diameter wire supplied by the Steel Company of Canada, Limited. A standard Tie Bender was manufacturedto bend the ties to the exact dimension so that longitudinal reinforcing steel would be accurately located within a tolerance of 1/16 inch. Approximately 33 ties were required for a single beam while 27 ties were used for each column. The uniform spacing of the stirrups was detailed at three inches in the beam and four inch in the columns throughout. Calculations showed that these ties would provide sufficient shear capacity for the frame.

The cages of reinforcing steel for the beam and columns were constructed separately. They were then welded to the Steel

Joint Connector (described later) to form a integrated cage for the frame.

The adjustable steel forms were constructed of nine inches angle sections bolted to a backing plate which was drilled to accomodate a number of specific dimensions of frame. This form, shown in the photograph in Figure 2.2, was designed to make double bay single story frames or one bay portal frames. By using a steel form, the accuracy in casting of frames could be maintained within an allowable tolerance of 1/8 inch. The form accomodated cross-sections from four to sixteen inches in depth in ½ inch increments. The steel form also provide durability, strength, and convenience for accurate fabrication of large-scale frames . Each part of the steel form was light enough to be cleaned and handled by two men. Smooth surface on the concrete were produced so that mechanical gage points, for strain measurements, and dial gage points, for monitoring deflection, could be conveniently applied.

Immediately before the installation of the reinforcing cage and pouring of concrete, the steel formwork was coated with a layer of Form-oil so that the form could be removed easily from the concrete after pouring and curing.

Steel spacers made from number three reinforcing bars were fabricated to hold the steel cage in its correct position in the steel form, so that proper location of the cage was assured. The arrangement of the reinforcing cage and steel form were shown in Figure 2.3 and in the photograph in Figure 2.2.

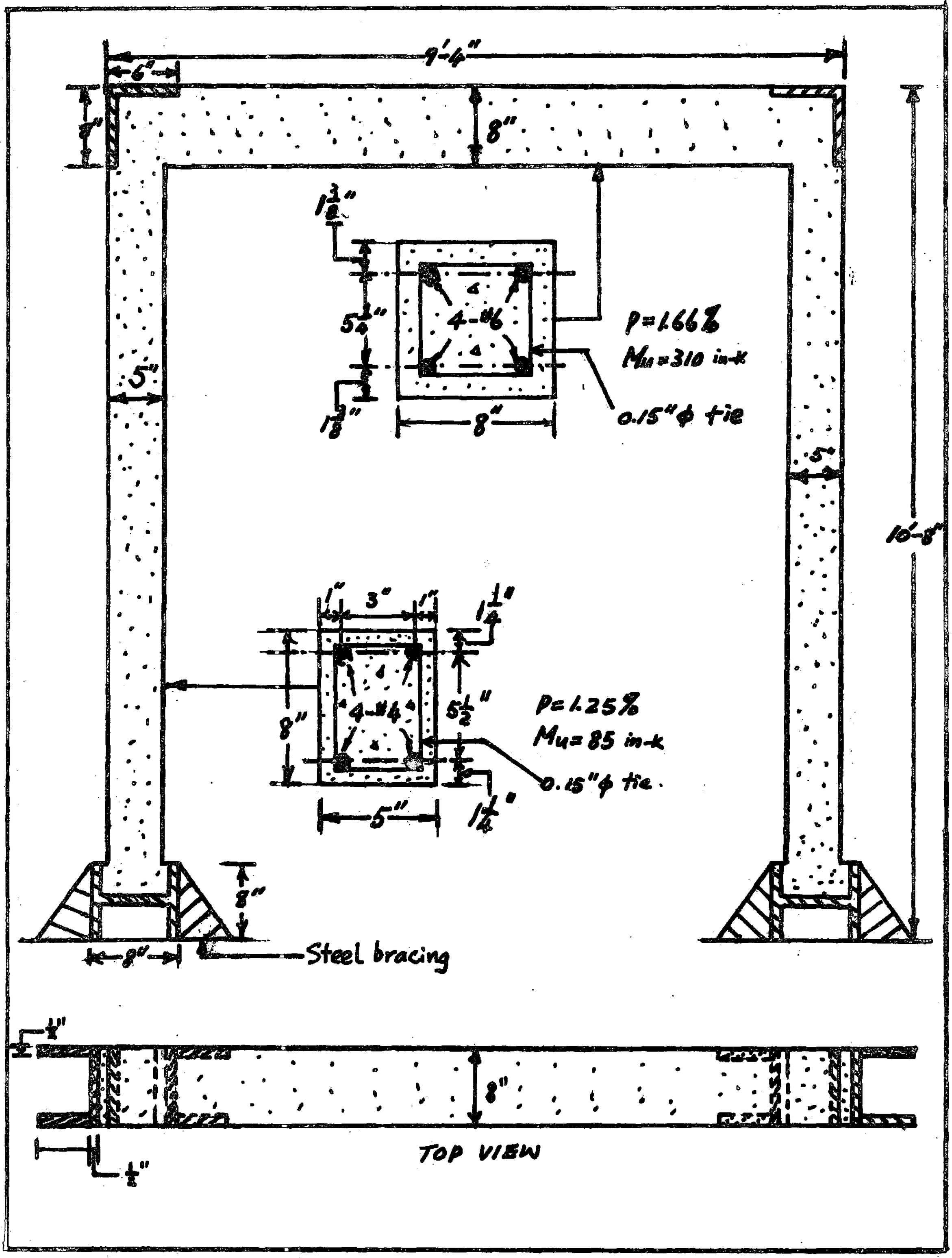

Figure 2.1

Dimension of Frame FS1 and FR1

Figure 2.2

Reinforcing Cage and Steel Form

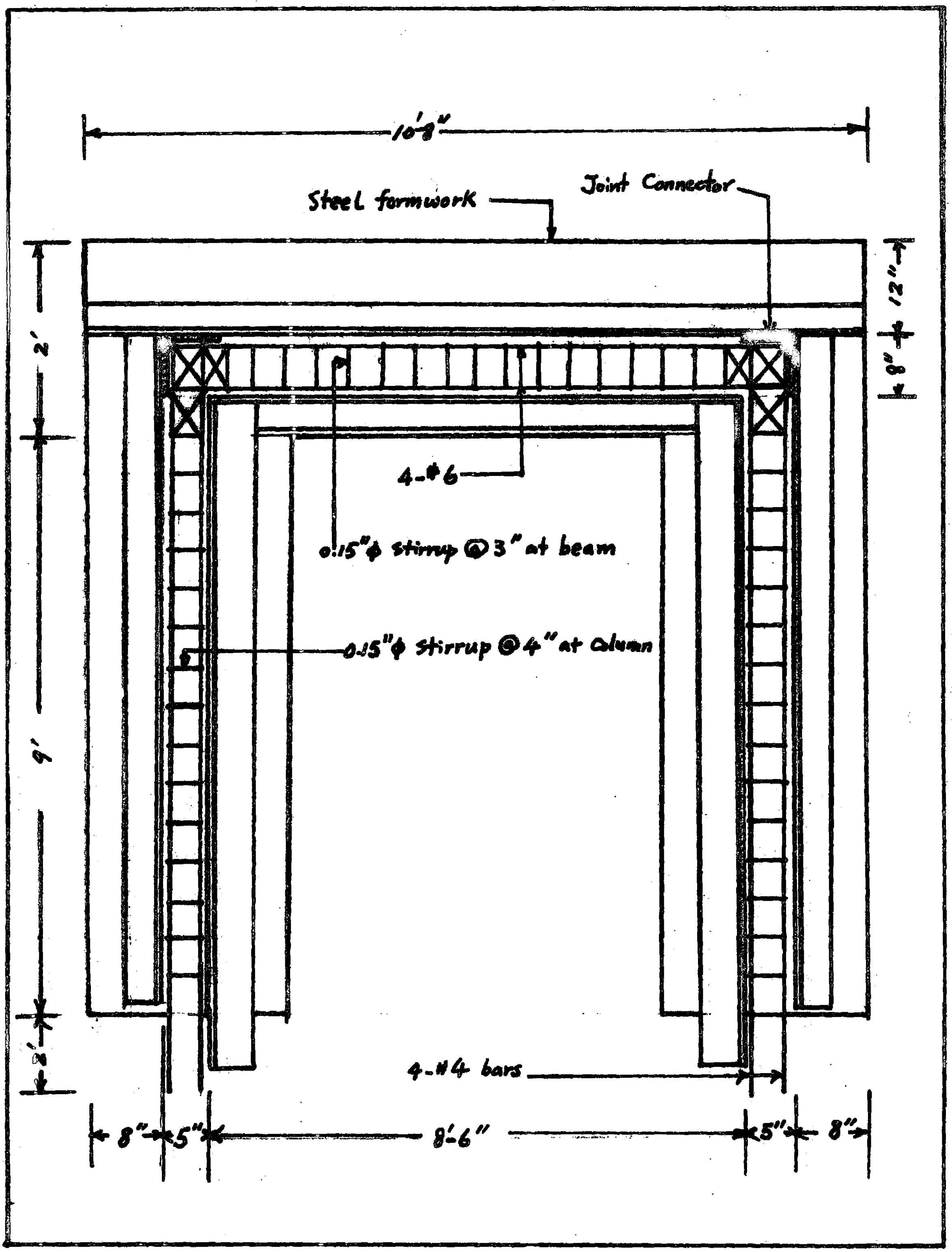

Figure 2.3

Reinforcing Cage and Steel Form

(2.3) Design of Steel Joint Connector:

A steel joint connector was used to integrate the individual beam and column cages into a continuous reinforcing cage for the frame. The connector was made from an eight inch by six inch by ½ inch steel angle with holes drilled as shown in Figure 2.4.a. The reinforcing bars of the beam and columns were designed to pass through the holes and were welded on both sides of the angle.

The reason for introducing special joint connectors in the frame was to make the joint rigid and prevent possible premature cracking of the joint. It was found that (19) bending the longitudinal bar around a small radius in the joint produce a corner which was susceptible to excessive cracking in the tension zone. The steel joint connector was thus designed to eliminate this problem. In addition, the connector served as a rigid base in the corner of the frame to accomodate application of the high column loads.

After the longitudinal reinforcing bars had been welded to the joint connector, addition al reinforcing was applied to the joint to fasten the bars together, as shown in Figure 2.4.b. and photograph 2.5. Three number three bars approximately eight inches long were welded to the inner faces of the joint connector on an inclined angle so that any possible tensile stress in the concrete due to opening of the joint would be counteracted by the steel. As will be discussed and visualized later , sufficient rigidity was created in the joint so that it could be regarded as being fully rigid for analytical purpose.

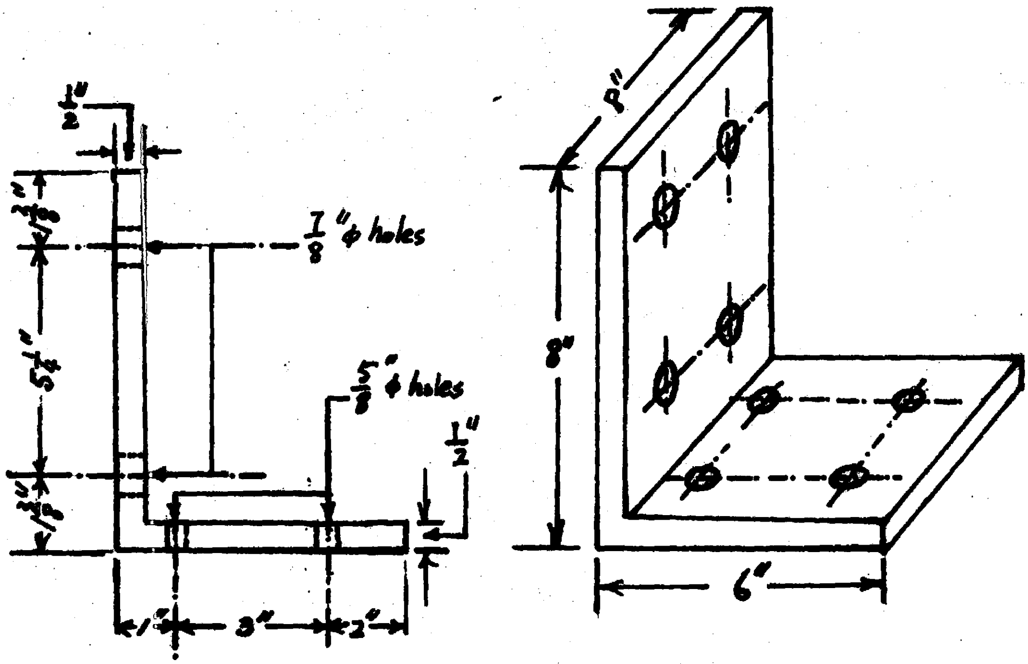

Figure 2.4.a

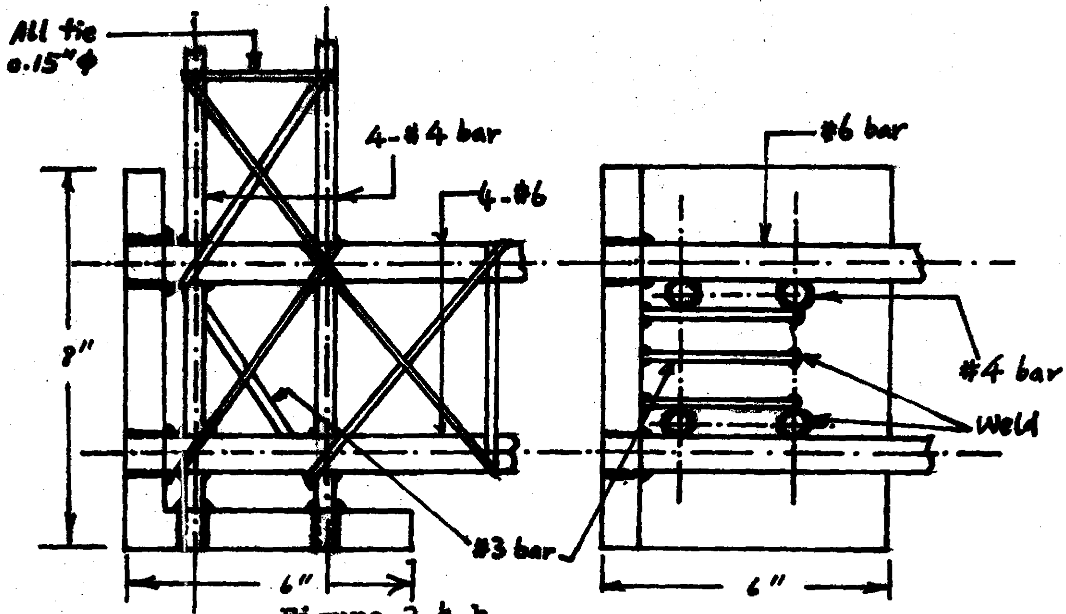

Figure 2.4.b

Figure 2.4 : Steel Joint Connector

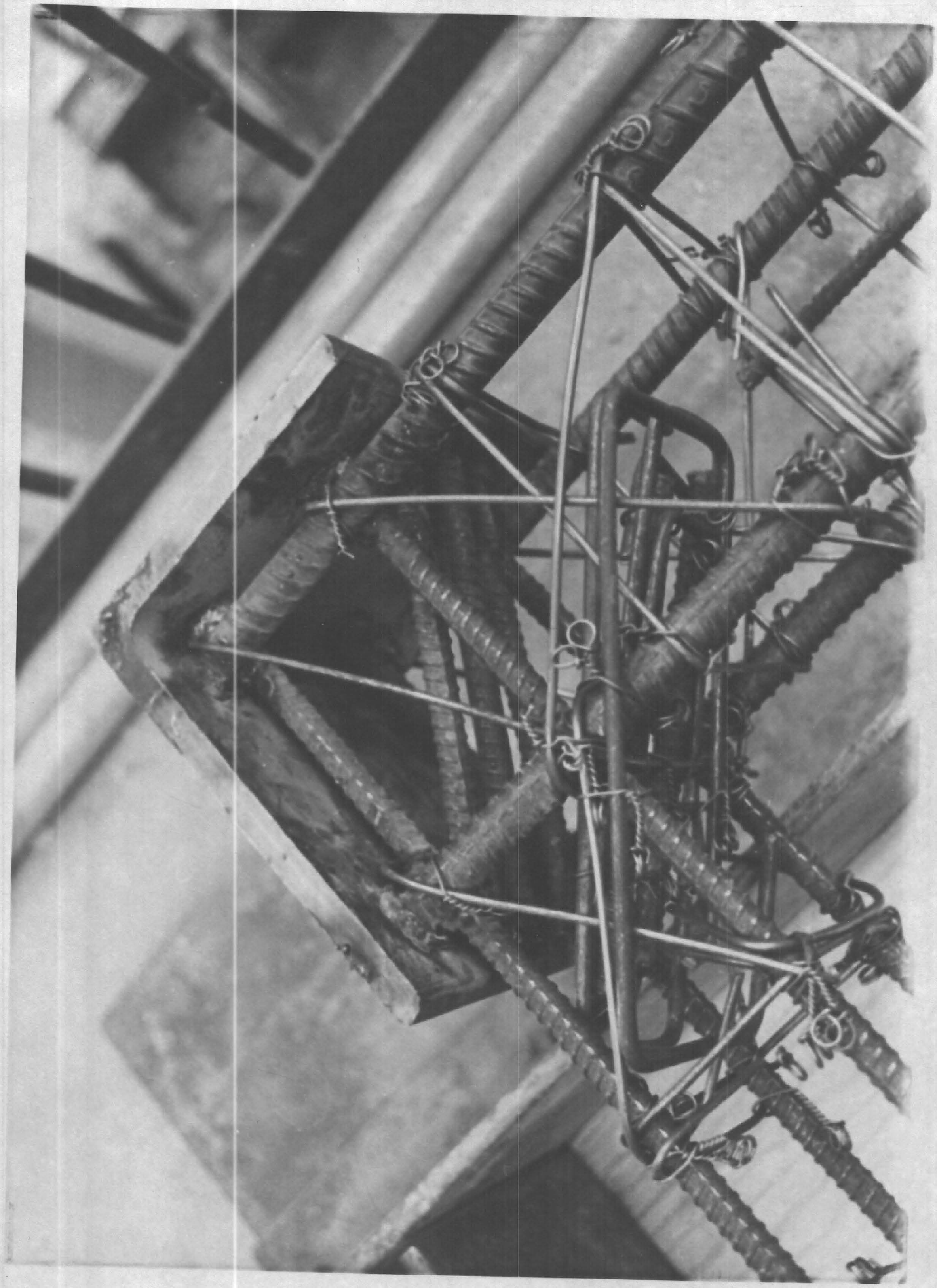

Figure 2.5

Detail of Joint Connection

(2.4) Concrete Column Bases:

The column bases were fabricated from eight inch by eight inch wide flange steel sections eight inches long as shown in Figure 2.6.a. Holes drilled in the web of the section anchored and positioned the column bars which were welded to the web. Additional reinforcement was welded to the section so that tension in the column due to uplift or bending could be properly transmitted to the base. The bottom of the web of each steel section was ground after welding to provide a smooth surface. The space below the web was required to insert a steel plate from the column loading device. The column axial load assembly for the frames will be described later.

The details of the rigid base assembly for the frames are shown in Figure 2.6.b. The steel wide flange sections were welded directly to the one inch thick steel plate of the frame base assembly. The lower plate was stiffened with eight inch channel sections. The entire base system was prestressed to the floor of the Applied Dynamic Laboratory using two $2\frac{5}{8}$ inch diameter anchor bolts, each stressed to approximately sixty kips in tension.

Triangular steel bracing wings cut from ½ inch plate were then welded to the column base and to the one inch base plate so as to stiffen the base connection and to provide a fixed end condition. A picture of the steel bracing wing may be observed in Figure 2.10.

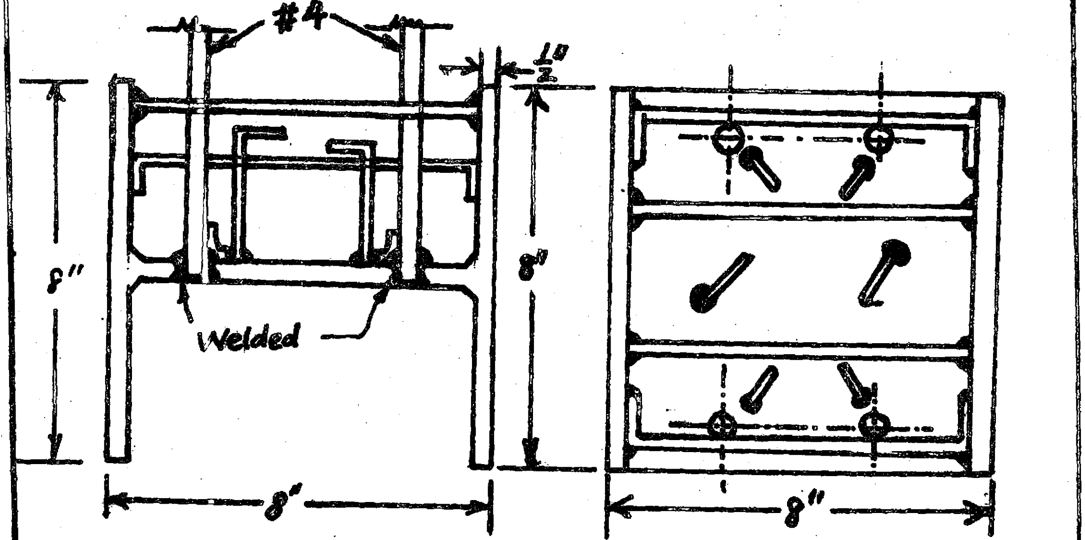

Figure 2.6.a

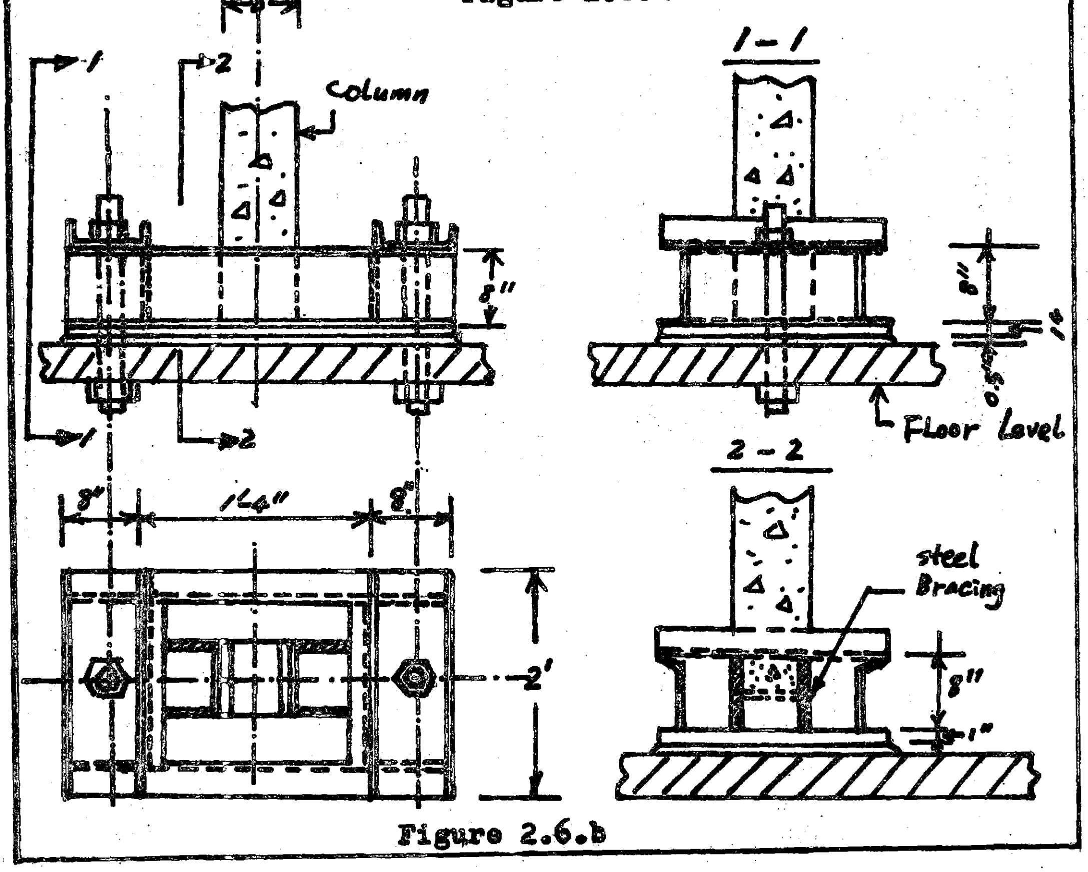

Figure 2.6.b

Figure 2.6 : Concrete Column Base

(2.5) Concrete Mixing Process :

The concrete mix design was the same as that used in the University of Toronto Column Test Series (20) so that predetermined data on creep and shrinkage derived by Drysdale (20) could be used. Table 2.1 gives the proportions of the mix design :

Table 2.1: CONCRETE MIX DESIGN

Ingredient	Weight per Batch (in lb.)	Weight by percent
Portland Cement Type I	127.4	14.0 %
Water	82.6	9.1 %
Fine Aggregate (wash pit sun sand, finess 2.51)	424.0	46.6 %
Coarse Aggregate (3/8 inch maximum size crushed stone)	275.5	30.3 %
Total	909.5 lb.	100.0 %

Slump Test result: Frame FR1: $2\frac{3}{4}$ inches

Frame FS1: 2 ½ inches

The quantity of concrete required for frame FS1 was about six cubic feet which would make one large scale frame, five creep and shrinkage prisms and twelve standard concrete cylinder test specimens. For frame FR1, only four cubic feet of concrete were needed to cast a large frame and six cylinders.

Concrete components were prepared by weight and mixed in a horizontal drum mixer. Batches were mixed in rapid succession to avoid drying out of the mix between batches. Each batch was allowed to mix for five minutes after the last of the water had been added. A slump test was performed immediately before pouring so that the quality and workability of the concrete was known and controlled. The designed ultimate strength of concrete for 28 day cylinder strength was 4000 psi. The concrete cylinder test results are given in Appendix B.

The concrete mixes were lifted by overhead crane to the second floor level of laboratory where the frames were fabricated. The concrete prisms and cylinders were made with the frame. Each specimen including the frame was poured in three layers, with each layer vibrated by a poker-type vibrator. The concrete was placed to overfill the form so that a smooth surface finish could be trowelled. It took approximately three hours for pouring, vibrating and surface finishing of the test specimens.

Approximately five hours after pouring, when the concrete began to harden, wet burlap was placed over the specimens so that excessive surface drying and cracking of concrete could be prevented. After approximately twenty four hours, the sides of the steel form were removed and moist curing of the concrete continued for another seven days, before the specimen was lifted into test position.

However, the procedures for making and curing the concrete followed the specification given in ASTM Standard C-192-69.

(2.6) Erection of Frames :

Two weeks after pouring, frame FS1 was lifted by crane and positioned in a tent covered by polyethylene. Inside the enclosure the temperature was kept at 75° F $\pm$ 2° F and the relative humidity was maintained at 50 % $\pm$ 2 %. The column bases were welded to the steel base assembly described in section 2.4.

To maintain a constant temperature and relative humidity, the tent was equiped with a humidifier, a dehumidifier, four electric fans and two electric heaters. The atmospheric conditions were controlled by two thermostats and a humidistat mounted on walls inside the tent. These instruments were electronically coupled and controlled so that relative humidity could be maintained within the allowable tolerance.

The design of frame FR1 was essentially identical to frame FS1. It was cast four weeks after frame FS1 was placed in the tent. Seven days after pouring, frame FR1 was lifted by crane to the main structural test floor of the laboratory to begin preparation for proportional load testing.

(2.7) Instrumentation:

Concrete strains were measured using a demountable mechanical strain indicator, the Demec Gauge, housing an eight inch gauge length. The gauge points consisted of 1/4 inch diameter brass gauge discs with a number 60 center hole. The gauge points were attached to the concrete surface with epoxy cement. To obtain a useful set of strain gradients for the frame, the gauge points were attached to the critical high moment sections of the frames. The positions of the gauge points are shown in Figure 2.7. It should be noted that these discs were cemented **onto the** smooth face of the frames which was the face of concrete inside the steel form. Both columns were instrumented with gauge points on the faces of the concrete lying perpendicular to the direction of bending.

Dial gauge with scale division of 0.001 inch were used to measure deflection of the frames. Since deflections in the base portion of the columns were very small, 0.0001 inch division gauge were employed in this region.

An independent system of pipe-framework was constructed to support the dial gauges. The bases of the dial gauge framework were glued to the test floor level for frame FR1 and were welded to the steel base assembly for frame FS1. The positions of dial gauges are shown in Figure 2.7 .

Various sizes of load cells were used to register the loads applied to **points on the frames.** A load cell consisted of a spool-shape steel cylinder with four electric resistance strain gages, two vertical and two horizontal, mounted on the outside surface midway between the ends. These **gauges** were wired as a full wheatstone bridge and therefore formed a temperature compensating system. Strains were recorded using a switch and balance unit and a Budd Model P-350 Strain Indicator. To avoid problems **with drift** of the calibration curves, the load cells were selected so that the strains for the maximum applied loads were limited to between 300 to 700 micro-inches per inch. This limit was sufficiently high to provide easy resolution of calibration curves.

Prior to each test, the load cells were calibrated in a Tinius-Olsen Universal Testing Machine. Loads and readings were recorded in increments up to the maximum value desired. Readings were made for several cycles of increasing and decreasing loads. Graphs of the load calibration curve were prepared for each load cell for use in the test.

In addition to the load cells, high-strength tensile steel rod were employed in the axial load assembly which is described in section 2.8. The steel rods for frame FS1 were gauged in the same manner as the load cells and then calibrated in the Tinius-Olsen Universal Testing Machine. Calibration graphs were prepared for use during testing.

(2.8) <u>Loading Systems:</u>

(a) <u>Column Axial Loading Assembly:</u>

The column loads were applied through a post-tensioning system consisting of two one-inch diameter steel rod as shown in Figure 2.8. The threaded tension rods were restrained at the bottom of the column base by a six inch by six inch by two inch steel plate inserted below the web of the H-section of the concrete column base.

At the top of the column, a load cell and hydraulic jack were mounted on the steel joint connector. The load was transfered to the tension rods through a hollow steel section of dimension fourteen inch by seven inch by half inch section. The load cell transmitted the compression force to the column and therefore was

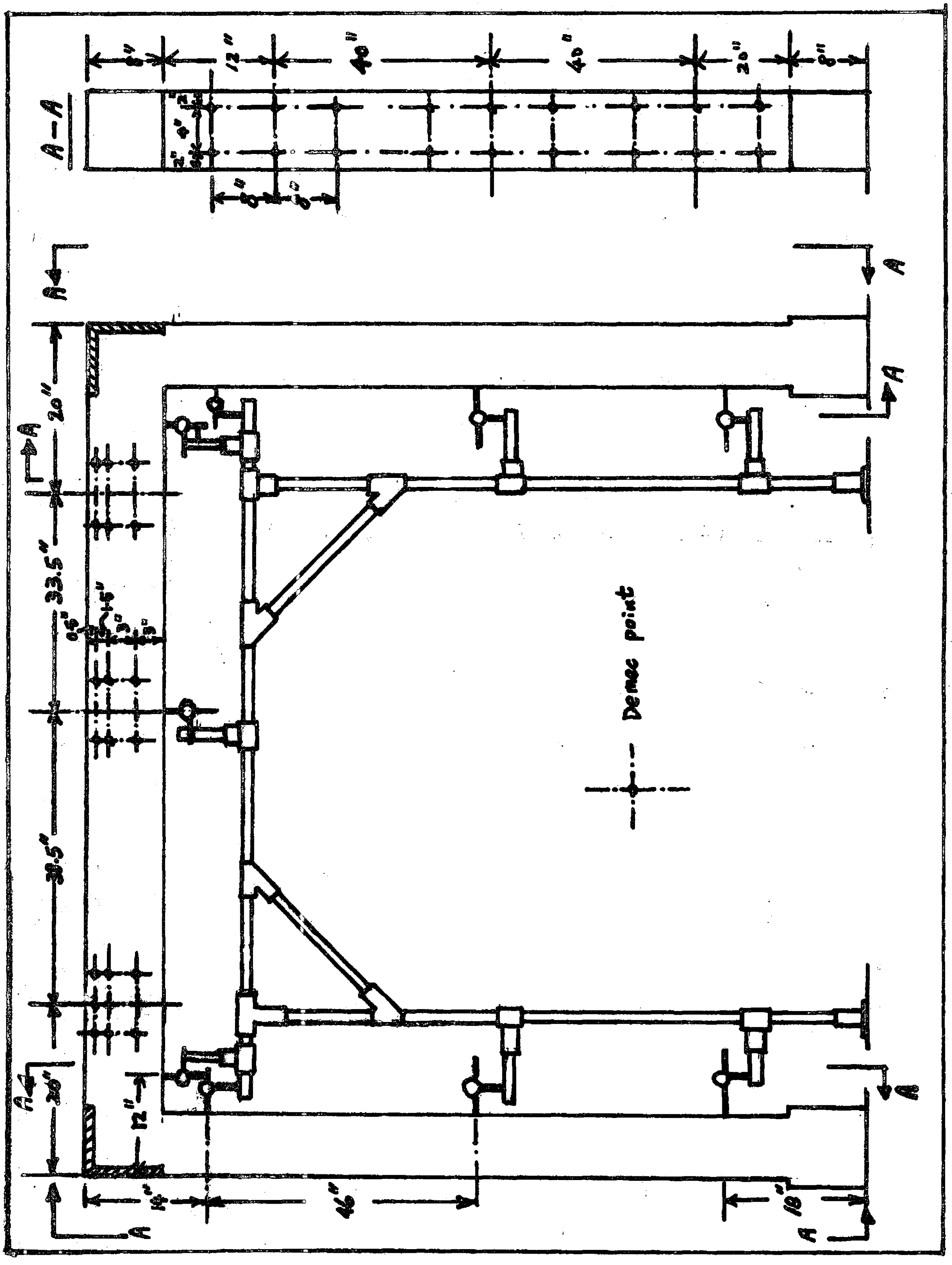

Figure 2.7

Dial Gauge and Demec Point Position for Frame FS1 & FR1 used to monitor and control the level of load.

For the short-term test of Frame FR1, the jack was kept in the loading position for the duration of the test. However, for the sustained load specimen, Frame FS1, the tension rods were fitted with strain gauges so as to act as a load measuring device while transmitting the axial loads. In this case, the tension rods were tensioned by jacking against a plate positioned over the top of the column and the load was maintained by tightening a nut to prevent change in the elongation of the rods after the jack pressure was removed. At regular intervals, the load on the columns had to be adjusted due to the decrease in load associated with creep and shrinkage.

(b) Beam Loading Assembly:

For the short-term test of Frame FR1, the beam load was applied by mounting a vertical load mechanism between the 14 inch wideflange steel columns of the loading system in the laboratory. The vertical load mechanism consisted of a 50 ton hydraulic jack mounted on a mechanical slide which allowed eight inches travel from the center of the beam in the direction of sidesway. Load was transferred to the beam through a ball seat. A load cell was used to record the loads applied.

The beam loading system for the sustained loading test of Frame FS1 was very different from Frame FR1. As shown in Figure 2.8 , four vertical load springs were stressed by pulling downward on four tension rods which extended from a plate on top of the springs to a base bolted to the test floor. The base consisted of a rigid steel box with a slide plate located under the top of the

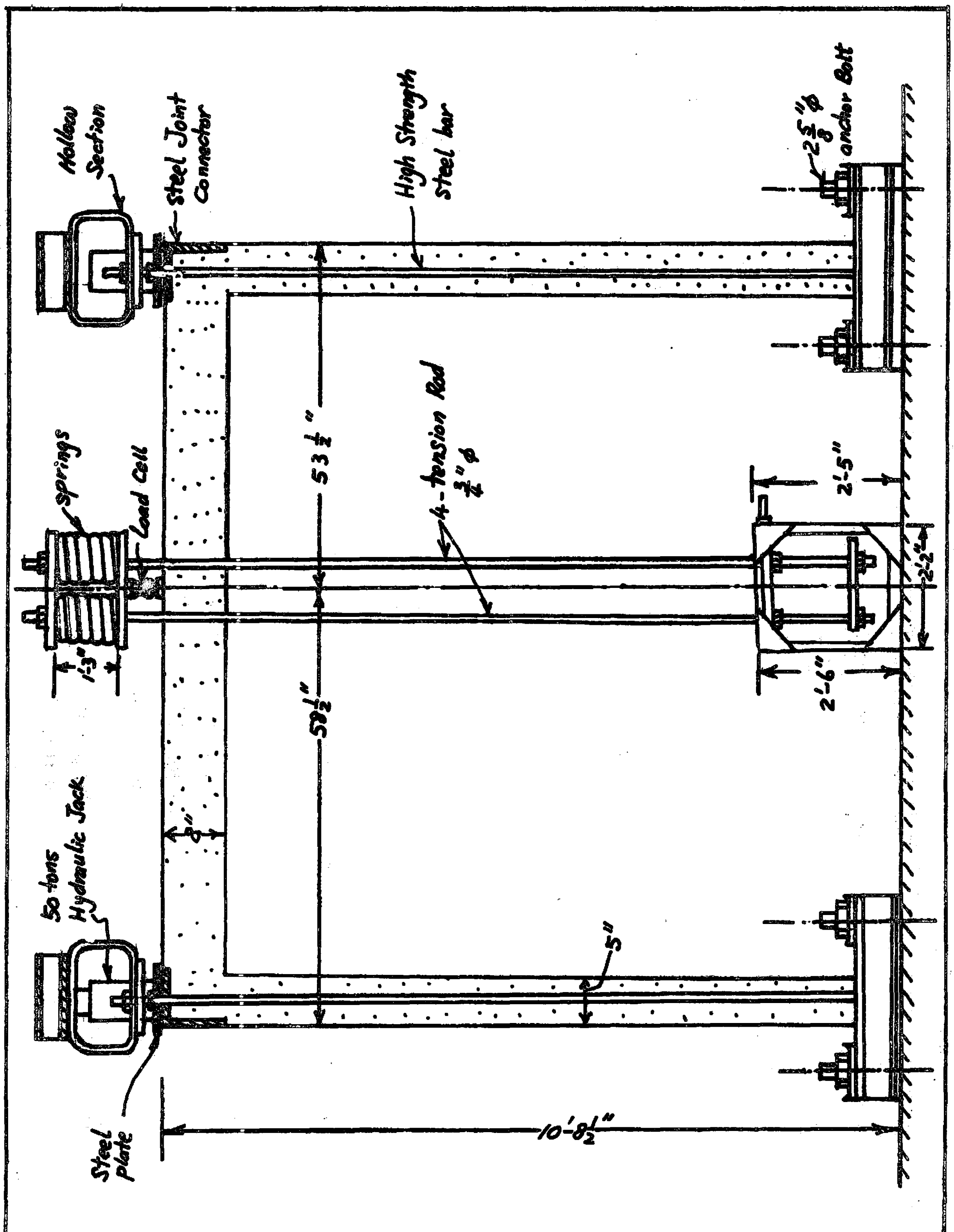

Figure 2.8

Loading System for Frame FS1

box. The tension rods passed through the top of the box and the slide plate. Both ends of the tension rods were threaded to accomodate the adjusting nuts. The slide plate was held against the underside of the top of the box by nuts on the tension rods.

A one inch thick plate was supported by the tension rods about one foot below the top of the box. On this plate, a fifty ton hydraulic jack was placed to load the springs. Load was applied by jacking against the top of the box, thereby pulling downward on the tension rods and compressing the springs which in turn transmit the load to the top of the beam through a plate and load cell. With jacking pressure applied, the nuts holding the tension rods against the slide plate were tightened thus maintaining the displacement of the springs so that the jack could be removed. The decrease in the load caused by deflection of the concrete frame with time was minimized through use of the springs. However , occassionally, the level of load had to be corrected by tightening the nuts.

(2.9) Testing and Observations :

(a) Short-term test, Frame FR1 :

For Frame FR1,the axial forces on the column and the vertical load on the beam were applied simultaneously in proportional increments. The columns were loaded from zero to sixty kips in increment of ten kips. The beam load was 20 percent of the column load, from zero to twelve kips and was loaded in increments of 2 kips.

When the loads on the columns reached sixty kips, these loads were maintained constant while the beam load was increased from twelve kips to failure of the frame. The dial gauge reading were recorded for each loading stage while the strain readings using the Demec Gauge were taken at selected stages of loading.

It was observed that the beam load became very unstable at the load level of fourteen kips and extensive cracking of concrete in the region near the beam center was noted. The beam load was further increased with one kip increments and the top of the beam under the load began to spall. At the load level of twenty kips, the load indicated by the load cells showed a rapid reduction of load within a few seconds of achieving this loading. Hence it was concluded that the structure had failed. For the applied loading condition, the frame appeared to have collapsed through formation of a beam mechanism.

(b) Sustained-load Test, Frame FS1:

The sustained load test specimen Frame FS1 was loaded in proportional stages to the load level desired. Upon reaching the column load level of 46 kips, on both columns, and a load of 10 kips on the beam, these loads were sustained so that effect of creep and shrinkage could be investigated. The deflection was observed to increase most significantly in the early stages of loading and correspondingly decrease the load level in the structure. It was therefore necessary to adjust the load level in the frame quite often to maintain the desired load intensities. Nevertheless, the load level was maintained within ± 2 % of the design load so that a constant sustained-load level can be assumed and compared to the analytical result. Dial gauge and Demec reading were taken at regular time intervals. After two months of loading at constant load level, it was observed that the deflection had ceased to increase significantly, thence, the load level was increased by 20 % and sustained for four additional weeks. After this three months of sustained loading, the frame was loaded to failure. The failure beam load was recorded to be 18 kips when a constant column load of 46 kips was sustained on both columns. The failure mode of the frame was observed to be a beam mechanism. Figures 2.9 and 2.10 show pictures of the sustained-load test specimen , Frame FS1 taken after failure of the frame.

(2.10) Conclusion:

This chapter has described the fabrication and testing of frames FR1 and FS1 for experimental verification of the proposed Matrix Stiffness-Modification method of inelastic analysis of concrete structures. Several details were presented. The test results are believed to be quite reliable due to constant care in fabrication and testing and through use of adequate recalibration procedures for load monitoring devices. The test results are shown in Chapter six where they are compared with the theore tical predictions.

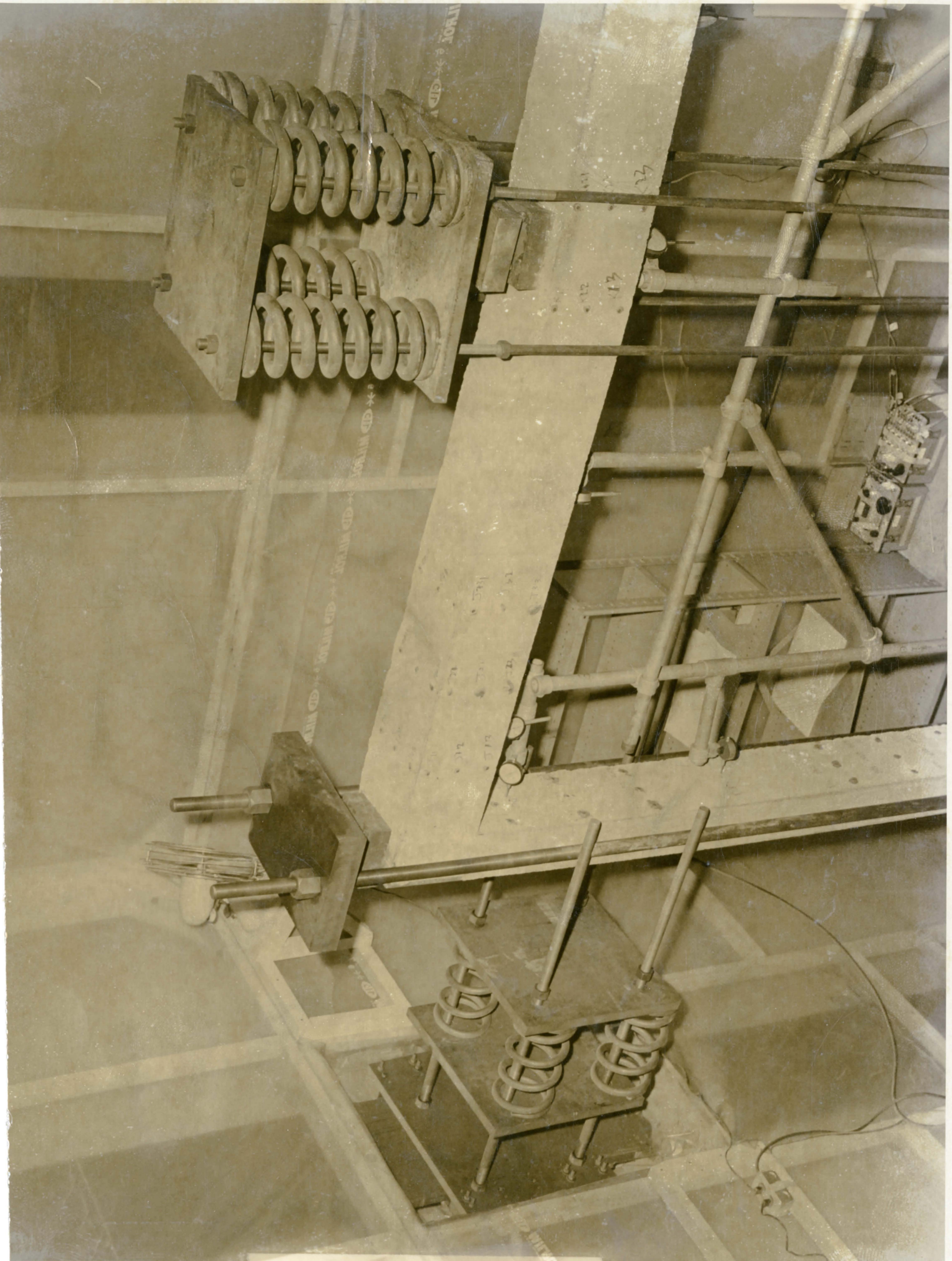

Figure 2.9 : Frame FS1

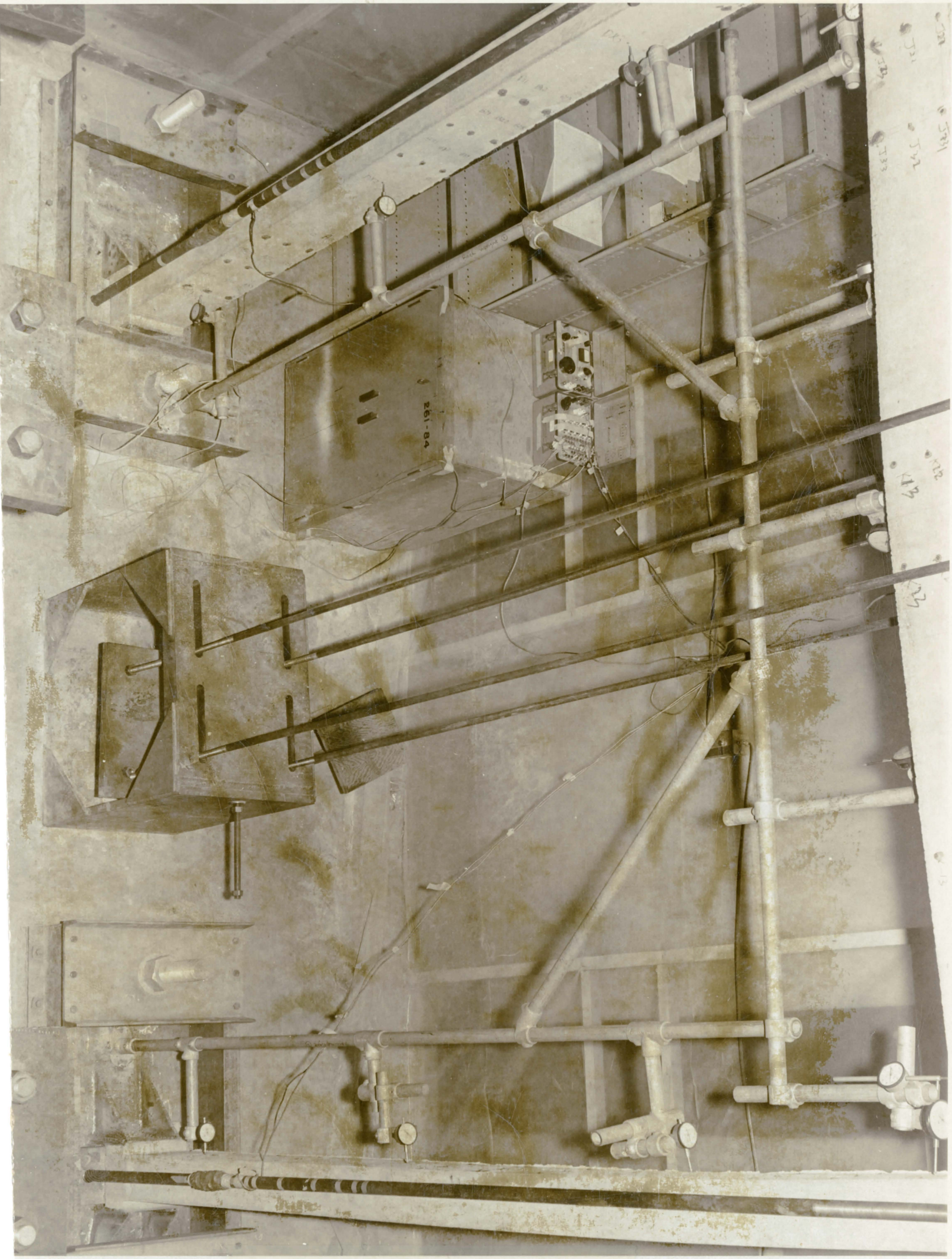

Figure 2.10 : Frame FS1

Chapter 3

PROPERTIES OF MATERIALS

(3.1) Introduction :

In this chapter, the general stress-strain relations of concrete and reinforcing steel are described. The phenomenon of creep and shrinkage of concrete and their method of computation are briefly introduced.

(3.2) Stress-Strain Curves for Concrete :

Concrete under applied load is known to exhibit a non-linear stress-strain relationship. The general shape of the stress-strain curve is shown as the solid line in Figure 3.1. The curve begins with a fairly linear portion that stretches to about 30 percent of the ultimate strength, then gradually deviates from the straight line up to a peak at the ultimate strength of concrete. After that, the curve starts to descend in a gradual manner until the ultimate strain of the concrete has been reached.

The nonlinearity of the stress-strain relationship of concrete can be attributed to the fact that the failure of concrete under load takes place through progressive internal cracking (43). At loads below the elastic limit, called the proportional limit of concrete, the stress concentrations within the heterogeneous internal structure remain at a low enough level that relatively minor microcracking occurs, and therefore the stress-strain curve in this region is rather linear. At loads above the proportional limit, the stresses in the concrete cause the development of increasing internal micro-cracking of the interfaces between the cement paste and the aggregate, and hence, the stress-strain curve starts to deviate from the straight line drawn in Figure 3.1. With increasing stress up to the ultimate strength of concrete, the propagation of crack increases vigorously within the cement paste, and between the cement paste and the aggregate thereby causing a progressive breakdown and discontinuity in the internal structure of concrete. For straining beyond ultimate load the ability of the section to withstand high stress is reduced and the stress-strain curve drops down with a decreasing stress until the ultimate strain of the concrete is reached.

For a numerical application of the concrete stress-strain relationship in the analysis of concrete structures, it is convenient and necessary to formulate standard mathematical curves to describe this relationship.It was pointed out as early as 1900 by the father of Aerodynamics, Von Karman (35) that the stress-strain relation of nonlinear material can be approximated by an exponential curve,

$$\frac{f_c}{f'_c} = 1 - e^{(-aw)} \qquad \ldots (3.1)$$

where,

f'_c = Ultimate strength of concrete

a = An experimental constant

w = Strain of material

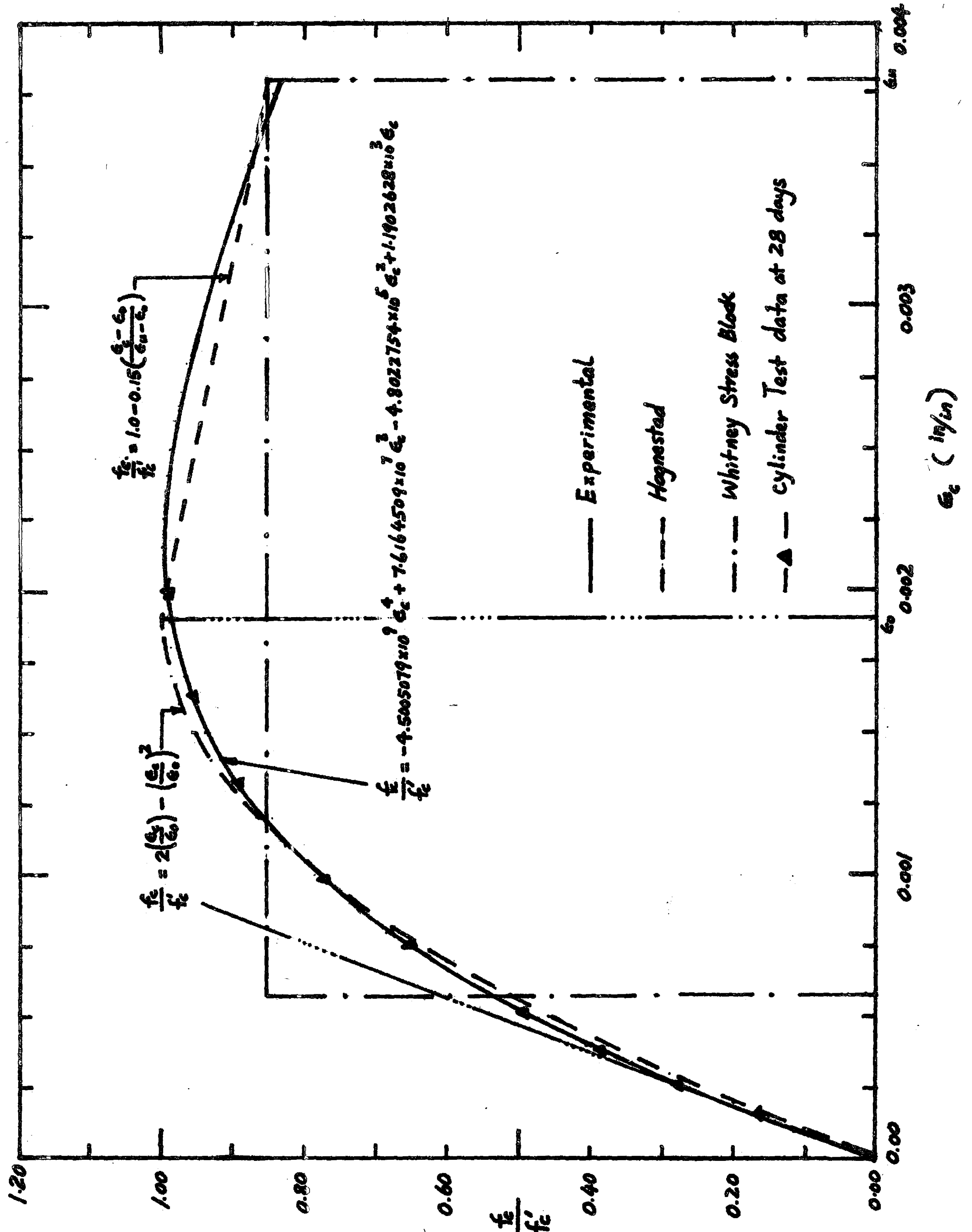

Figure 3.1

Stress-Strain Curve for Concrete

The exponential term of equation 3.1 can be expanded in series forms as,

$$e^{(-aw)} = 1 - aw + (aw)^2/2! - (aw)^3/3! + \ldots$$

Hence Equation 3.1 can be simplified as a series,

$$\frac{f_c}{f'_c} = C_1 w + C_2 w^2 + C_3 w^3 + \ldots + C_i w^i + \ldots$$

$$= \sum_{i=1}^{n} C_i w^i \qquad \ldots (3.2)$$

where,

$i = 1, 2, 3, 4, \ldots$

C_i = experimental constants

Generally, it is considered that a fourth order polynomial will yield a sufficiently accurate approximation of the actual stress-strain characteristic of concrete. The constants C_i are determined from a least-square fitting of large number of test data. For the concrete used in Frames FS1 and FR1, and for the other concrete research done at McMaster University, the values of the constants are derived as follows,

$$C_1 = 1.1902628\text{x}10^3$$
$$C_2 = -4.8022754\text{x}10^5$$
$$C_3 = 7.6164509\text{x}10^7$$
$$C_4 = -4.5005079\text{x}10^9$$

In Figure 3.1, the experimental curve reaches its ultimate strength at a strain of 0.00215 in./in., and then gradually decreases until the ultimate strain of 0.0038 in./in. is reached.

(3.3) Comparison of the Experimental Stress-Strain relation with Hognestad's and Whitney's Curves:

The Ultimate Strength Design method for proportioning concrete members has brought the stress-strain relation of concrete into focus. Due to simplicity in application, the Whitney's stress block has been accepted by the ACI-318-63 (2) as a satisfactory representation of the magnitude and position of the resultant of the stress distribution in concrete for the Ultimate Design Method. On the other hand, for more realistic analysis of the behavior of concrete, the Hognestad's curve (32) has been widely used. It is thus the purpose of this section to evaluate the experimental stress-strain relation by comparing it to the well-known Hognestad's and Whitney's Curves.

Hognestad assumed a parabolic distribution of stress in the rising branch of his curve up to the maximum stress occuring at a strain which is one-half of the ultimate strain of concrete. A discontinuity existed at the point of maximum stress, and a straight line approximated the falling branch of the curve. Practically, the straight line approximation of this curve in the falling branch portion is not true and was introduced to provide a means of achieving compatible stress resultants. It has been proved by strain controlled experiments (5,48) that the falling branch is a tailing curve. However, the falling branch behavior is important only to ductility of concrete but not to strength. Hognestad originally suggested that the ultimate stress of concrete should be taken as 85 percent of the actual experimental ultimate strength of concrete. However, for research, the author sees no reason for using only partial strength of the concrete. This point was also discussed by Furlong (28) where using 85% of the experimental ultimate strength of concrete proved to be too low. Thus the author used the full strength of concrete in this comparison and in his research. In Figure 3.1, the Hognestad's curve is shown as a dash line whereas the Whitney's stress block is shown as a solid-dash line. It is therefore noted that the experimental curve follows fairly closely to the Hognestad curve in the rising branch of the curve and with minor difference in the falling branch.

The area under the curves and above the strain axis is computed as,

$$\text{Area} = \int_0^{\epsilon_u} f_c(w)\, dw$$

the moment of area of the curves about the zero stress axis is given by,

$$\text{Moment of Area} = \int_0^{\epsilon_u} f_c(w)\, w\, dw$$

Table 3.1 gives a summary of the integration by using an ultimate strain of concrete of 0.0038 in./in., as recommended by Hognestad. From the table, the experimental and Hognestad's curves differ in area by 1.4 %, and in moment of area by less than 1.5 %. However, Whitney's stress block seems rather conservative. It is 10.8 % less in area and 8.5 % less in moment of area than the experimental curve; and is 9.4 % less in area and 7.2 % less in moment of area than the Hognestad's curve.

Table 3.1

COMPARISON OF THE EXPERIMENTAL STRESS-STRAIN RELATION WITH HOGNESTAD AND WHITNEY CURVES

Curve	Area	Moment of Area
Experimental	3.07229×10^{-3}	6.55833×10^{-6}
Hognestad	3.02423×10^{-3}	6.46741×10^{-6}
Whitney	2.74202×10^{-3}	6.00113×10^{-6}
Ratio		
Hognestad/Experimental	0.986	0.985
Whitney/Experimental	0.892	0.915
Whitney/Hognestad	0.906	0.928

(3.4) Stress-Strain Relationship for Reinforcing Steel :

The reinforcing steel is assumed to be an idealized elasto-plastic material. The effect of strain hardening in steel has been neglected. Hence , the curve can be depicted as a perfectly straight line up to the yielding point and after that a flat line of constant stress follows. The relationship between stress and strain can be represented by the following equation,

$$f_s = f_y \left(\frac{w_s + w_y - |w_s - w_y|}{2\, w_y} \right) \quad \ldots (3.3)$$

where,

f_s, f_y = stress and yield strength of steel respectively

w_s, w_y = strain and yield strain of steel respectively

Figure 3.2 shows the theoretical and experimental stress-strain curve

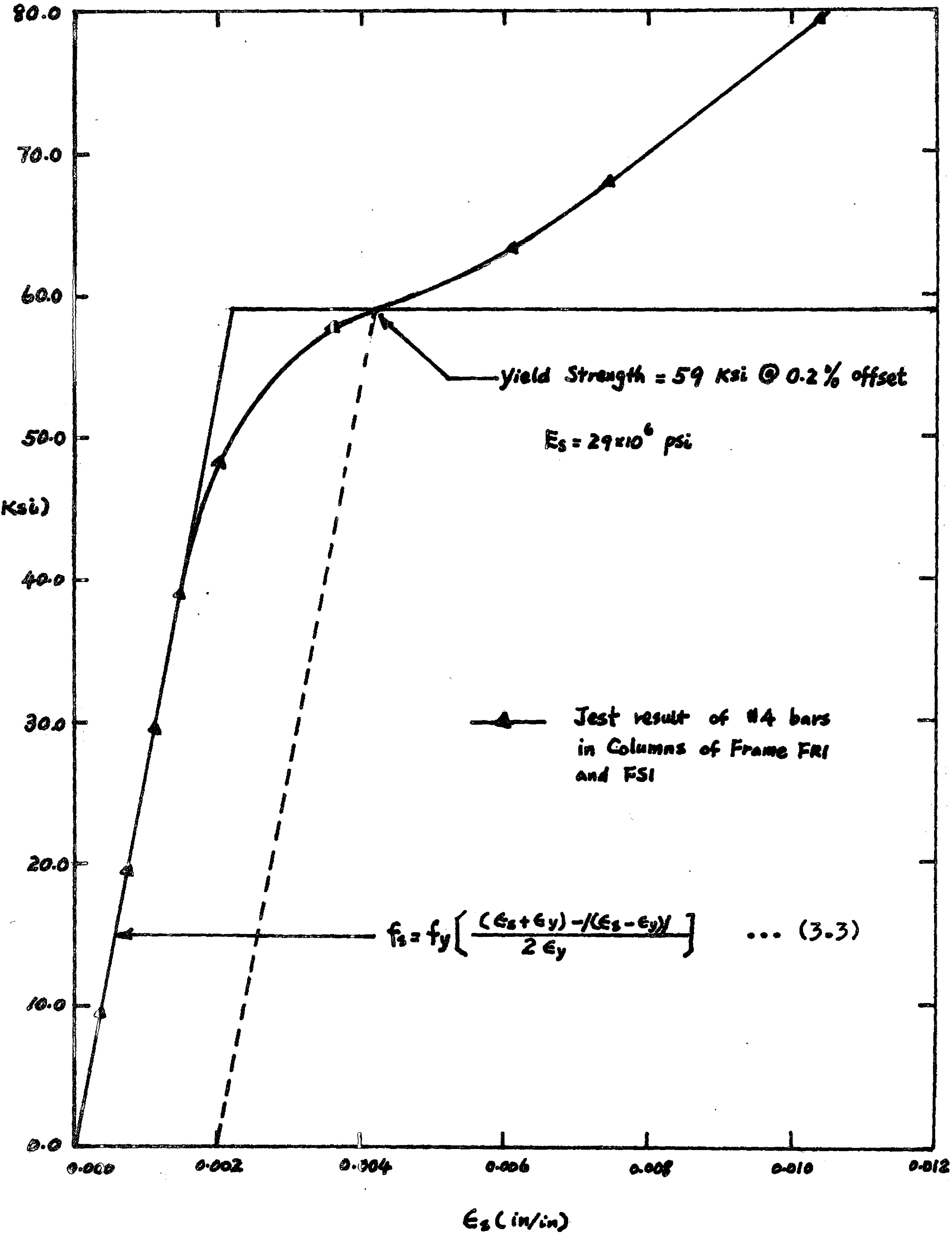

Figure 3.2

Stress-Strain relationship for Steel

for the number 4 bar used in Frames FR1 and FS1. It is noted that an accurate analysis of Frames FS1 and FR1 requires exact knowledge of the stress-strain relationship of number 4 bar if failure of the frames occurs in the columns. Fortunately, for the loading condition designed for Frames FR1 and FS1, the higher moment occurs in the beam where the number 6 bar has a distinct yield region which closely follows the idealized curve (19).

(3.5) Shrinkage of Concrete :

Shrinkage of concrete is the volumetric deformation that the concrete undergoes when not subjected to load or restraint. It is due mainly to the loss of moisture of the concrete by diffusion to, or evaporation from free surfaces. The existence of a moisture gradient within the concrete hence causes differential shrinkage which can induce internal stresses.

The magnitude of shrinkage strain is of the same order as the elastic strain of concrete under usual ranges of working stress. Shrinkage can produce tensile stress large enough to cause extensive cracking of concrete, hence, it should be taken into account in the analysis of concrete structures.

Figure 3.3 shows the shrinkage function used in this analysis. It was derived by Drysdale (20) from a least square fitting of prism results. The derivation assumed uniform shrinkage acting at a given cross-section. The shrinkage function is given mathematically as,

$$\text{Shrinkage} = 0.000111 + 0.000224 \operatorname{Log}_{10}(\text{Time}) \quad \ldots (3.4)$$

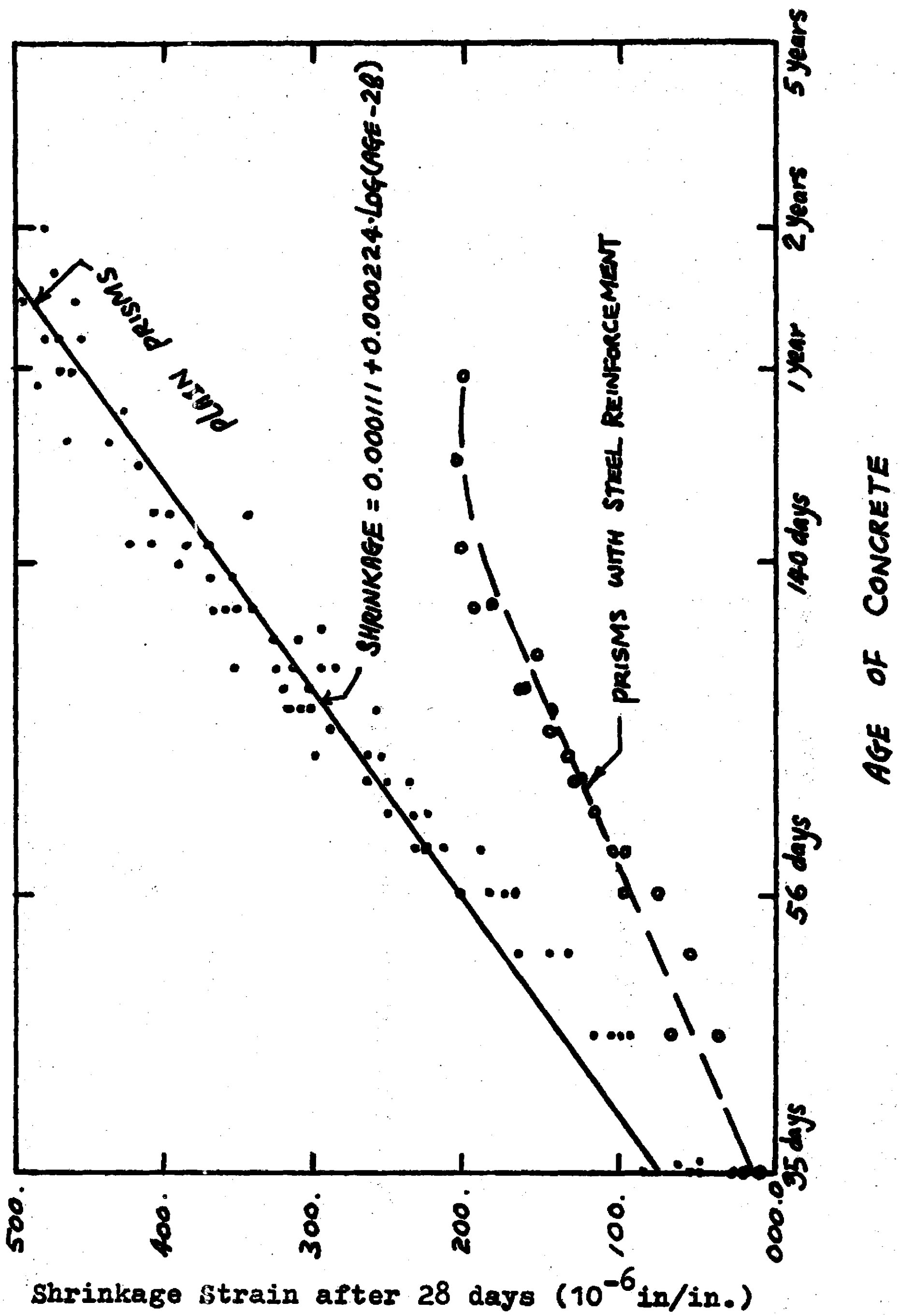

Figure 3.3

Shrinkage Function

(3.6) Creep of Concrete :

Creep is the increase in strain of concrete under sustained stress. Creep strain can be several times as large as the elastic strain of concrete under load, and hence is of considerable importance in analysis of concrete structure. There are several theories explaining the phenomenom of creep. They attributed creep to be viscous flow of cement water paste, closure of internal voids, crystalline flow in aggregate, and by seepage flow of colloidal water from the gel that is formed by hydration of the cement.

Neville (31) however suggested that creep is due to oriented internal moisture diffusion caused by a free energy gradient of the absorbed water and to slow deformation of the elastic skeleton of the gel induced by viscous deformation of absorbed water. When concrete is under stress, some gel particles moved closer to one another while some moved apart. The free energy of water then varies accordingly, and local energy gradients results. This is the driving force for local moisture diffusion.

Creep is influenced by the aggregate-cement ratio, water-cement ratio, kind and grading of aggregates, composition and finess of cement, age at time of loading, intensity and duration of stress, moisture content of concrete, relative humidity of ambient air, and size and shape of the concrete member. The rate of creep deformation is relatively rapid at early ages after loading, and decreases exponentially with time. Concrete also exhibits creep recovery upon unloading. It can be explained (31) as the release of the increased strain energy stored in the gel during creep. Creep recovery is gradual because of the viscous restraint of the absorbed water.

This section only briefly introduces the concept of creep. However, for further detail of creep, the readers are recommended to read references 26, 40, 50.

(3.7) Method of Computing Creep under Variable Stress:

Several methods have been proposed for computing the magnitude of creep under varying stress. Nevertheless, three methods, the Rate of Creep method, the Effective Modulus method and the Superposition method, have been found to be most widely used (33, 50) . A summary of these methods is given in Table 3.2.

Accordingly, the rate of creep method usually overestimates creep while the effective modulus method underestimates creep. The method of superposition generally gives fairly accurate result but still underestimates creep.

(3.8) Modified Superposition Method:

This method is proposed by Drysdale (20) and is briefly described here. The method can predict creep more accurately by accounting for the stress history of the concrete.

For a concrete creep specimen subjected to sustained stress, the "elastic strain" is defined as the short-term concrete strain corresponding to a given applied loads. The magnitude of the creep is then given by,

$$\text{Creep} = A + B \operatorname{Log}_{10}(\text{time}) \qquad \ldots (3.5)$$

Table 3.2

METHOD OF COMPUTING CREEP UNDER VARIABLE STRESS

Method	Formula	Remark
Rate of Creep	$c = \int f \frac{dc}{dt}\,dt$	For a given specific creep curve, the total creep is given by c, where f is the imposed stress and dc/dt is the rate of creep .
Effective Modulus	$E_c' = E_c/(1+c_1E_c)$	E_c is the modulus of elasticity of concrete, c_1 is the specific creep.
Superposition	$c = c_1 + c_2$	A specimen of concrete is loaded to stress f_1 from time T_o to T_1, and the stress was changed to f_2 and maintained from T_1 to T_2 . c_1 is the creep due to f_2 for time $T_2 - T_1$ minus the creep due to stress f_1 over the same time interval. c_2 is that creep which would have occurred at stress f_1 during the time T_o to T_2 when loaded at time T_o .

where A and B are creep coefficients derived by least square fitting of experimental data. For the concrete used in making Frames FR1 and FS1, the functions A and B are given as,

$$A = A_1 w^3 + A_2 w^2 + A_3 w + A_4$$

$$B = B_1 w^3 + B_2 w^2 + B_3 w + B_4$$

where,

$$\begin{aligned}
w &= \text{elastic strain of concrete} \\
A_1 &= -1.03050\times10^{6} \\
A_2 &= 5.748870\times10^{2} \\
A_3 &= -3.77674\times10^{-1} \\
A_4 &= -3.072250\times10^{-6} \\
B_1 &= 1.858390\times10^{6} \\
B_2 &= -1.012295\times10^{3} \\
B_3 &= 1.5213225 \\
B_4 &= -7.986250\times10^{-6}
\end{aligned} \quad \ldots (3.7)$$

If an element of concrete is loaded so that the elastic strain is w_1 and maintained at that stress f_1 for a period of time T_o to T_1, the amount of creep which would occur would be C_1. After that, an increased stress f_2 which results in elastic strain w_2 is in turn maintained for the period T_1 to T_2, and the amount of creep which would occur during this time if the specimen had been loaded to f_2 at time T_o is then denoted as C_2. To account for the change in stress, C_3 is the amount of creep which would occur for the change of elastic strain w_2-w_1 over a time interval from zero time to T_2-T_1. The total creep C, is given by,

$$C = C_1 + C_2 + C_3$$

The modified superposition method will slightly underestimate creep for increasing stress, and the effect of creep recovery is not taken into account. Figure 3.4 gives the curves for functions A and B and Figure 3.5 illustrates the method of modified superposition.

(3.9) <u>Summary</u> :

This chapter has discussed the material properties of concrete and steel. The stress-strain relationship of steel and concrete must be known in advance so that a rational second order analysis of inelastic concrete structures can be made. Creep and shrinkage of concrete have been known to have considerable importance in structural analysis of sustained load behavior of concrete structures, and therefore their method of computation consists of a very important aspect of the present research.

Creep and shrinkage curves which have been derived by Drysdale (20) in his University of Toronto Column Test, have been used in this research .

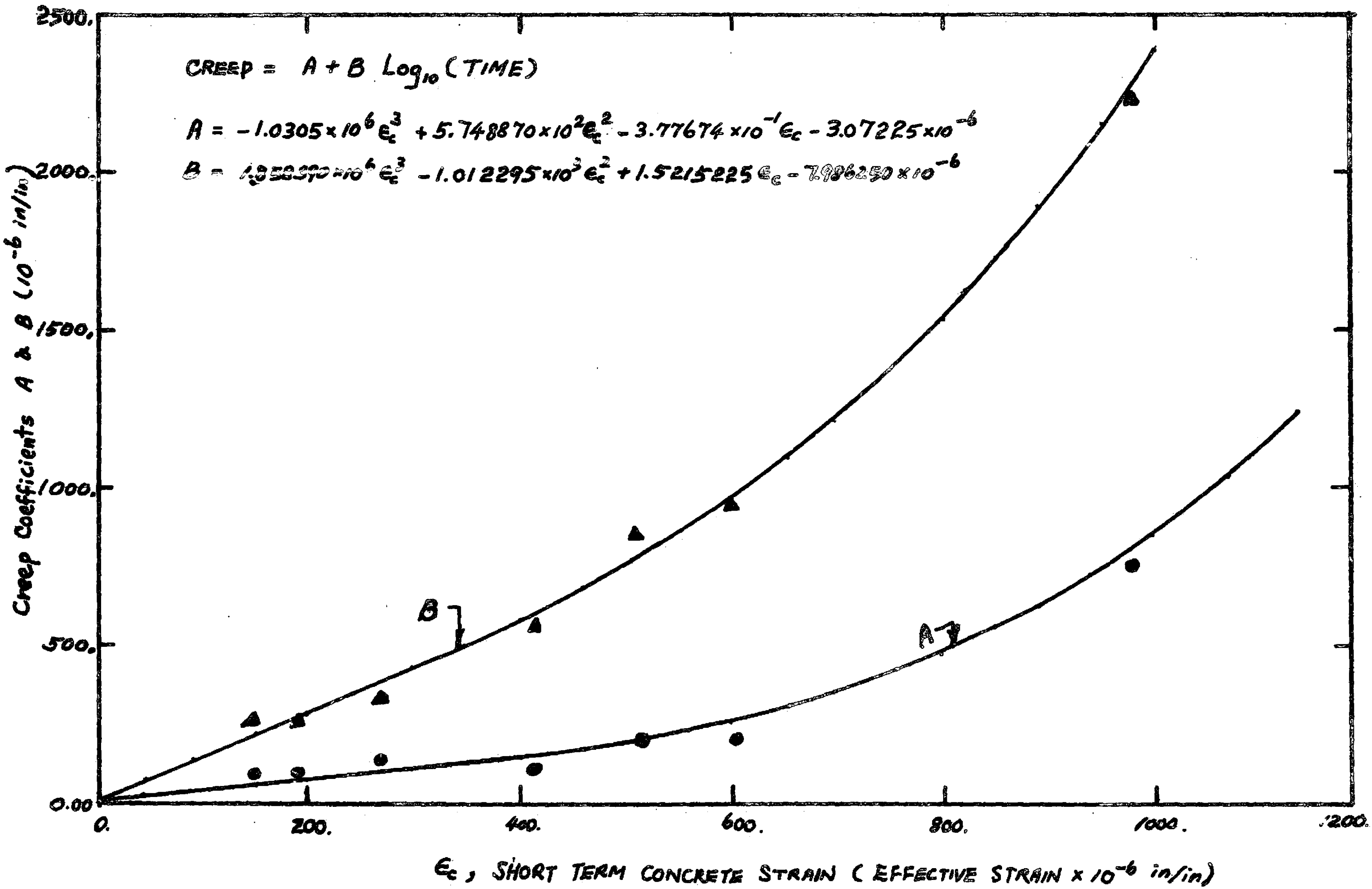

Figure 3.4
Creep Functions

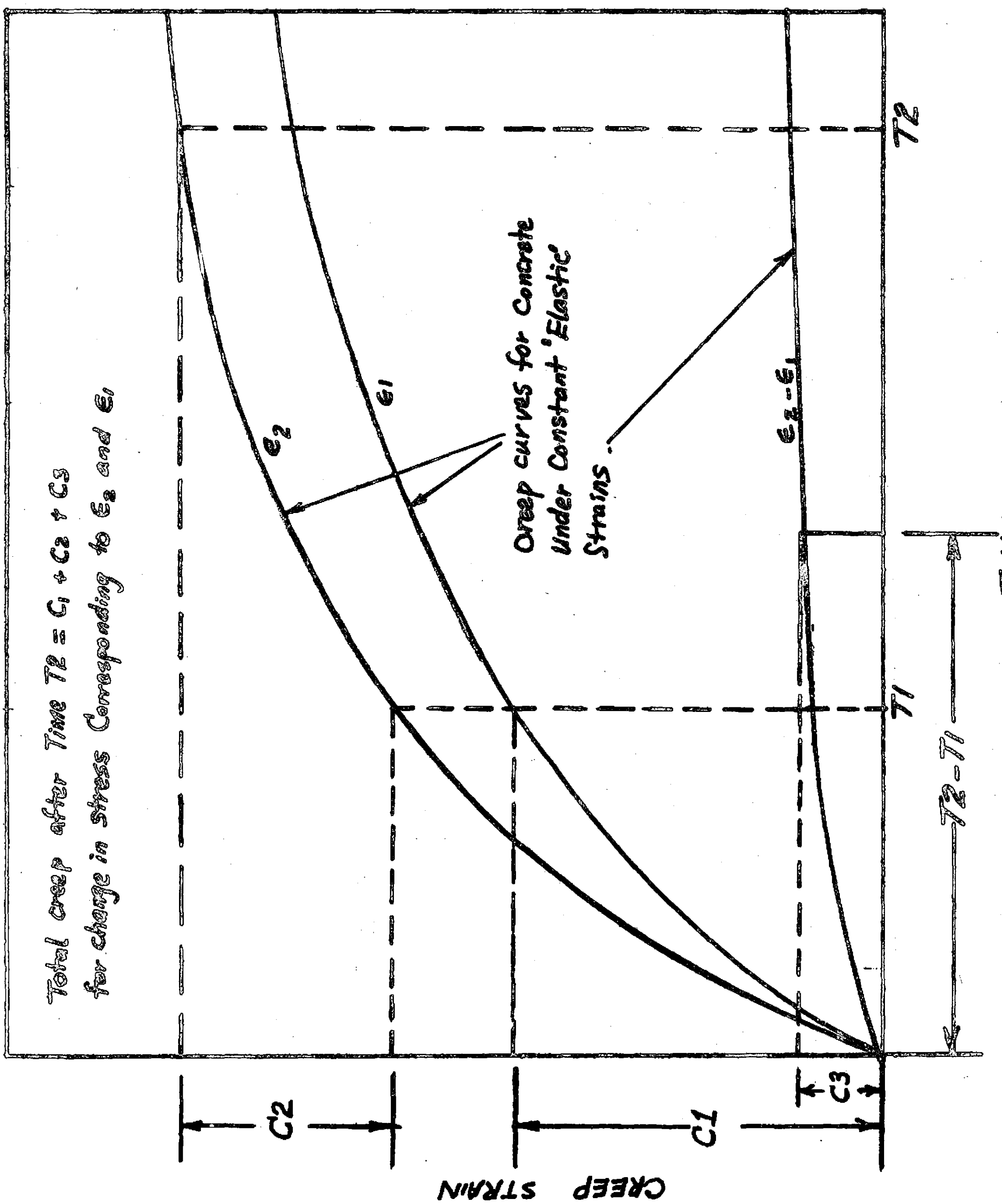

Figure 3.5
Modified Superposition Method

Chapter 4

DEFORMATION CHARACTERISTICS OF CONCRETE SECTIONS

(4.1) Introduction :

In this chapter, some aspects of the deformation properties of a given cross-section of concrete are discussed. An extended Newton-Raphson method (49) has been used to determine the strain and curvature distribution in a concrete section subjected to externally applied bending moment and axial force. The short term and sustained load effect on the load-moment-curvature-time characteristics and the stiffness properties of concrete sections have been derived by the numerical approximation. The digital computations were performed using a high-speed CDC 6400 electronic computer in the Computing Center of McMaster University, and the results are presented in graphical form. The computer program for determination of the deformation characteristics of a section forms part of the program for the Matrix Stiffness-Modification Technique (to be discussed in detail in Chapter 5) which is included in Appendix A.

The material presented here is of fundamental importance for understanding the proposed stiffness modification method of inelastic concrete structural analysis which is presented in Chapter 5. In addition, it is hoped that this chapter will offer a clear picture of the nonlinear response of concrete sections subjected to applied bending moment and axial load through the discussion of the graphs contained herein.

(4.2) Internal Load Vector for a Concrete Section :

For a concrete cross-section subjected to a given strain distribution, the internal forces and bending moments can be computed provided that the stress-strain properties of materials are known.

The assumption that plane sections remain plane after loading has been confirmed by other investigators (49) and is incorporated in this analysis. Hence, for a given cross-section of concrete, assuming a linear strain distribution over the section, the corresponding stress at any point can be computed from the compatible stress-strain relationship. Figure 4.1 shows the given concrete section, the strain distribution diagram and the corresponding stress diagram.

Let w denotes strain and f denotes stress, hence, if the stress-strain relationships of the materials are given as,

$$f_c = f_c^* (w)$$
$$f_s = f_s^* (w)$$

where,

f_c , f_s = stress of concrete and steel respectively.

f^*_c, f_s^* = stress function of concrete and steel respective

Thus, for a given strain distribution over the cross-section, the internal axial force and bending moment can be computed as follows,

$$P = C_c + C_s - T_c - T_s$$
$$= \frac{a}{w_1}\int_0^{w_1} b\ f_c^*(w)\ dw + A_s'\ f_s^*(w_2) - A_s f_s^*(w\ \ ) - \frac{g}{w_t}\int_0^{w_t} b\ f_c^*(w)\ dw$$

$$M = \frac{a^2}{w_1^2}\int_0^{w_1} b\ f_c^*(w)\ w\ dw + A_s'\ f_s^*(w_2)\ (a - d') + A_s f_s^*(w_3)(d - a) + \frac{g^2}{w_t^2}\int_0^{w_t} b\ f_c^*(w)\ w\ dw - P\ (a - c)$$

Where,

P = internal axial force

M = internal bending moment

w_1= concrete strain of extreme compressive fibre

w_t= tensile strain of concrete

ϕ = curvature of section

a,b,c,d,d',g = length given in Figure 4.1

A_s, A_s' = area of tension and compression steel respectively.

However, the calculations of P and M are so tedious that hand computation is almost not feasible for a large number of calculations. Fortunately, the high-speed computer can be utilized to solve the problem easily. With the addition of creep and shrinkage strains, numerical integration must be resorted to. The cross-section is then subdivided into a finite number of fibers, with equal height as shown in Figure 4.1. The internal axial force and bending moment can be computed by summing the average normal stresses times the area over which they act, and by summing the moment caused by the axial force in each element strip respectively. Therefore,

$$P = (b_1 l_1 f_{c1} + b_2 l_2 f_{c2} + \dots + b_n l_n f_{cn}) + (A_{s1} f_{s1} + A_{s2} f_{s2} + \dots + A_{sm} f_{sm})$$

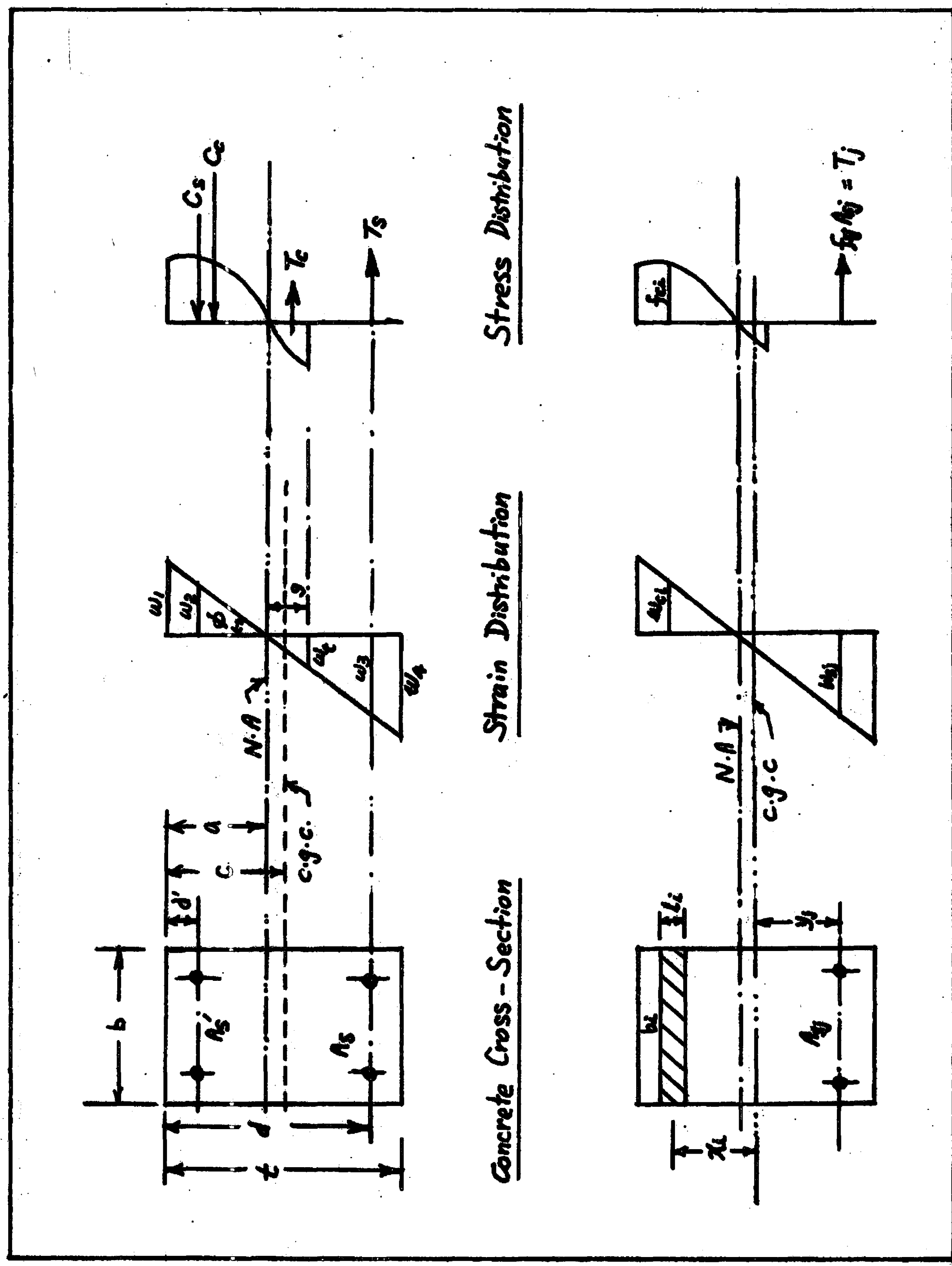

Figure 4.1

Concrete Stress and Strain Distribution

$$M = (b_1 l_1 f_{c1} x_1 + b_2 l_2 f_{c2} x_2 + \dots + b_n l_n f_{cn} x_n) + (A_{s1} f_{s1} y_1 + A_{s2} f_{s2} y_2 + \dots + A_{sm} f_{sm} y_m)$$

or,

$$P = \sum_{i=1}^{n} b_i l_i f_{ci} + \sum_{j=1}^{m} A_{sj} f_{sj}$$

$$M = \sum_{i=1}^{n} b_i l_i f_{ci} x_i + \sum_{j=1}^{m} A_{sj} f_{sj} y_j \qquad \dots \quad (4.1)$$

where,

n = number of element strip

m = number of row of reinforcing steel

x_i = distance from the centroid of each element strip to the geometric centroid of section

y_j = distance from the centroid of each row of steel to the geometric centroid of section.

It is known that concrete cannot take any tensile stress beyond a specified limit. Therefore, some of the force components in Equation 4.1 corresponding to tensile stress in the concrete will be zero if the tensile strain of the concrete is beyond the cracking stress. Due to the non-linear nature of the stress-strain characteristic of concrete, coupled with the effects of creep and shrinkage, the only feasible process was to employ a numerical trial and error iteration to determine the unique strain distribution which would yield an internal load and moment compatible with the externally applied axial load and bending moment. To speed up the process of convergence of the iteration, an extended Newton-Raphson method (49) is presented in next section.

(4.3) Extended Newton-Raphson Method:

For a given set of applied load and moment, the Newton-Raphson method of successive approximation can be conveniently applied to determine the compatible strain distribution. By referring to Figure 4.1 again, the internal load and moment can be determined provided that the extreme concrete fibre compressive strain and the curvature are known, or,

$$\begin{aligned} P^* &= P\,(w_1\,,\,\phi) \\ M^* &= M\,(w_1\,,\,\phi) \end{aligned} \qquad \ldots \quad (4.2)$$

where,

w_1 = extreme concrete fibre compressive strain

ϕ = curvature acting over the cross-section

P^*, M^* = internal axial load and bending moment respectively.

P, M = load and moment function respectively.

By using Taylor's theorem with linear term only,

$$\begin{aligned} P^* &= \bar{P} + \frac{\partial P^*}{\partial w_1}\,dw_1 + \frac{\partial P^*}{\partial \phi}\,d\phi \\ M^* &= \bar{M} + \frac{\partial M^*}{\partial w_1}\,dw_1 + \frac{\partial M^*}{\partial \phi}\,d\phi \end{aligned} \qquad \ldots \quad (4.3)$$

where,

$\bar{P}$, $\bar{M}$ = known axial load and moment for a known $\bar{\phi}$ and $\bar{w}_1$

$\frac{\partial P^*}{\partial w_1}$, $\frac{\partial M^*}{\partial w_1}$, $\frac{\partial P^*}{\partial \phi}$, $\frac{\partial M^*}{\partial \phi}$ = rates of change of P^* and M^* for which ϕ and w_1 are sought

dw_1, $d\phi$ = increment of strain and curvature necessary to produce P^* and M^*

so that,

$$\begin{aligned} \phi^* &= \bar{\phi} + d\phi \\ w_1^* &= \bar{w}_1 + dw_1 \end{aligned} \qquad \ldots \quad (4.4)$$

where ϕ^* and w_1^* can be used to compute P* and M*. Equation 4.3 can also be expressed in Matrix form as,

$$\begin{Bmatrix} P^* - \bar{P} \\ \hline M^* - \bar{M} \end{Bmatrix} = \left[\begin{array}{c|c} \partial P^*/\partial\phi & \partial P^*/\partial w_1 \\ \hline \partial M^*/\partial\phi & \partial M^*/\partial w_1 \end{array}\right] \begin{Bmatrix} d\phi \\ \hline dw_1 \end{Bmatrix} \qquad \ldots \quad (4.5)$$

or, rewriting equation 4.5 as,

$$Q^* \quad = \quad E^* \quad W^*$$

Hence, if the square matrix E* and the load vector Q* are known, the increment vector W* can be easily determined if E^{*-1} exists,

$$W^* \quad = \quad E^{*-1} \quad Q^*$$

The increment in curvature and strain contained in the W* vector can then be substituted into Equation 4.4 to obtain a new set of w_1 and ϕ and therefore a new set of load and bending moment. The computed P and M are then compared to the applied P and M, and if the difference between them does not vary by more than an allowable error, the process of iteration is then terminated. Otherwise, the iteration is repeated by substituting into equation 4.3 the computed P and M as a new initial value of $\bar{P}$ and $\bar{M}$, and the computed w_1 and ϕ as a new $\bar{w}_1$ and $\bar{\phi}$.

The Newton-Raphson method is just briefly introduced in this section. However, in section 5.6.c, a more detail description of this method with its application to computer programming is given. Further details may be found in an excellent paper by Robinson (49).

(4.4) Selection of Increments for Convergence Control :

The selection of suitable initial values of $\bar{w}_1$ and $\bar{\phi}$ to compute the initial values of $\bar{P}$ and $\bar{M}$, and the increments of concrete strain and curvature, ∂w_1 and $\partial \phi$, for the corresponding increments ∂P and ∂M, were among the most difficult tasks facing the author for the design of a general program for multi-storey frame analysis. After running a great number of frame analysis programs for different loading conditions and durations of time, it was found that selection of initial values of "Elastic Strain" and "Elastic Curvature" for a known applied axial load and bending moment, will give satisfactory result for most situations.

However, when creep and shrinkage have been taken into account, the elastic strain of concrete may exhibit nonlinearity and the convergence of the Newton-Raphson method to obtain a compatible set of w_1^* and ϕ^* for known values of P^* and M^* may become difficult. It is sometimes necessary to change the initially selected value of $\bar{\phi}$ and $\bar{w}_1$ to catalize the convergence of the method. Thus, if after 50 cycles of numerical iteration with each cycle begining with a selected ϕ^* and w_1^* for computing P^* and M^*, then comparing the computed P^* and M^* with the applied P and M, it is found that convergence cannot be obtained, the initial value of $\bar{\phi}$ and $\bar{w}_1$ are incremented linearly as follows,

$$\bar{\phi} = (\bar{\phi}_{\text{initial}})\ 0.20\ K$$
$$\bar{w}_1 = (\bar{w}_{1\ \text{initial}})\ 0.20\ K \qquad \dots (4.6)$$

where,

$$K = 1, 2, 3, 4, \dots$$

By the above mentioned procedure, provided that a reasonable first estimate of ϕ and w_1 are chosen, convergence by the extended Newton-Raphson method has proved successful.

(4.5) Short-term Load-Deformation Curves :

From the Newton-Raphson method described in the last section, the short-term load-deformation curves for a given cross-section of concrete can be easily determined. The typical section used in this chapter is the beam section for Frames FS1 and FR1. The ultimate compressive strain of concrete has been set at 0.004 in. per in., while the cracking tension strain of concrete was assumed to be 0.00015 in/in. for cases where tension of concrete was included. However, in most cases the analysis does not include the effect of tension in the concrete . The reason will be explained later.

(4.5.a) Moment - Curvature Relationship :

As described previously, for a given applied bending moment and axial load acting on a cross-section, a compatible strain distribution was obtainable and the short-term moment - curvature curves with different values of constant axial load can be plotted as shown in Figure 4.2.

The failure envelop is defined as the limiting line at which concrete had reached its ultimate strain for different load levels. The effect of tension of concrete on the moment - curvature behavior is shown as dotted lines. When the section is uncracked, or the strain at the extreme fibre of the concrete is less than 0.00015 in/in, the entire section acts to resist the applied bending moment and axial load. This implies that the moment-curvature curves have constant slopes up to the maximum uncracked moment capacity of the section. When the tension strain in the extreme tensile fibre is reached, the concrete starts to crack which in turn causes loss of equilibrium which produces more cracking until a new state of equilibrium is reached. This unstable moment curvature region may be thought of as the transition region between uncracked and cracked section behavior. Further increase in applied moment reduces the effect of tension on the behavior of the section and the curve gradually approaches the one without tension. Thus, at high values of applied moment, it can be observed that tension has a relatively insignificant influence on the behavior and capacity of the section.

When tension is included, the cracking moment capacity increases with increase in axial load since the presence of axial load produces a compression effect which counteracts the tension resulting from the applied moment. The increase in axial load also caused a decrease in the slope of the moment curvature curves prior to cracking because the increase in axial load at constant moment level will increase the curvature of the section.

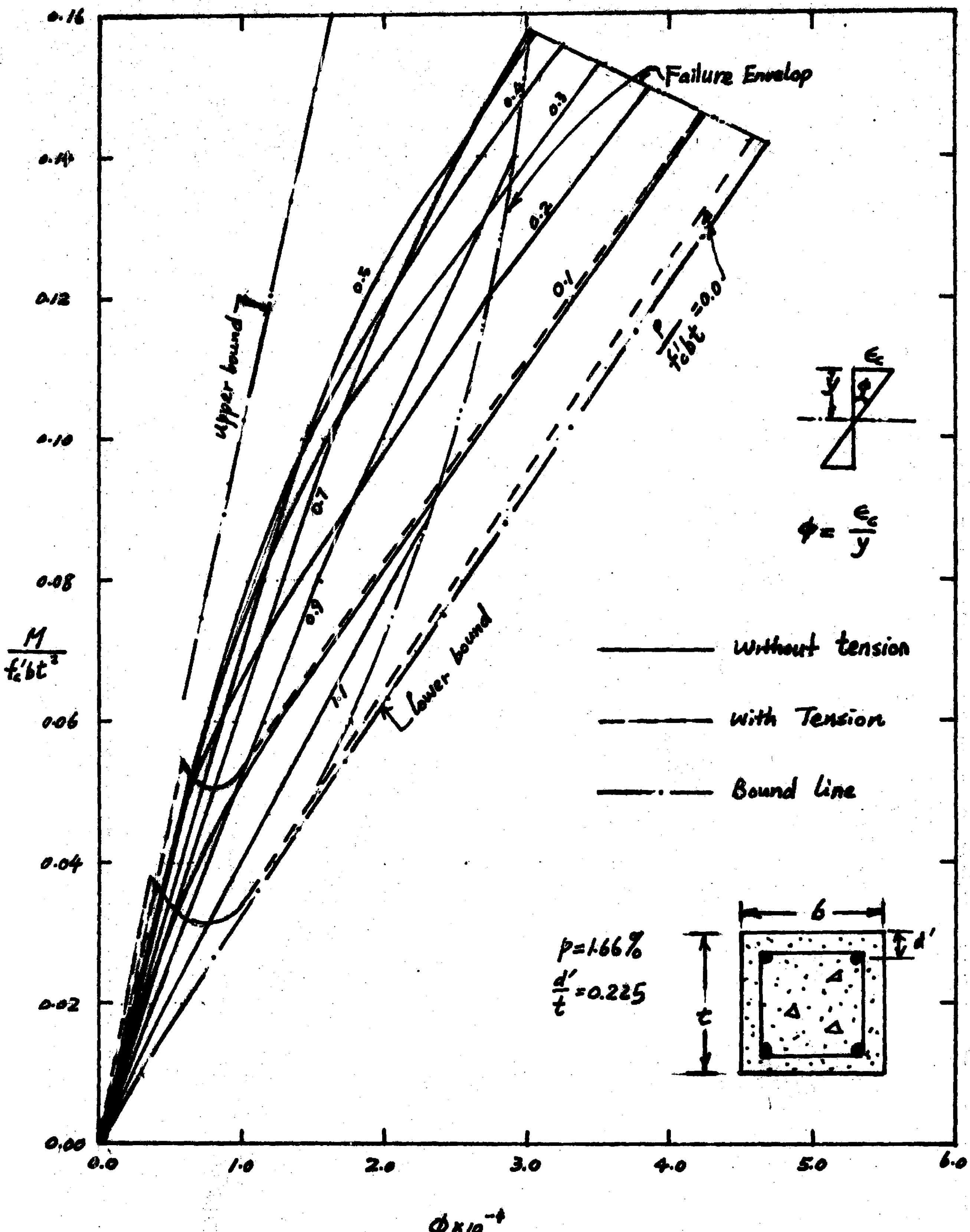

Figure 4.2

Short-term Moment-Curvature Curves

When tension is not included, the initial slope of the curves will be increased by the increase in axial load. Nonetheless, when the curve has reached a slope equal to the slope of the zero-load curve with tension included, further increase in axial load will then decrease the initial slope of the curve in such a manner to approach the zero-load without tension curves.

From the above discussion, it is quite clear that bounds on the moment-curvature curves can be conveniently established by the zero-load curves with and without included tension of concrete. The lower bound is given directly by the zero-load curve without including tension of concrete, while the upper bound is limited by a line drawing from the origin having the same slope as the initial slope of the zero-load with tension curve. The failure envelop serves to terminate the curves from further extension from the origin.

(4.5.b) Axial Load - Curvature Relationships :

The short-term axial load- curvature curves are plotted in Figure 4.3 with different value of constant moment. Tension of concrete is not included here or in subsequent sections unless otherwise specified. The curves are terminated at the failure envelop as determined by the concrete reaching the compression failure strain.

It can be observed that the curvature of the section increases as moment increases at constant load. However, at constant moment, by increasing the applied axial load starting from zero is equivalent to shifting the neutral axis away from the

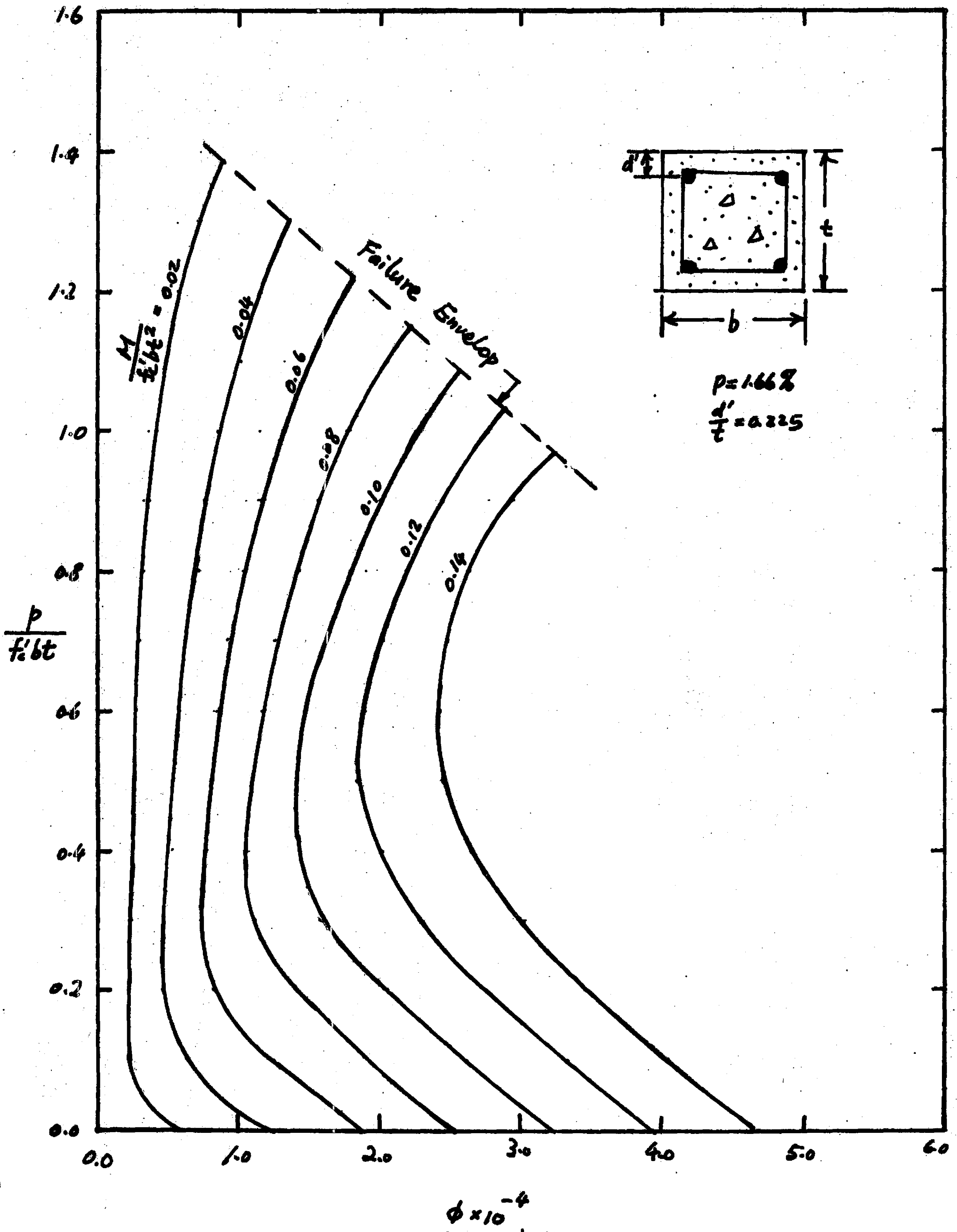

Figure 4.3

Short-term Axial Load - Curvature Curves extreme compressive fibre so that more uncracked section has been provided to resist the applied bending moment. Hence, the curvature is decreased to a critical point at which minimum value of the curvature has been reached. Further increase in axial load beyond that point will cause the curvature to increase . It is also noted that the load at minimum curvature for constant moment increases with increasing moment which also implies that at high moment, the presence of axial load will help to provide more stiffness to the section for cases where length effects are not taken into consideration.

(4.5.c) Load - Axial Strain Curves :

The axial strain is defined as the concrete strain at the centroid of a given cross-section which is subjected to axial force only. Due to the nonlinearity in the stress-strain relationship of concrete coupled with the effect of creep and shrinkage, it is considered that the computation of axial strain should include the effect of bending moment. Therefore, the axial strain is defined by the author as the difference between two components of strain, namely, w_{a1} which is the strain at the centroid of the section subjected to combined bending moment and axial load, and w_{a2} which is the strain at the centroid of the section due to pure bending only. The axial strain, w_{axial}, can then be given as,

$$w_{axial} = w_{a1} - w_{a2} \qquad \ldots (4.7)$$

Figure 4.4 gives the Load-axial strain curves with different level of bending moment.

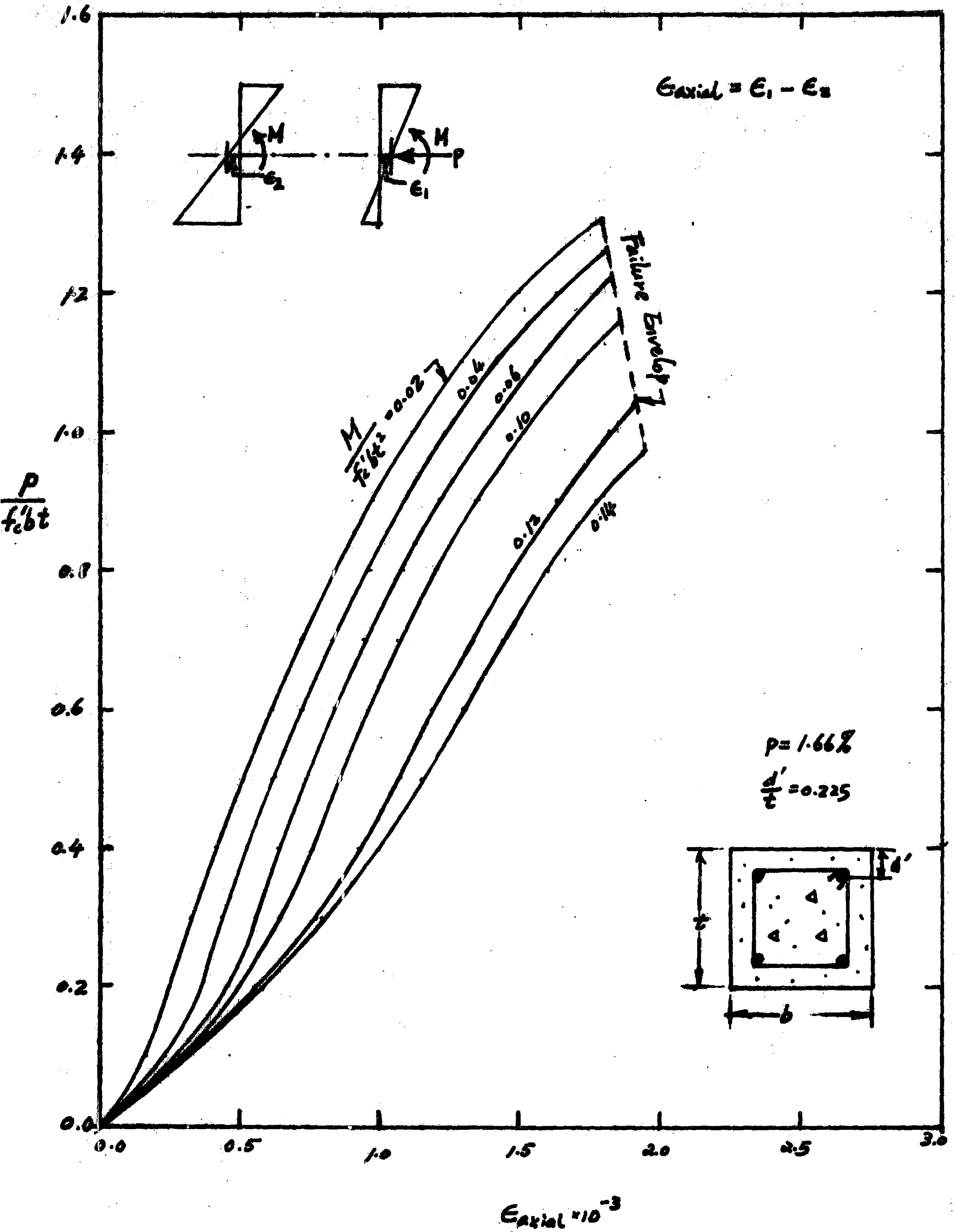

Figure 4.4

Short-term Load - Axial Strain Curves

At constant load, it can be observed that the axial strain increases with the increasing moment. At constant moment, the slope of the curves increases gradually up to a point of inflection and then decreases with increasing load. The physical implication is that at constant moment and low axial load, the axial deformation is decreasedby the increase in the axial load because the presence of axial load produces a compression effect which counteracts the tensile strain resulting from the applied moment. However, at higher load above the point of inflection, the higher stresses in the section for a known constant moment start to override the effect of bending moment and hence cause the axial strain to increase with increasing load.

(4.6) Short-term Stiffness Properties :

This section describes the stiffness properties of a cross-section of concrete subjected to applied axial load and bending moment. The flexural stiffness EI is defined as the secant modulus of the moment-curvature curve , or,

$$EI = \frac{M}{\phi} \qquad \ldots (4.8)$$

The axial stiffness EA is defined as the secant modulus of the load-axial strain curve, or

$$EA = \frac{P}{w_{axial}} \qquad \ldots (4.9)$$

where P and M are the applied axial load and bending moment and ϕ is the curvature of section.

(4.6.a) Flexural Stiffness-Moment-Axial Load Curves :

The short-term flexural stiffness-moment curves with different value of axial load are plotted in Figure 4.5 and the flexural stiffness-axial load curves with different value of constant moment are plotted in Figure 4.6. The stiffness for cracked transformed section of concrete, $E_c I_c$ is the product of the modulus of elasticity of concrete by the moment of inertia of the cracked transformed section of concrete. The EI value given by the new ACI 318-71 for the recommended Moment Magnifier method for design of slender column has also been included in the graphs. The formula used by the Moment Magnifier method (37) is given as,

$$EI = \frac{E_c I_g}{2.5\ (1 + R_m)} \qquad \ldots (4.10)$$

where,

$$E_c = 33\ (W)^{1.5}(\ f'_c)^{1/2}$$

I_g = moment of inertia of gross-section of concrete

R_m = ratio of dead load moment to total moment

The bounds for the moment magnifier method have been given by the lines $R_m = 0$ and $R_m = 1$.

From Figure 4.5 and Figure 4.6, it can be noted that the short-term EI is decreased by the increase in moment which also means that at high moment, the stiffness is reduced by the cracking of the concrete section. At low moment, the difference between the theorectical EI and the $E_c I_c$ can be as high as 70 % but is reduced by the increasing moment. Nevertheless, at high moment and low load, the theorectical EI can be 40 % less than $E_c I_c$ which also indicates

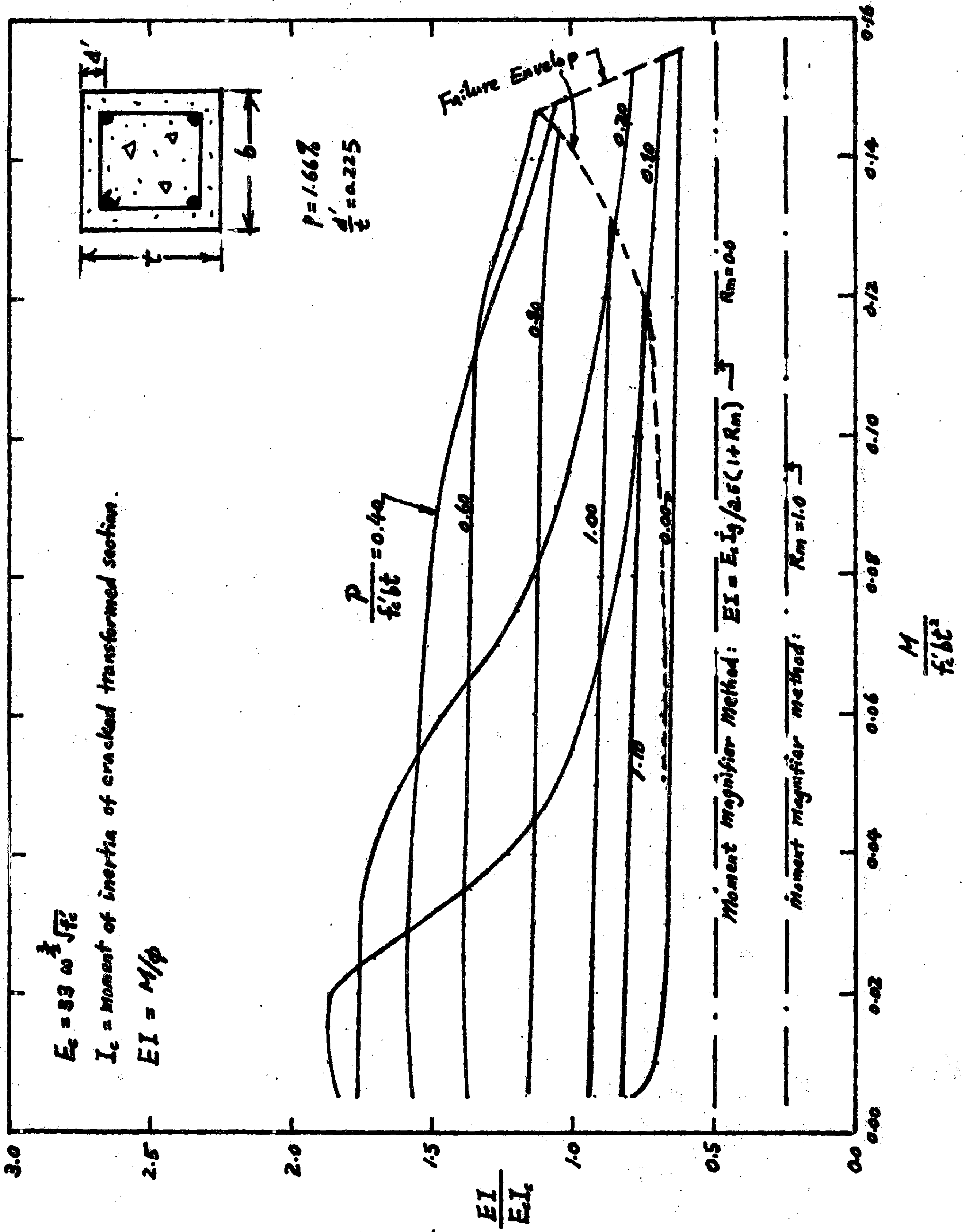

Figure 4.5

Short-term Flexural Stiffness - Moment Curves

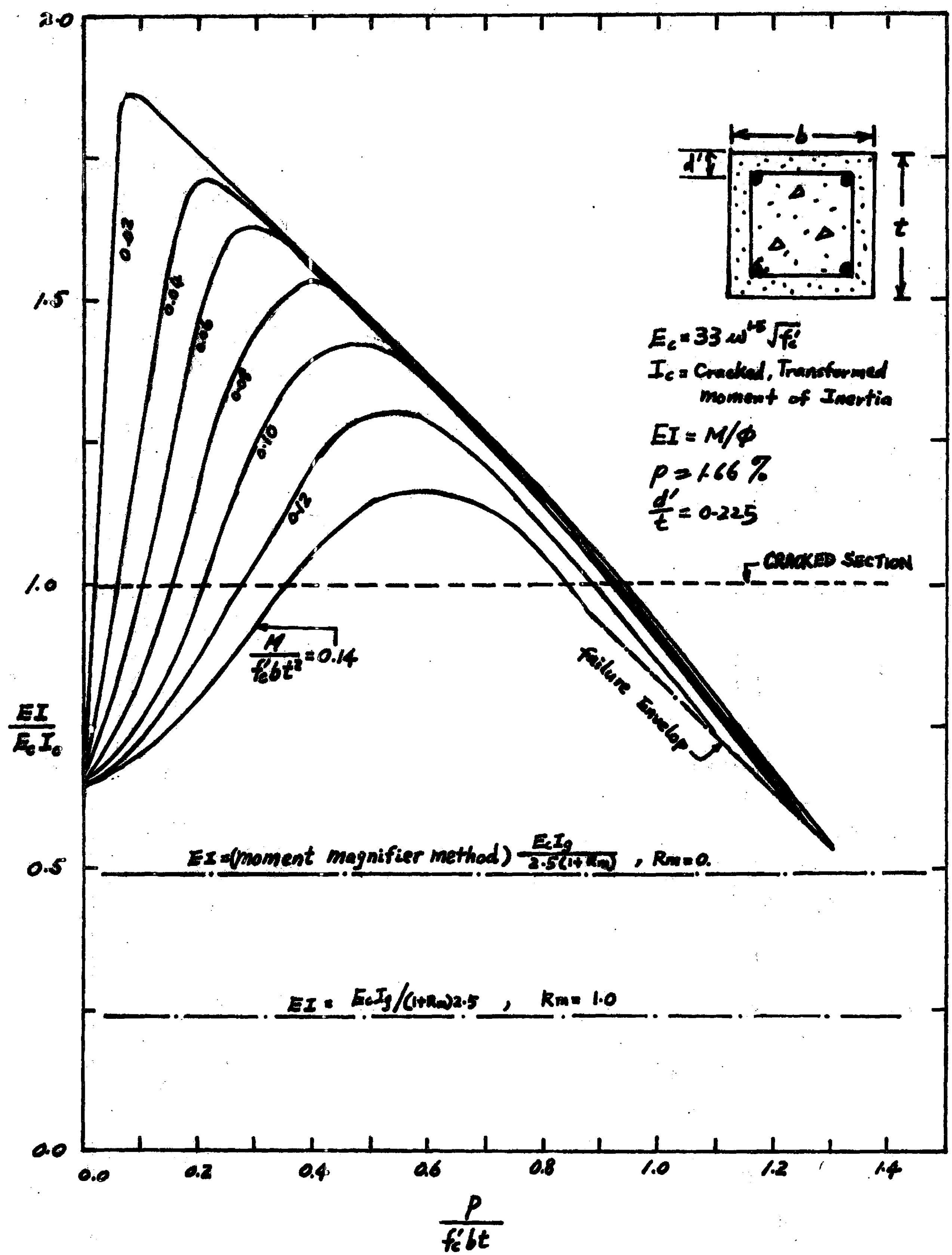

Figure 4.6

Short-term Flexural Stiffness - Axial Load Curves that using the stiffness for a cracked transformed section in analysing inelastic concrete structures may underestimate the deflection under short-term loading. For the section analysed, the EI proposed by the Moment Magnifier method underestimates the theorectical short-term flexural stiffness of the cross-section and is about 50% less than the stiffness for the cracked transformed section of concrete.

(4.6.b) Axial Stiffness-Load-Moment Curves :

The contours of short-term axial stiffness-load curves with different value of constant bending moment are plotted in Figure 4.7. The axial stiffness for an uncracked section $E_c bt$, is the product of the modulus of elasticity of concrete by the gross section area of the section, and is shown in Figure 4.7 as a dotted-solid line.

At zero moment, where the section is subjected to axial force only, the axial stiffness decreases as the axial load increases. However, this possiblity has been ruled out in the design of concrete column sections since the 1963 ACI Code (2) required that a minimum eccentricity should be considered in cases where the applied moment is zero. Therefore, generally, the axial stiffness at low load, for instance, at 5 % of $f'_c bt$, is confined to a range of 35 % to 50 % of $E_c bt$ but increases with the applied axial load at different values of constant moment. However, the increase in EA with axial force stops at a maxima, corresponding to the point of inflection discussed in section 4.5.c for the load-axial strain curves, after which EA is decreased by the increasing axial force.

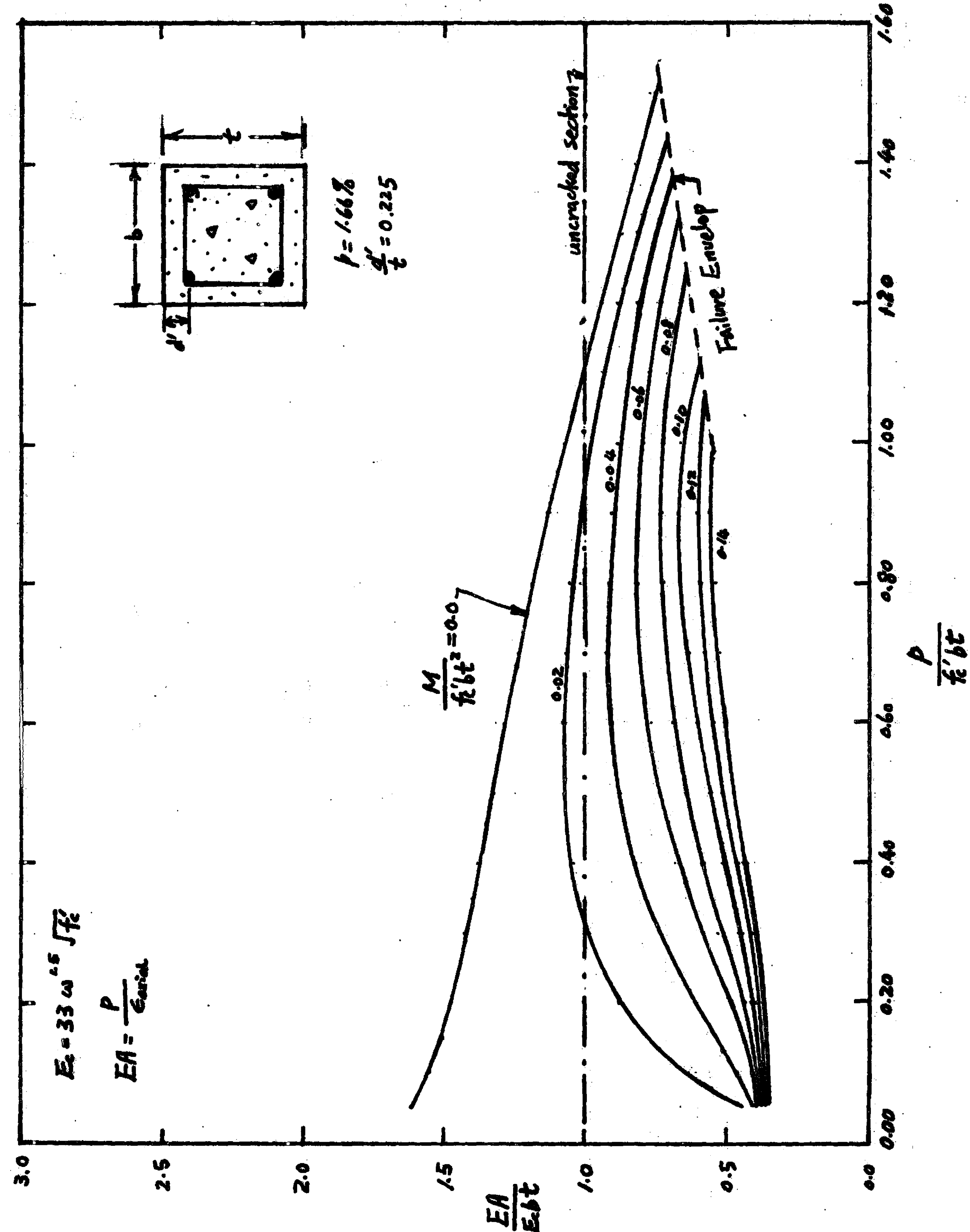

Figure 4.7

Short-term Axial Stiffness-Load Curves

At constant axial load, the axial stiffness decreases as the moment increases which also implies that the presence of bending moment will increase the axial deformation of a member in a structure. For most cases, the uncracked stiffness overestimates the theore tical EA which implies that the axial displacement will be underestimated by using $E_c bt$ for axial stiffness. For the working stress region the main reason is due to the fact that the section will crack under loads which will subsequently reduce the effective area of the section to resist applied load and bending moment.

(4.6.c) Unit Slenderness-Moment-Load Curves :

When the length effects of a member are taken in account, the radius of gyration, r, of the section plays an important role in defining the slenderness of the member. The radius of gyration is given by,

$$r = \left(\frac{I}{A} \right)^{1/2}$$

Due to cracking of the concrete section, the moment of inertia I, and the area of the section A, are not constant for a section subjected to applied load and moment. Hence it is not possible to define an axact I and A for a section under varying loads. However, this difficulty may be overcome by defining the EI and EA values discussed previously. Therefore, the radius of gyration can be determined by the square root of the ratio of EI to EA. Hence, a characteristic measure of slenderness has been defined as the Unit Slenderness as follow:

$$\frac{t}{r} = t \left(\frac{EA}{EI} \right)^{1/2} \quad \ldots (4.11)$$

The unit slenderness-moment relationships with different values of constant load are plotted in Figure 4.8 and the unit slenderness-axial load curves with varying levels of constant moment are given in Figure 4.9. The radius of gyration recommended by the 1963 and 1971 ACI Code is also drawn in the graphs as the alternate dot-dash line for rectangular sections.

From the graphs, the unit slenderness at low moment and under constant applied axial force tends to decrease with increasing moment until a minimum value of t/r is reached after which the curve increases with increasing moment and finally terminates at the failure envelop shown as dashed line in the diagram. Physically, at constant load and low moment, the presence of axial force tends to stiffen the section and therefore reduce the slenderness effect on the cross-section. At higher moments above the minimum value of t/r , the section starts to crack which reduces the effective area of the cross-section contributing to the evaluation of radius of gyration. Hence the radius of gyration begins to decrease with increasing moment. The minima of unit slenderness tends to shift to higher moments as load increases because the higher the axial load, the larger the moment required to crack the section or to decrease the radius of gyration of the section.

From a practical point of view, the unit slenderness seems to give a measure of the degree of cracking or the cracking profile of the section. By comparison with the ACI recommended value of t/r, it indicates that the code may underestimate the radius of gyration of a section subjected to short term loading.

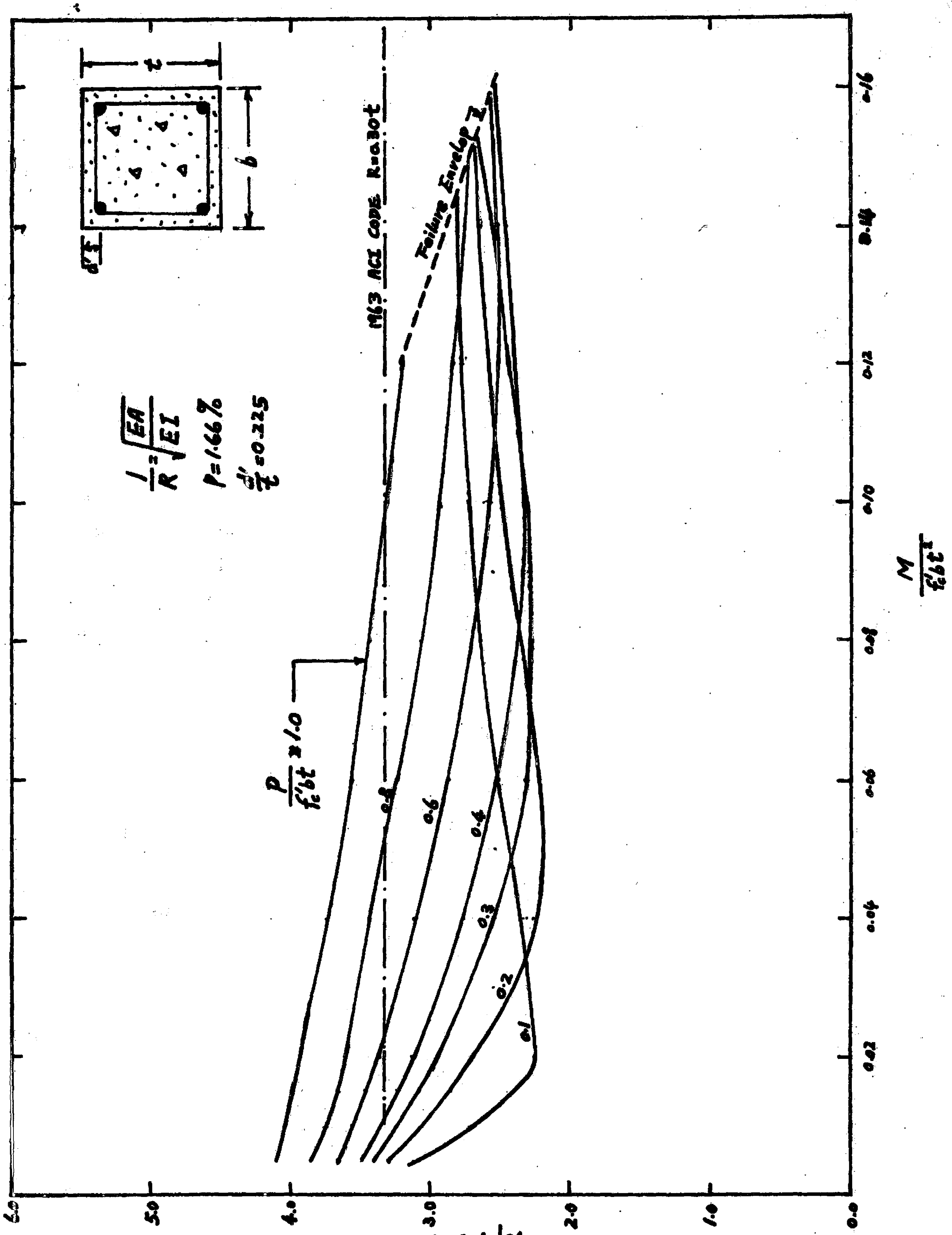

Figure 4.8

Short-term Unit Slenderness - Moment Curves

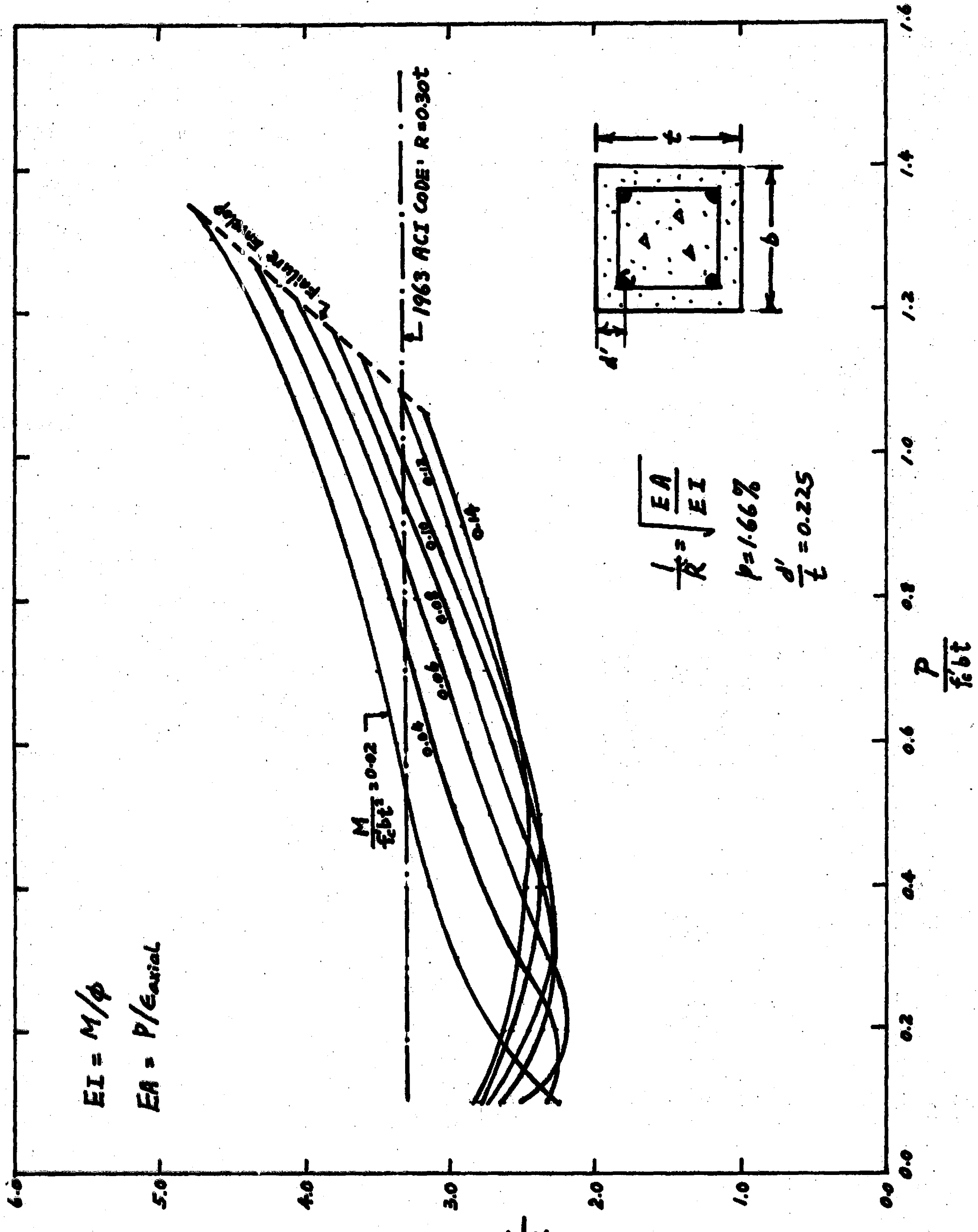

Figure 4.9

Short-term Unit Slenderness - Axial Load Curves

(4.7) Long-term Stiffness Properties :

The long-term stiffness properties of a concrete cross-section subjected to constant sustained applied bending moment and axial force are discussed briefly in this section. The modified superposition method for determining creep, which was described in section 3.8, was used to predict creep deformation. Tension and shrinkage of concrete are not included in this analysis. A total time period of two years has been used in the computation of stiffness properties and the time was divided into discrete intervals for convenience of analysis.

(4.7.a) Flexural Stiffness - Time Relationships :

The long-term flexural stiffness-time curves with different values of applied moment and axial force are plotted in Figure 4.10 and Figure 4.11. The value of flexural stiffness for the cracked transformed section of concrete and for the proposed Moment Magnifier method are also drawn in the graphs.

It is interesting to note that the flexural stiffnesses converge to a near constant value as time elapses. In addition , no matter how the load and bending moment vary, the EI for the sustained loading condition tends to be limited by the bounds imposed by the ACI moment magnifier method. The cracked transformed section of concrete gives a flexural stiffness which overestimates the theorectical EI values by more than 100 %.

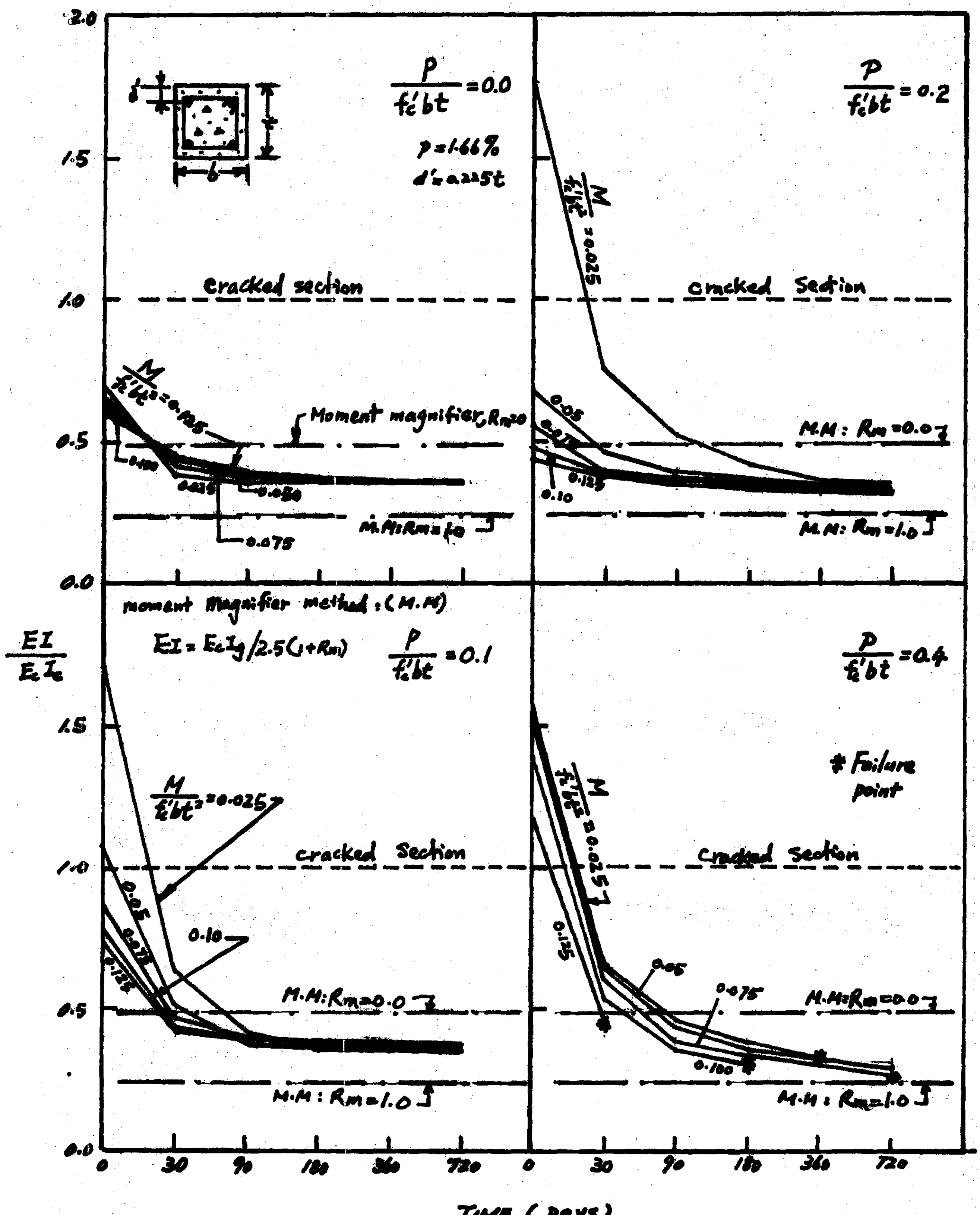

Figure 4.10
Long-term Flexural Stiffness-Time Curves

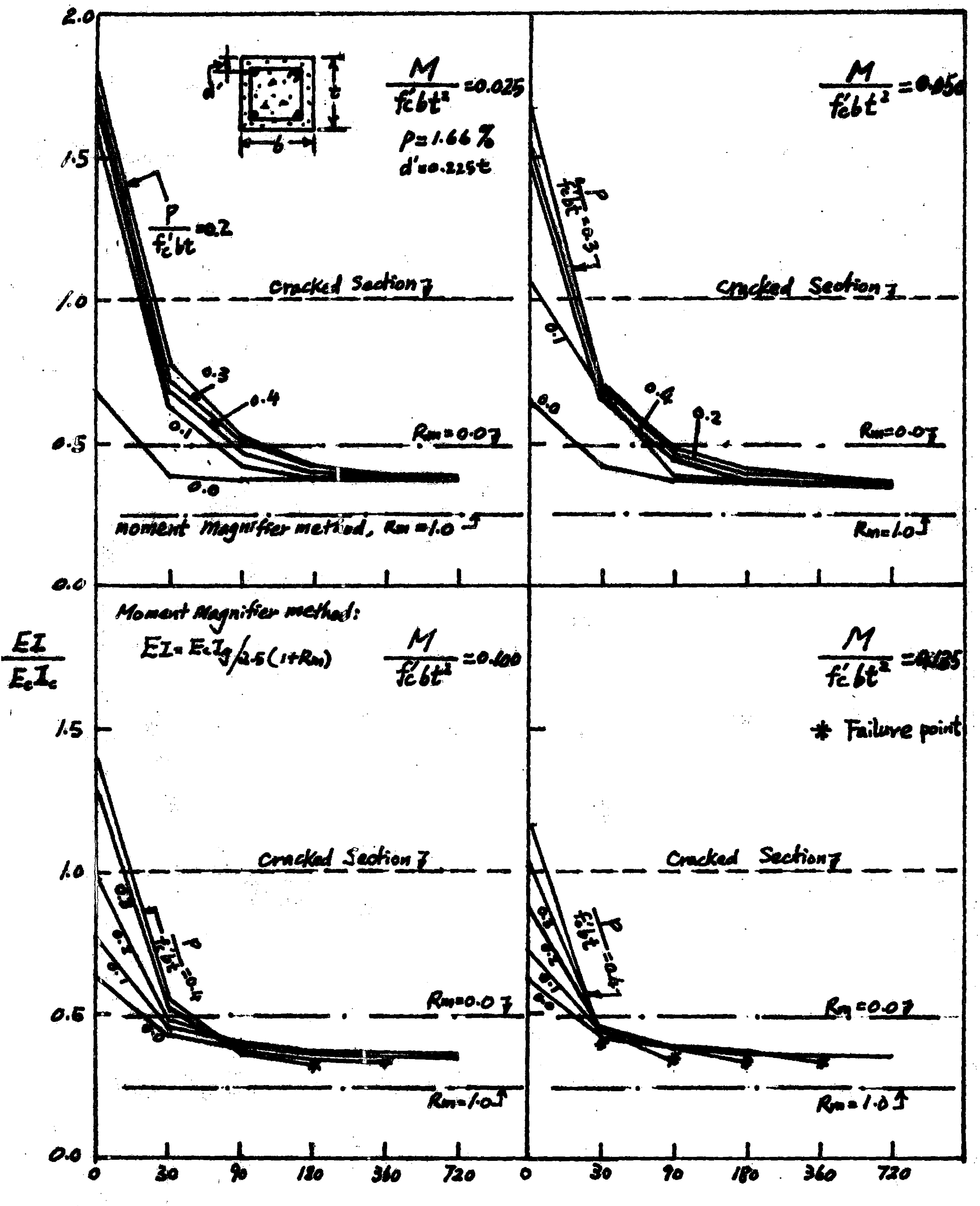

Figure 4.11

Long-term Flexural Stiffness-Time Curves

(4.7.b) Axial Stiffness - Time Curves :

The sustained-load axial stiffness-time curves with different values of constant axial load and bending moment are shown in Figures 4.12 and 4.13 . The axial stiffness has also shown the tendency to converge to a constant value in the course of time regardless of the combination of load and bending moment in the section. The theorectical values of EA are only 30 % of the uncracked axial stiffness, $E_c bt$.

It is now quite apparent that an appropriate expression for the axial stiffness of a concrete section can be derived by refering too the graphs. Hence, the author recommends the following EA value according to Figure 4.12 and Figure 4.13,

$$EA = \frac{E_c A_g}{C(1 + Rm)} \qquad \ldots (4.12)$$

where,

A_g = gross-section area of concrete section

E_c = $33\ (W)^{1.5}\ (\ f'_c\ )^{1/2}$

Rm = Ratio of dead load moment to total moment

C = 2.5 to 3.0

The Equation for EA is similar to the EI value proposed by the Moment Magnifier method which is given in Equation 4.10, and the bounds for $R_m = 0$ and $R_m = 1$ for Equation 4.12 are drawn as shown in Figures 4.12 and 4.13.

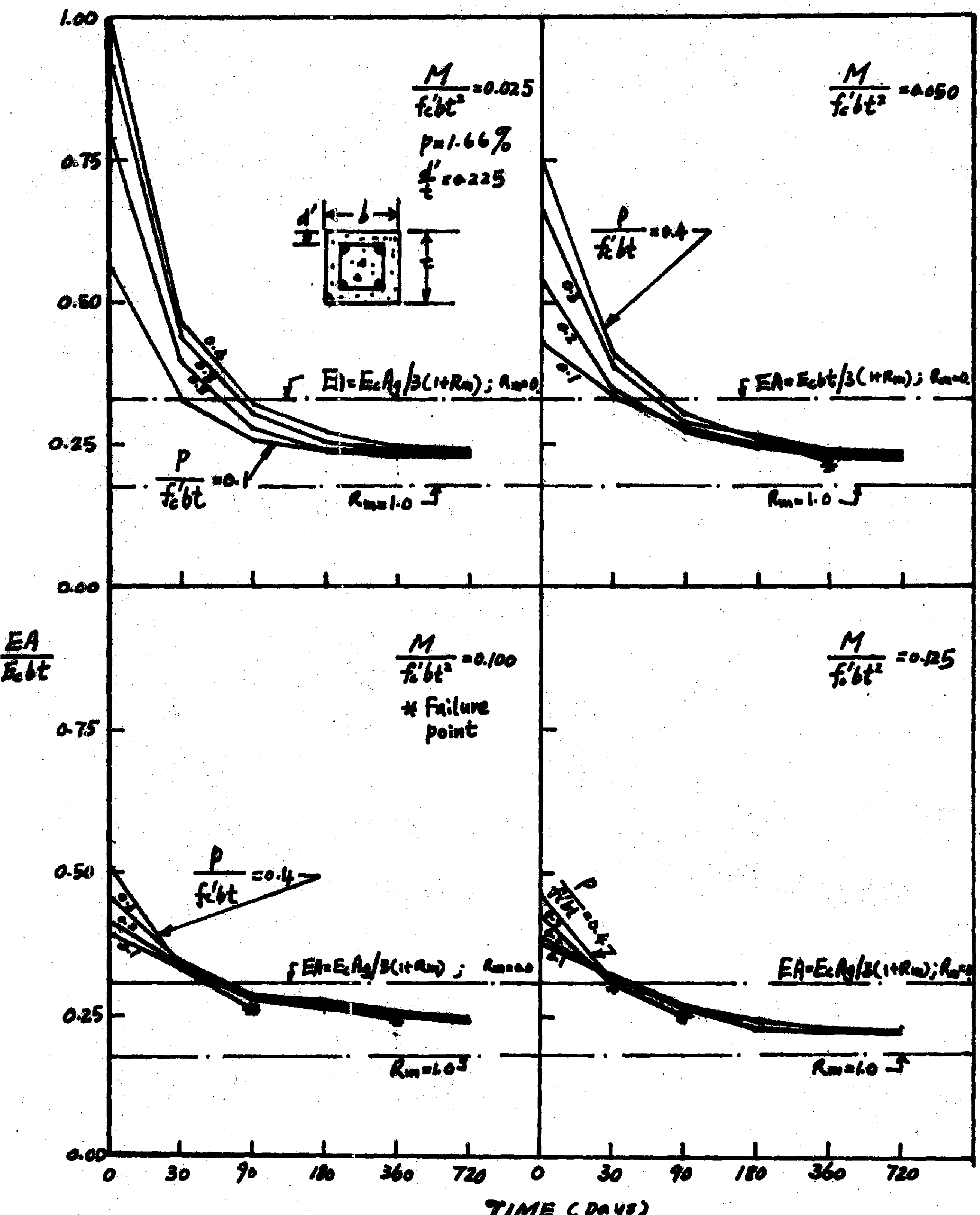

Figure 4.12

Long-term Axial Stiffness - Time Curves

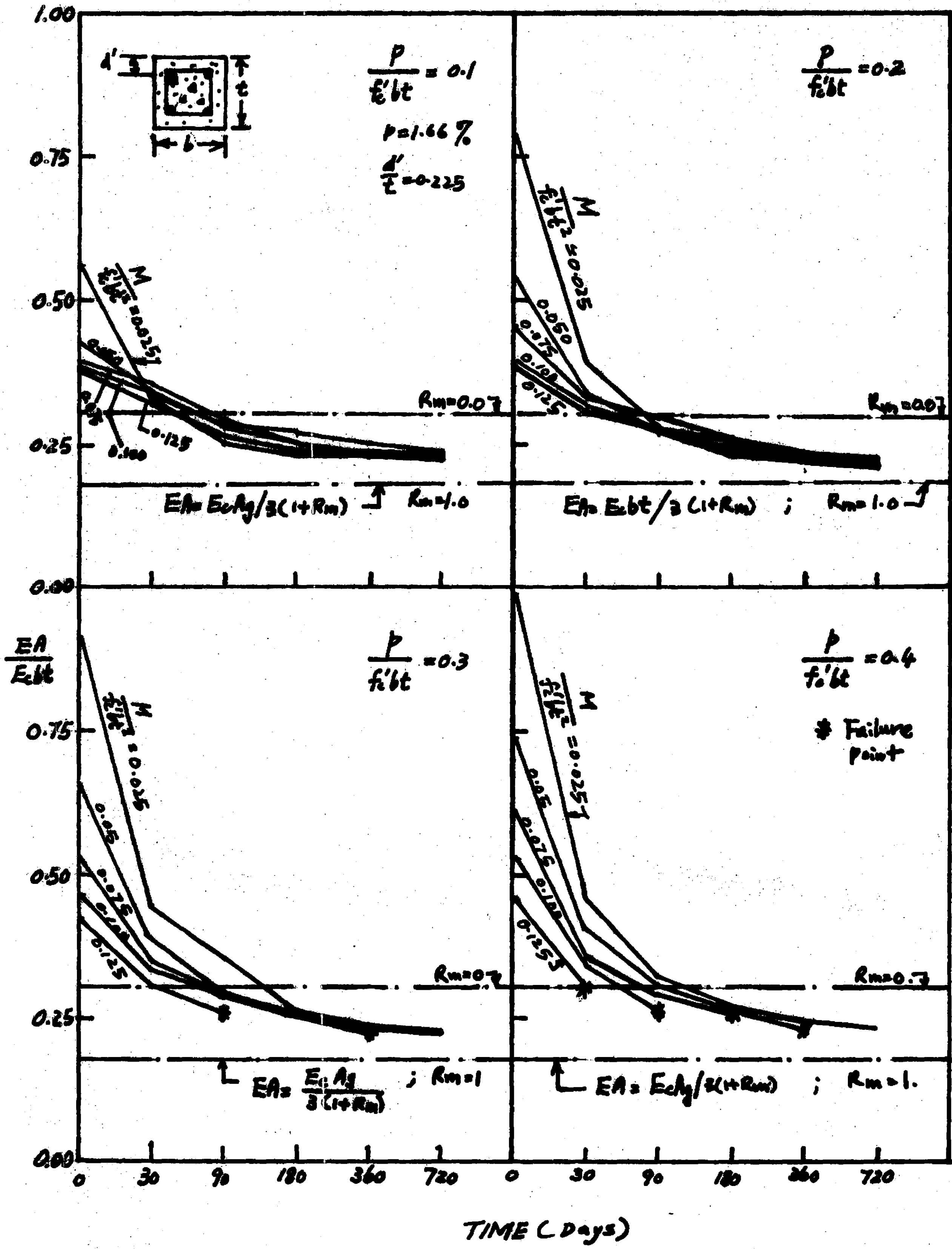

Figure 4.13

Long-term Axial Stiffness - Time Curves

(4.8) Summary :

The various short-term and sustained load deformation characteristics and stiffness properties for a typical concrete cross-section have been studied. The following conclusion can then be drawn:

(1) For short-term analysis, the cracked transformed section does not give an adequate estimate of the flexural stiffness and will in most cases overestimate the actual EI of the section.

(2) The EI value recommended by the ACI Moment Magnifier method underestimates the short-term theorectical EI but provides accurate bounds for the long term theorectical flexural stiffness.

(3) The axial stiffness EA for an uncracked section usually overestimates the theorectical EA value in a section. A recommended value for EA has been given in Equation 4.12.

(4) The radius of gyration recommended by the ACI code may either underestimate or overestimate the actual radius of gyration of a section subjected to short-term loading.

Chapter 5

MATRIX STIFFNESS-MODIFICATION TECHNIQUE

(5.1) Introduction :

This chapter presents a matrix stiffness modification method for nonlinear analysis of concrete structures. Reference is made to a computer program which was developed to incorporate the above analytical technique for predicting behavior of concrete frames subjected to short-term and sustained loading. Convergence of the iterative method of stiffness modification is discussed.

As an indication of the ability of this method to predict non-linear behavior, the deflection data for short-term test frame FR1 are compared to the analytic results. The description of the computer program is included in this chapter. A copy of the program is also presented in Appendix A.

(5.2) Concept of Stiffness Modification and its Limitation :

It has been discussed in section 1.2 that for a structure subjected to given applied loads, an equivalent set of stiffnesses for the whole structure may be obtainable if an appropriate modification process has been devised. The equivalent stiffnesses EI and EA for an element of a structure can be derived from the characteristic curves for moment-curvature and load - axial strain relationships as described in Chapter 4.

If an estimated set of equivalent stiffness is arbitrarily assumed for each element of a structure subjected to a particular type of loading, the compatible strain distribution for equilibrium of external and internal load can be used to recalculate the estimated equivalent stiffness in an iterative sequence until the change in the stiffnesses approaches an acceptable value. This set of equivalent stiffnesses can be used to generate the realistic behavior of structures. Then it is necessary to develop a general computer program incorporating the idea of stiffness modification to acquire the correct set of equivalent stiffness for inelastic analysis of concrete structures.

However, by comparison of a large number of experimental and analytical results, it is concluded that the convergence of the stiffness modification method in predicting the behavior of actual structures is limited by the following criteria:

> "No plastic hinge is allowed to form in the structure under consideration"

By this limitation, the frame is loaded only below the ultimate capacity of any section and thus no plastic hinge is allowed to form anywhere in the structure. Hence, for studies of failure, failure is defined when any part of the structure reaches its ultimate capacity and no account is taken of the redistribution of load which can occur due to plastic deformation. The reason for this limitation is that when plastic hinge has formed in the structure, the hinge will allow an undefined increase in rotation at the hinge without further increase in the moment capacity of the structure under increasing applied loads. Therefore, the stiffness modification procedure cannot insure a definite set of equivalent stiffnesses for the whole structure.

(5.3) Mathematical Model of the Frame :

This section describes the mathematical model of a specified frame and indicates the data required for the computer analysis of the structure.

A mathematical model of the frame is formed by dividing the frame into a number of interconnected discrete elements of member lengths, with the nodal points of each element being selected at points of geometric discontinuity, points under concentrated load and at any suitable points which are considered important in the analysis. Theoretically, a large number of elements can be selected for a given structure. However, within the tolerable limits for accuracy, this selection is limited principally by the storage capacity and the computing time required for the computer. For the CDC 6400 computer used at McMaster University, 26 elements for a single-bay one-storey frame can yield sufficient accuracy (19) in the predicted result.

When the frame has been divided into elements, the following numbering rules should be followed in setting up the model for the structure:

(1) Assign joint numbers and element numbers to all joints and elements.

(2) Loads can be located at nodal points only.

(3) All bases must be assigned number zero.

(4) Those elements which require modification of their stiffnesses are numbered first.

Rules 1, 2, 3 are required for conventional matrix manipulation and can be found in textbooks on matrix structural analysis(36,44). Rule 4 provides the computer with the addresses of the elements which need no modification of their stiffnesses.

As an illustration, Figure 5.1 shows the mathematical model of Frame FR1 for the short-term test. The idealized beam and column line represents the centroid of the actual beam and columns. The frame is divided into 26 elements and 25 joints. All the elements and joints have been numbered successively. In this case all elements require modification of their stiffnesses due to inelastic behavior. The bases have been assigned number zero. Vertical loads are positioned only at nodal joints 19, 22 and 25 respectively.

The mathematical model required the following input to the computer which can be generalized in the following sequence:

> Title of the frame, allowable cycle of iteration for the main program, a conversion factor which converts the unit of length of the coordinate of the mathematical model into inches, total number of joints in the structure, total number of elements , total number of inelastic elements which require modification of their stiffness, number of element strips desired for the element cross-section, allowable number of iteration for the Newton-Raphson method (to be described in section 5.6.c.) , cracking tensile strain for concrete, shrinkage strain of concrete, concrete cylinder strength, steel yield strength, modulus of elasticity of steel, coordinates of each element , location and amount of the tension and compression steel in each

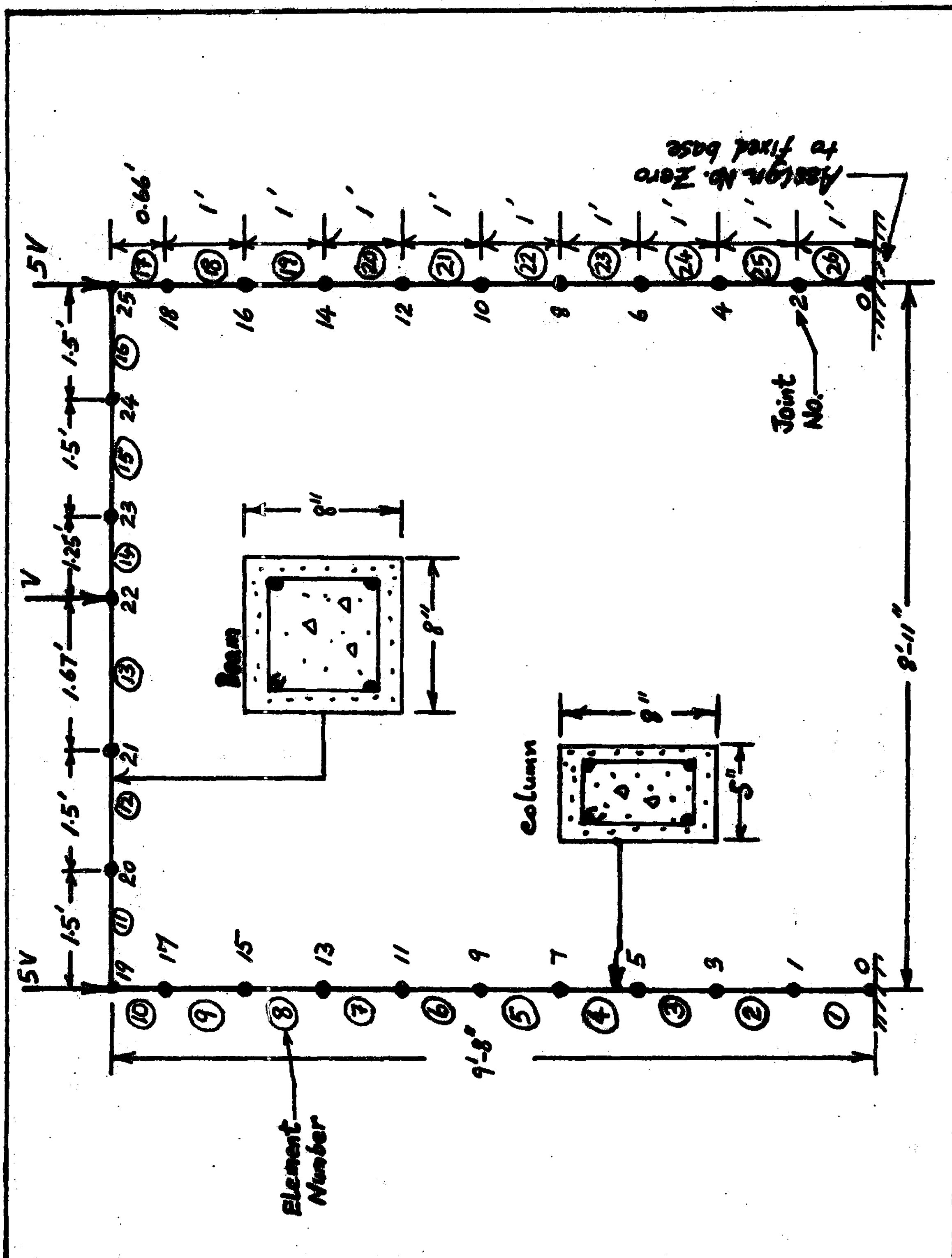

Figure 5.1

Mathematical Model for Frame FR1

element cross-section, the specified loading system, the duration of sustained load desired.

(5.4) The Element Stiffness Matrix :

Before describing the technique of stiffness modification, it is also necessary to understand the reason for modifying the stiffness matrix and identifying where the modification occurs. Hence, in Figure 5.2, the element stiffness matrix for a slender member is formulated in its member coordinates which are the coordinate system whose X-axis coincides with the direction of the centroid of the unloaded element and the Y-axis is orthogonal to the X-axis in the direction of principal bending. The derivation of this element stiffness matrix can be found in textbooks on Matrix method of structural analysis (36,44).

The element stiffness matrix describes the responses of each element subjected to externally applied loads. If the element stiffness matrix for each element of the structure can be formulated, the assembly stiffness matrix for the whole structure can be assembl ed and inverted to obtain the displacement and internal force vectors for the whole structure.

With structures made of elastic materials, such as steel, the element stiffness matrix is readily determined but this is not true for inelastic concrete structures. It has been shown in Chapter 4 that the stiffnesses EI and EA contained in the element stiffness matrix of the structure vary significantly with the degree of cracking of concrete and the level of stress in the concrete.

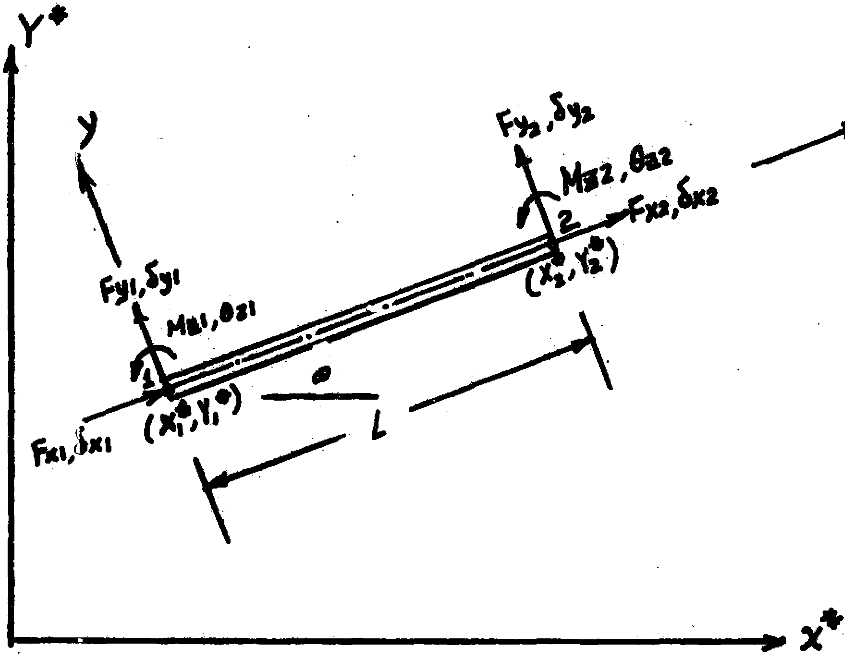

$$
[K] = \left[\begin{array}{ccc|ccc}
\frac{EA}{L} & 0 & 0 & \frac{-EA}{L} & 0 & 0 \\
0 & \frac{12EI}{L^3} & \frac{6EI}{L^2} & 0 & \frac{-12EI}{L^3} & \frac{6EI}{L^2} \\
0 & \frac{6EI}{L^2} & \frac{4EI}{L} & 0 & \frac{-6EI}{L^2} & \frac{2EI}{L} \\
\hline
\frac{-EA}{L} & 0 & 0 & \frac{EA}{L} & 0 & 0 \\
0 & \frac{-12EI}{L^3} & \frac{-6EI}{L^2} & 0 & \frac{12EI}{L^3} & \frac{-6EI}{L^2} \\
0 & \frac{6EI}{L^2} & \frac{2EI}{L} & 0 & \frac{-6EI}{L^2} & \frac{4EI}{L}
\end{array}\right]
$$

Figure 5.2

Element Stiffness Matrix

It is thus not possible to formulate a constant set of stiffnesses EI and EA for a structure subjected to loads which will cause inelastic behavior. However, by incorporating the idea of stiffness-modification proposed in section 5.2, an arbitrarily assumed set of initial stiffnesses EI and EA can be modified to obtain an unique set of equivalent stiffnesses under a specific loading condition. These equivalent stiffnesses are substituted into the element stiffness matrix for each element for subsequent generation of displacement and internal force vectors of the structure.

The stiffness modification process is described in the next section.

(5.5) Matrix Stiffness-Modification Method :

The proposed stiffness modification method as applied to nonlinear analysis of concrete structures is presented in this section. The method implements the concept proposed in section 5.2, and operates the steps in stiffness modification as follows :

(1) From the geometric properties of each element, the cross-section of each element is subdivided into a number of element strips.

(2) The elastic axial stiffness EA and flexural stiffness EI are computed using the following values:

$E_c = 33\ (W)^{1.5}\ (f'_c)^{\frac{1}{2}}$ (W = 145 pcf. for concrete)

A = gross section area of concrete

I = moment of inertia of cracked transformed section

These stiffnesses are substituted into the element stiffness matrix for each element.

(3) With the element stiffness matrix for each element formulated, the assembly stiffness matrix for the whole structure can be assembled and used to determine the displacement and force vectors for the structure.

(4) With the deflected shape of the structure known, the secondary bending moment due to deflection of the members (P-Delta effect) are computed and added to the primary moment acting at the center of the length of each element.

(5) For the known bending moment and axial force acting on a given element cross-section, the Newton-Raphson method is employed to determine the unique strain distribution for each element, thereby permitting the computation of the modified values of EI and EA. For the sustained loading condition, the shrinkage and creep deformation and stress history are included in the unique strain distribution which provide equilibrium of the section.

(6) These new equivalent stiffnesses EI and EA for each element are then compared to the previous stiffnesses, and when the error between them is less than 1 % for each element, the set of modified stiffness is said to have converged to the equivalent stiffnesses for the structure, and the process of iteration is terminated. Otherwise, the new stiffnesses are substituted into the element stiffness matrix for each element and the process in steps 2, 3, and 4 is repeated.

A flow chart showing the execution steps is given in Figure 5.3.

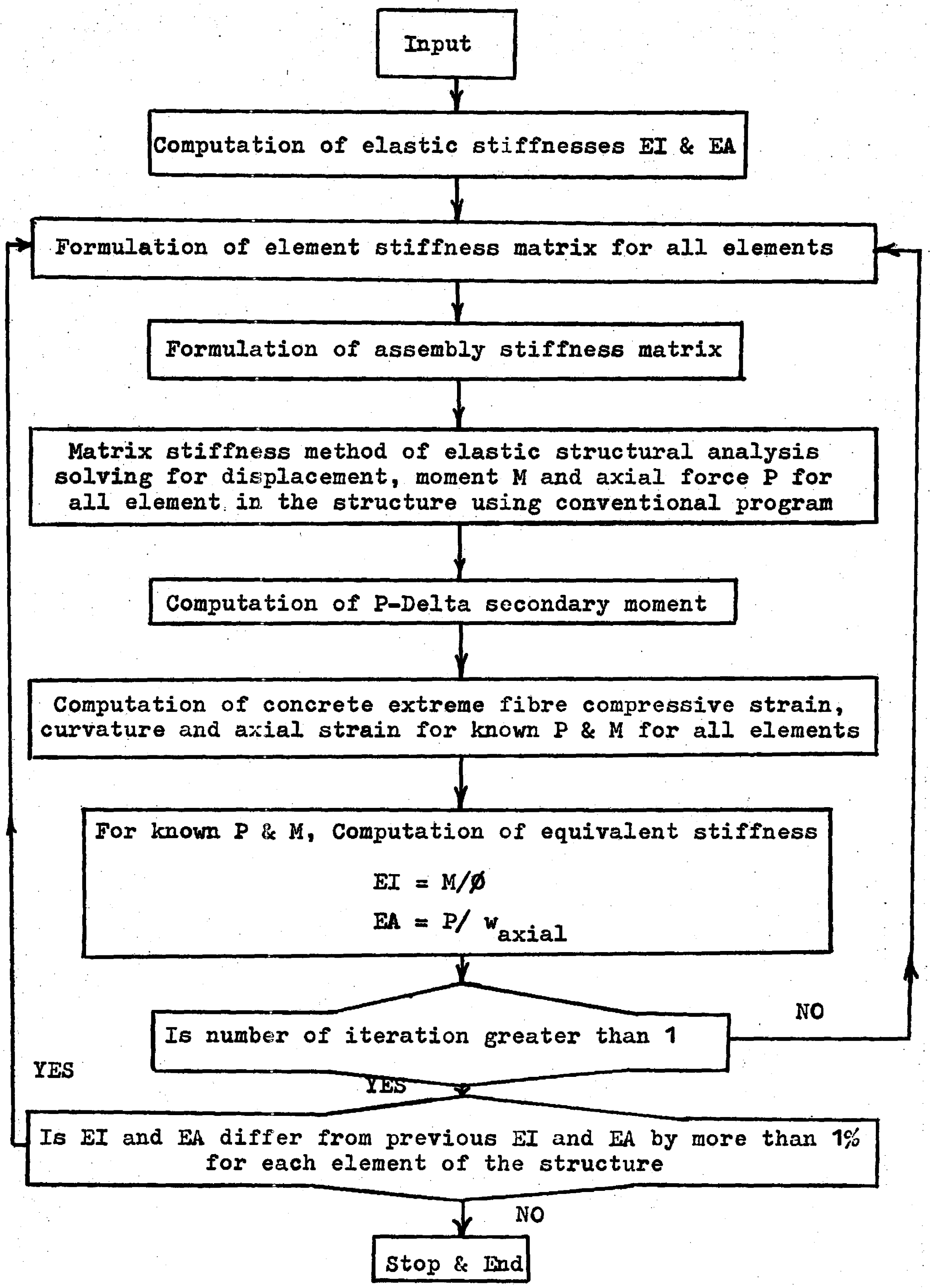

Figure 5.3 : Matrix Stiffness-Modification Method (I), Flowchart

Generally, for loads applied below the ultimate capacity of the structure, the stiffness criteria can be easily satisfied within a few cycle of iteratio (3 to 7 cycles was generally observed). However, for loads near ultimate capacity of the structure, or when creep, shrinkage and stress-history were included, the analysis usually required more cycles of iteration. This was due to the large modification in equivalent stiffnesses required to account for these large inelastic deformations.

(5.6) The Computer Program :

A brief description of the computer program developed for frame analysis using the matrix stiffness modification technique is given in this section.

The program consists of a main program and eight subprograms. In Figure 5.4, a flow chart is drawn to show the location and function of each subprogram.

The procedure for the elastic structural analysis which is performed by the subroutines "ARRANGE", "BALANCE", "ENLARGE", "TRANSF" and "STIFFN" , can be found in textbooks on matrix methods of structural analysis (36,44) and is therefore not discussed in here.

The subroutines "MPHI", "BMPCAL" and "CREEP" were developed for the stiffness modification process and are described in the following sections. In addition, the computation of secondary bending moment is also given in this section.

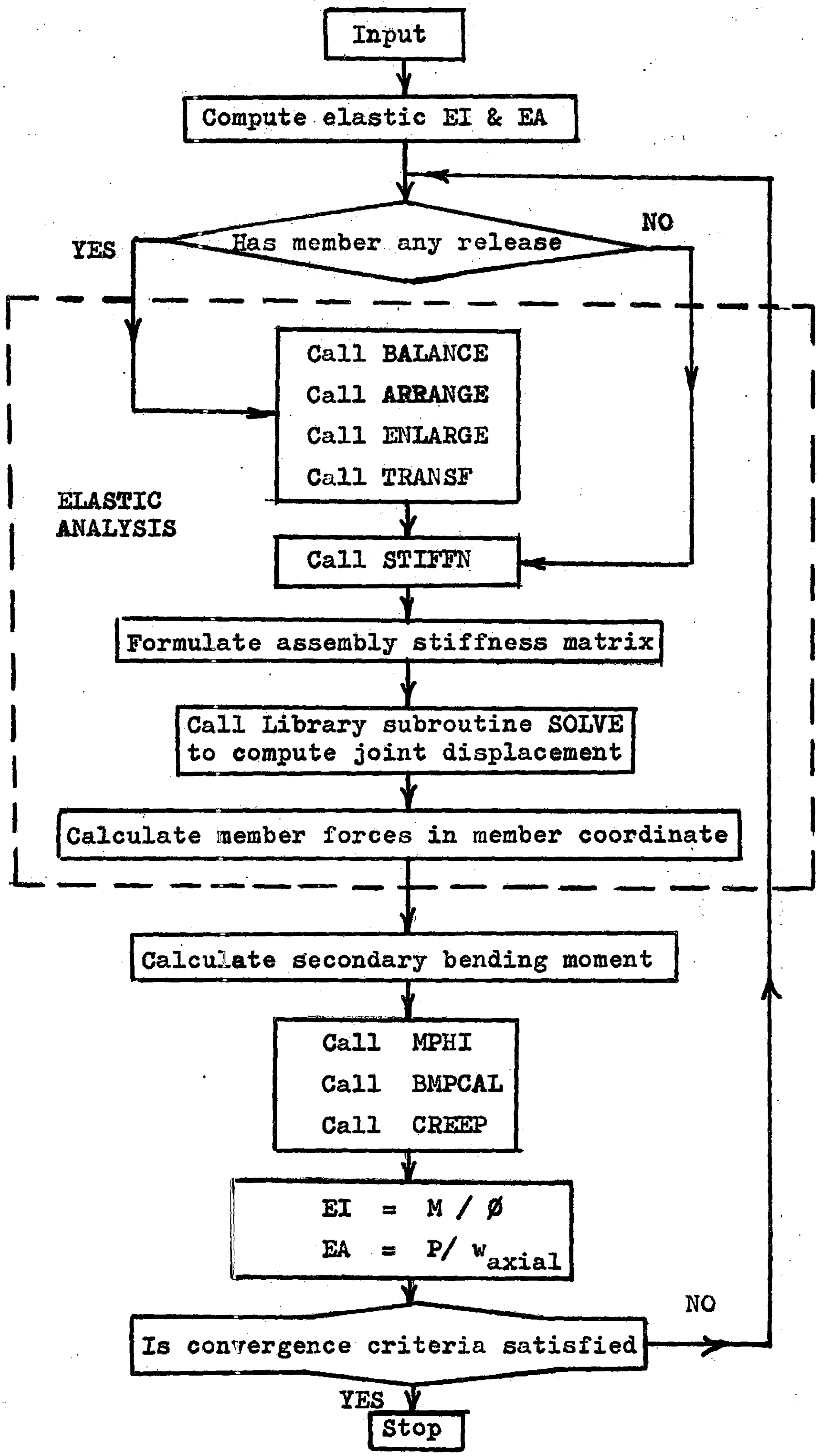

Figure 5.4: Matrix Stiffness-Modification Method (II), Flowchart

(5.6.a) Subroutine "BMPCAL" :

This subroutine operates the numerical integration procedures as described in section 4.2. Its function is to compute the internal force and moment for a concrete cross-section subjected to a given strain distribution. The following sign conventions are used in this subroutine,

(1) Compressive stresses or strains in concrete or steel are positive.

(2) Distances from the neutral axis of the section towards the concrete extreme compressive fibre are positive.

The steps for numerical integration are as follows,

(1) The geometric properties and the number of element strips of a given cross-section are read and transferred from the main program. The depth of the section is thus subdivided into a finite number of element strips and all the elements of the structure are assumed to have the same number of element strips.

(2) A known linear strain distribution from subroutine "MPHI" (to be described later) is transferred. From this linear strain distribution, the neutral axis is computed and the total strain acting at the centroid of each element strip are calculate. Similarly, the strain acting at the level of the steel reinforcement can be determined. The strain in the steel and concrete due to shrinkage are included from data obtained from prism tests.

(3) Where sustained loads are studied, the creep strain and additional shrinkage strain for a specific increment of time are included so that the total strain of concrete is comprised of :

$$w_{total} = w_{elastic} + w_{creep} + w_{shrinkage}$$

where, w = strain in concrete .

Therefore the elastic strain in concrete, or the strain contributing to stress acting on each element strip, is calculated by subtracting the creep and shrinkage strain from the total strain at the centroid of each element strip .

(4) From the stress-strain relationships of the concrete and the steel given in Equations 3.2 and 3.3 respectively, the stress acting at the centroid of each element strip and at the level of the steel are computed and Equation 4.1 is used to calculate the total axial force and bending moment acting at the centroid of the cross-section.

(5.6.b) Subroutine "CREEP" :

For cases where sustained loading is included, this subroutine is called upon to calculate and store the creep strains for a specified increment of time. The modified superposition method as described in section 3.8 is used to compute the creep for variable stress conditions. The computational steps for this routine are summarized as follows,

(1) The additional shrinkage strain in concrete for the specified time increment is computed by Equation 3.4.

(2) The loads and stress levels acting on a concrete cross-section are assumed to remain constant for the specified increments of time. The elastic strain acting at the centroid of each concrete element strip of the section which were computed and stored in subroutine BMPCAL , are then transferred and stored in this subroutine. The creep strains for each concrete element are then computed by the process described in section 3.8 .

(3) For the next time interval, the stresses on the element strips may be different from the previous values. These changes can result from a change in load intensity on the structure or from the redistribution of load caused by changes in stiffnesses associated with the sustained load deformation. The nonlinearity of creep versus stress also could cause a redistribution of stress on a cross-section. Therefore, for a new set of elastic strains after the first time interval, the stress history must be taken into account, and the creep strain due to stress history is calculated by the procedure described in section 3.8.

(4) The total inelastic strain due to time effect is thus given by,

$$w_{total} = w_{creep} + w_{additional\ shrinkage} + w_{stress\ history}$$

This total inelastic strain is transferred to subroutine BMPCAL for the computation of the elastic strain of the concrete.

(5.6.c) Subroutine "MPHI" :

In this subroutine, the Newton-Raphson method as described in section 4.3 is utilized to facilitate convergence on an unique strain distribution for a specified axial force and bending moment combination. The computational procedure is described below:

(1) The applied bending moment and axial force acting at the cross-section which were calculated in the main program are transferred to this subroutine.

(2) For an initially assumed strain distribution, the subroutine BMPCAL is called to calculate the axial force and bending moment corresponding to this assumed strain distribution.

(3) The computed axial force and bending moment are compared to the applied load and moment. The difference is measured by the following ratios,

$$R_1 = \left|\left(\frac{P_{applied} - P_{calculated}}{P_{applied}} \right)\right|$$

$$R_2 = \left|\left(\frac{M_{applied} - M_{calculated}}{M_{applied}} \right)\right|$$

where, if R_1 and R_2 are not greater than 1%, the iteration process is terminated, and the concrete strain and curvature are transferred to the main program for evaluation of equivalent stiffnesses EA and EI. In cases where the applied load P is equal to or near zero, the convergence procedure requires the calculated P be less than 0.01 kip. If the applied M is less than 10 in-kips, it is required that the computed M be less than or equal to 10 in-kips.

(4) If either R_1 or R_2 exceeds the allowable tolerance of 1 %, the convergence process is carried on by incrementing the concrete strain and curvature as follows,

$$\delta w_1 = G w_1 + H$$
$$\delta \phi = G \phi + H$$

where,

$$G = 0.0005$$
$$H = 1.0 \text{x} 10^{-10}$$

These will then generate a new concrete strain and a new curvature as,

$$w_{1\ new} = w_{1\ previous} + \delta w_1$$
$$\phi_{new} = \phi_{previous} + \delta \phi$$

To find the terms $\partial P/\partial w_1$, $\partial P/\partial \phi$, $\partial M/\partial w_1$, $\partial M/\partial \phi$ required for Equation 4.5, it is necessary to call the subroutine BMPCAL twice. Firstly, the curvature remaining constant and the new concrete strain $w_{1\ new}$ is substituted, a new set of P and M values which are due to the increment of w_1 only will be calculated. Therefore,

$$\frac{\partial M}{\partial w_1} = \left(\frac{M_{new} - M_{previous}}{w_{1\ new} - w_{1\ previous}} \right) \qquad \phi = \text{constant}$$

$$\frac{\partial P}{\partial w_1} = \left(\frac{P_{new} - P_{previous}}{w_{1\ new} - w_{1\ previous}} \right) \qquad \phi = \text{constant}$$

Secondly, by calling the subroutine BMPCAL, with the concrete strain remaining constant,the new curvature ϕ_{new} is substituted, and the remaining terms for Equation 4.5 are calculated as shown below ,

$$\frac{\partial P}{\partial \phi} = \left(\frac{P_{new} - P_{previous}}{\phi_{new} - \phi_{previous}} \right) \qquad w_1 = \text{constant}$$

$$\frac{\partial M}{\partial \phi} = \left(\frac{M_{new} - M_{previous}}{\phi_{new} \quad \phi_{previous}} \right) \qquad w_1 = \text{constant}$$

These values are then substituted into Equation 4.5 which is inverted to calculate the increment values of concrete strain and curvature dw_1 and $d\phi$. The new concrete strain and curvature are now given by,

$$w^*_{1\ new} = w_{1\ previous} + dw_1$$

$$\phi^*_{\ new} = \phi_{\ previous} + d\phi$$

These new values are used to compute a new set of axial force P and bending moment M, and the process in steps 2,3 is repeated.

(5.6.d) <u>Computation of Secondary Bending Moment</u> :

The computation of P-Delta secondary bending moment which is the effect of axial load multiplied by the additional eccentricity due to deflection, is performed in the main program. The matrix analysis generates a displacement vector for each element in the member coordinate system for the element, and then transforms this displacement vector into global coordinates which is the coordinate system for the whole structure. Hence in member coordinates the deflection in the X-direction indicates the longitudinal shortening or elongation of the element. Displacement in the Y-direction thus shows the amount of lateral deflection from the original undeflected position. Therefore, the secondary moment or P-Delta moment is computed by multiplying the axial force acting at the element centroid by the Y-direction deflection from the undeflected position of the element.

(5.7) Illustration :

To illustrate the convergence procedure for the matrix stiffness modification technique used in the analysis, the test results from the large scale frame FR1 under short-term loading are compared to the analytical prediction during the iterative process . As shown in Figure 5.5, the ratio of the predicted deflection to the measured deflection is plotted against the number of iterative cycles of stiffness modification. The predicted deflection in the first cycle of iteration differs quite significantly from the test result. However, after 3 cycles of iteration, the convergence is apparent. Considering possibility of experimental error and some simplifying assumptions, convergence has been obtained after 5 to 10 iterations.

(5.8) Summary :

In this Chapter, a detail description of the computer program for the matrix stiffness-modification method has been present. By comparison of the short-term test results of Frame FR1 with the

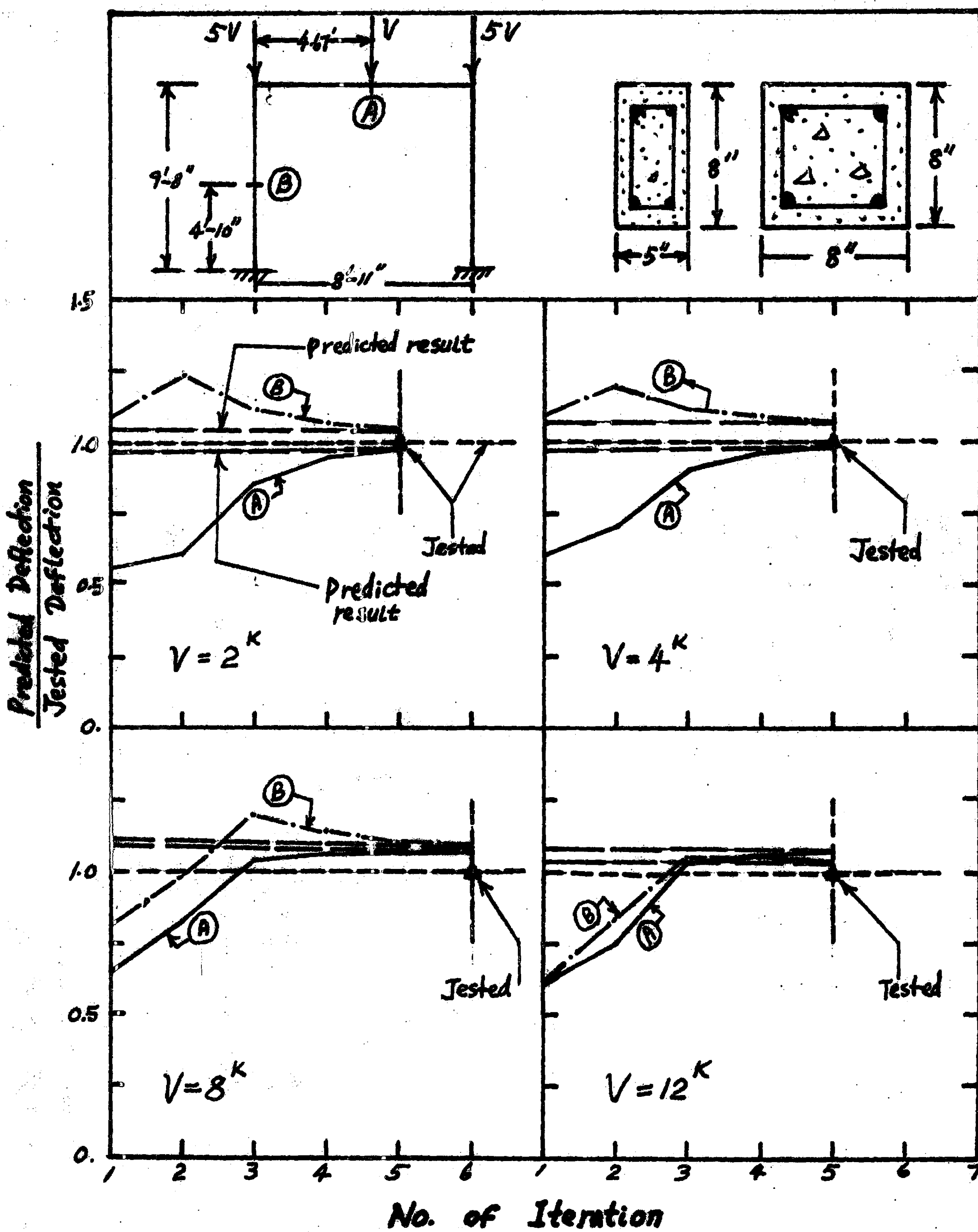

Figure 5.5

Illustration of Convergence

predicted values as well as the results in Chapter 6, it can be observed that the stiffness modification procedure is an effective method for analysing inelastic concrete structures. The accuracy of the method will be discussed in Chapter 6.

Chapter 6

COMPARISON OF ANALYTICAL AND EXPERIMENTAL RESULTS

(6.1) Introduction :

This chapter presents an extensive evaluation of the applicability of the proposed matrix stiffness modification method by comparison of the analytical results with the measured results of several reinforced concrete frames tested at McMaster University (19,52), McGill University (4,51) and the Cement & Concrete Association (17). In all cases, deflection was used as the main basis for comparison because it is directly measurable and is least susceptible to experimental error and analytical misinterpretation as compared to those measurable quantities such as strain, slope, rotation and crack width. However, in a few cases, the comparison of analytical and experimentally derived bending moment are included to add evidence for the applicability of the proposed analysis. A word of caution is that the experimental bending moment is derived from measured strain reading from which the numerical integration procedure as described in section 4.2 is used to obtain the moment . Therefore, the term "experimental bending moment" is really a combination of experimental strain reading and analytical interpretation.

In addition, an elastic analysis using the same mathematical model of frames as used for the nonlinear analysis, was developed to compute the elastic response of the frames. The stiffnesses were based on a cracked transformed section of concrete. This elastic method through use of small elements takes into account the distribution and amount of reinforcement in the frames.

(6.2) Short-term Test Results :

In this section, the comparison of the analytical and measured results of a total of 24 frames tested by the author and by others (4,17,19,51,52) has been reported. The dimension of the frames and the initial purpose of the tests are briefly introduced.

(6.2.a) Tan's Frames :

The measured deflections of Frame FR1 under short-term proportional loading, were compared to the analytical prediction as shown in Figure 6.1. The load-deflection data for three critical points on the frame were plotted. The fabrication and testing of this frame has been described in detail in Chapter 2. Refering to the figure, it can be concluded that excellent agreement has been observed between the modified stiffness analysis and the test results for three points compared . Except for point C, the analytical prediction slightly overestimates the tested deflection at high loads. The elastic solution which is also shown underestimates significantly the vertical deflection at point A and C. This has added evidence for the inaccuracy of the elastic analysis in predicting behavior of real structures.

In Figure 6.2, the predicted concrete strain distributions are compared to the measured values for points B and E. Close agreement between analytical and measured results is evident.

Figure 6.3 shows the comparison of deflection for Frames FG1 and FG2 tested by Mr. Golec, an undergraduate student , during the summer of 1970. The dimension and cross-section of these frames

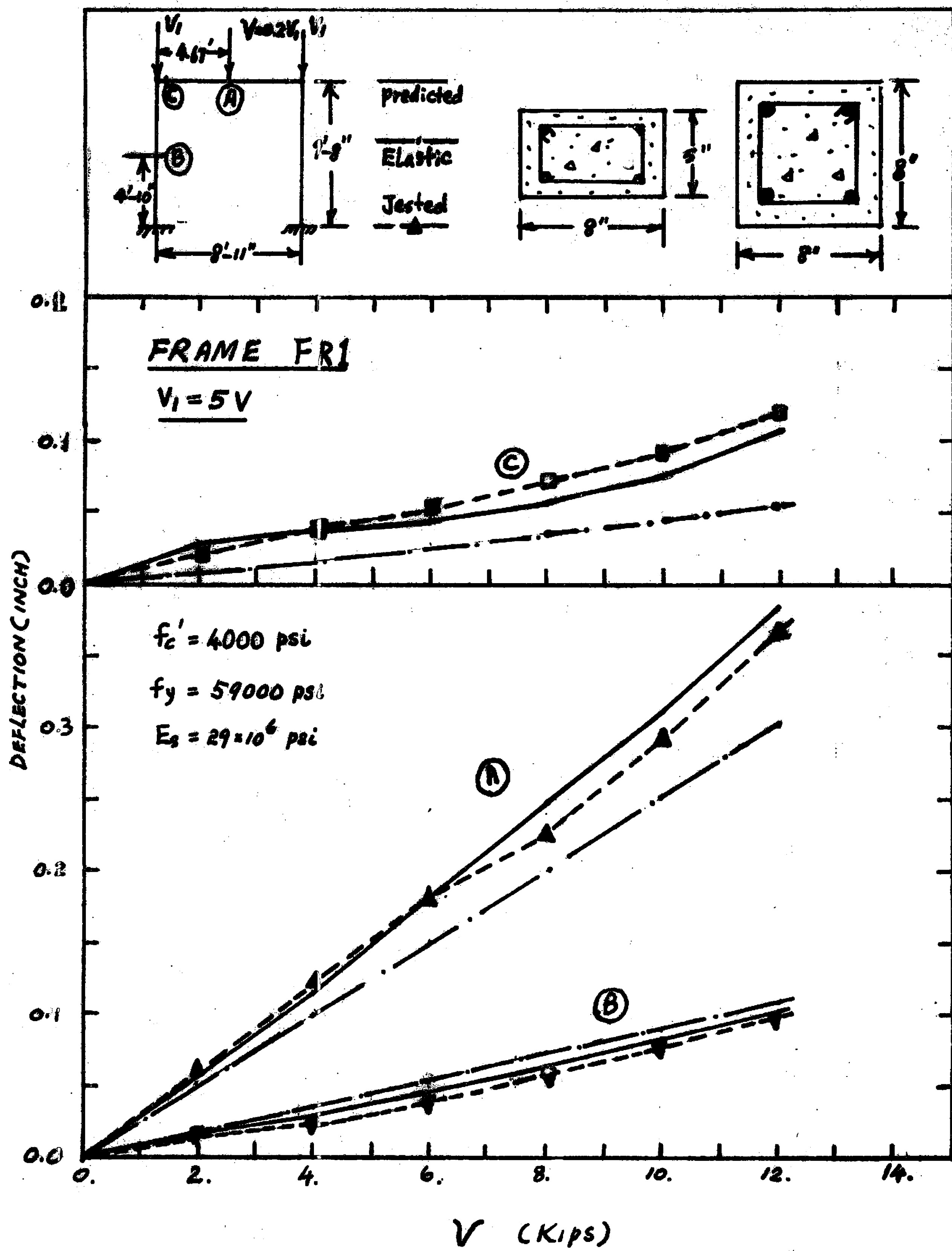

Figure 6.1

Comparison of Deflection for Tan's Frame FR1

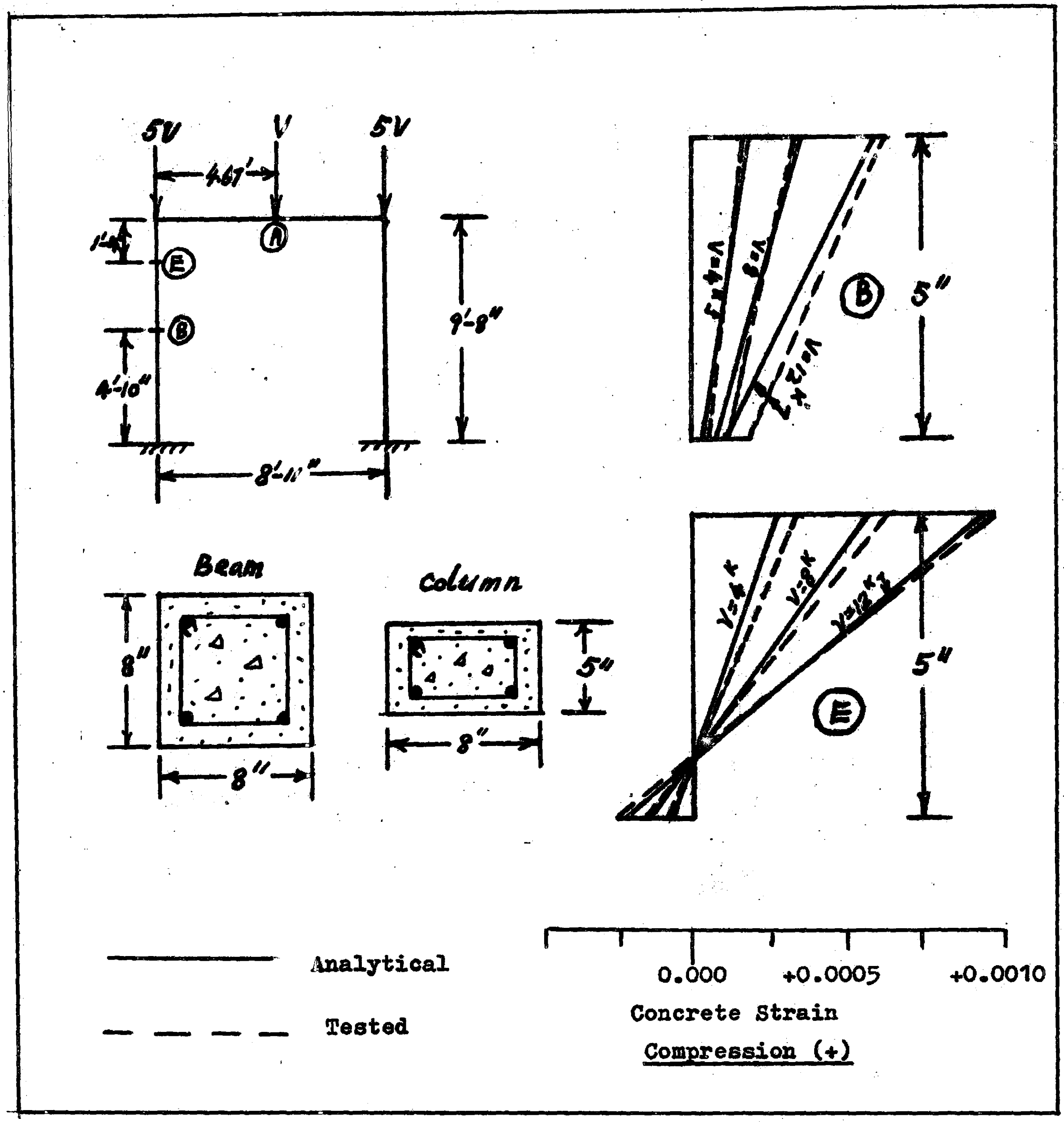

Figure 6.2

Comparison of Concrete Strain for Tan's Frame FR1

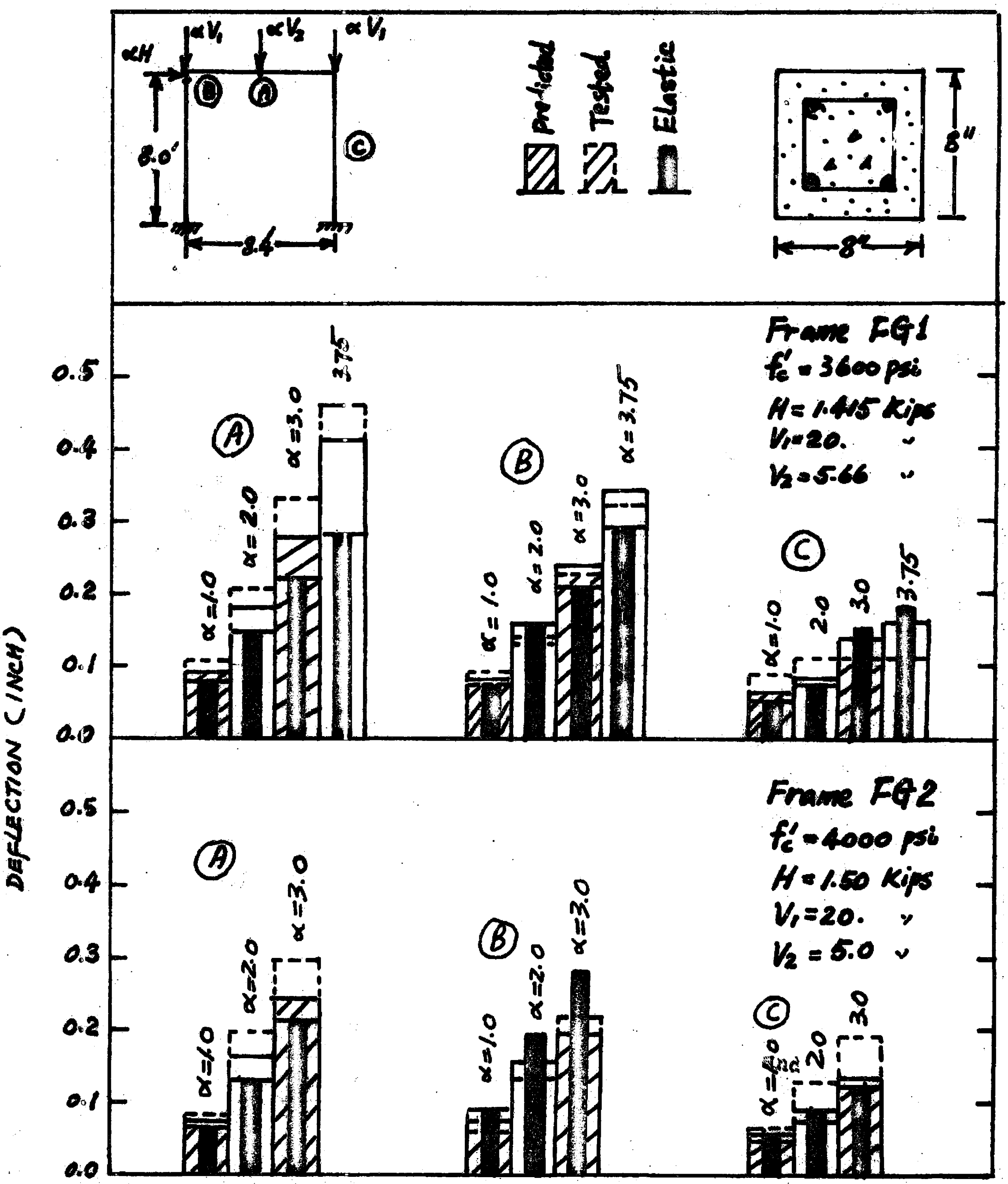

Figure 6.3

Comparison of Deflection for Tan's Frames FG1 and FG2 frames are the same as those tested by Danielson (to be discussed later). It can be seen that the predicted deflection follows quite closely with the test result except at higher loads. At high loads, cracking of the joint was very severe and likely contributed to the discrepancy between predicted and tested deflections.

(6.2.b) Svihra's Frames (52) :

Svihra in 1970 tested four two-bay single-storey frames in McMaster University to investigate the behavior and capacity of concrete frames subjected to cyclic loadings. The dimension of these frame are shown in Figure 6.4 to have a clear span of 8.3 feet for the beams and the columns were 8 feet high measured to the mid-height of the beam. The cross-section of the frames is constant and is identical to the beam section for Frame FR1 which was described in Chapter 2.

The experimental and analytical result for one of Svihra's frame, Frame BF-4, is presented in Figure 6.4. For the loading configuration, the sidesway deflection of the frame was the dominant displacement. The non-linear analysis predicts values which quite closely follow the measured values. The difference between predicted and tested deflection increases with increasing load but the percentage of error remained relatively small. The elastic analysis differs from the test results by a much greater error especially at high loads.

In Figure 6.5, the load-moment curves at various location on the frame were plotted and compared. The same trends as discussed for Figure 6.4 are evident.

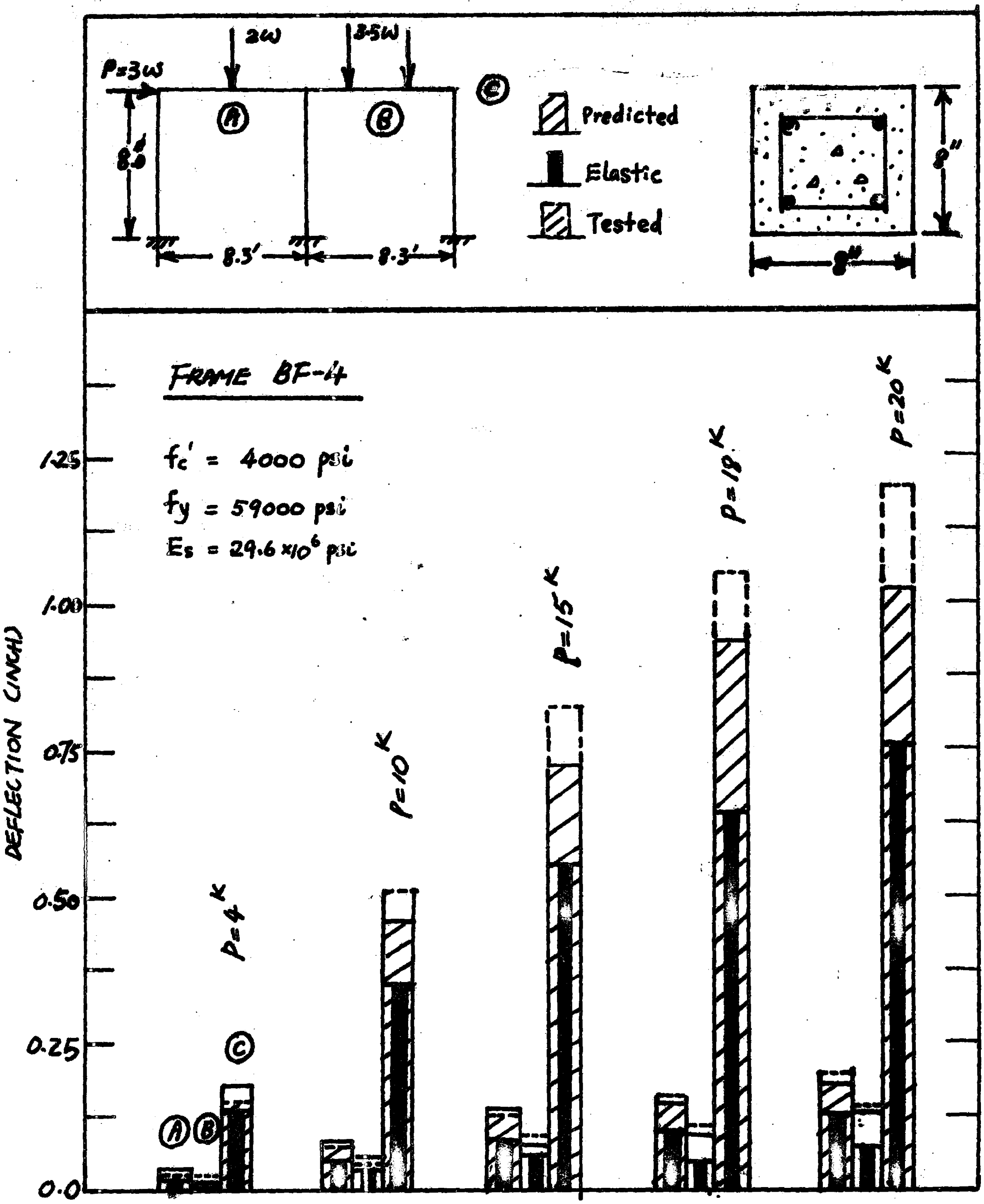

Figure 6.4

Comparison of Deflection for Svihra's Frame BF-4

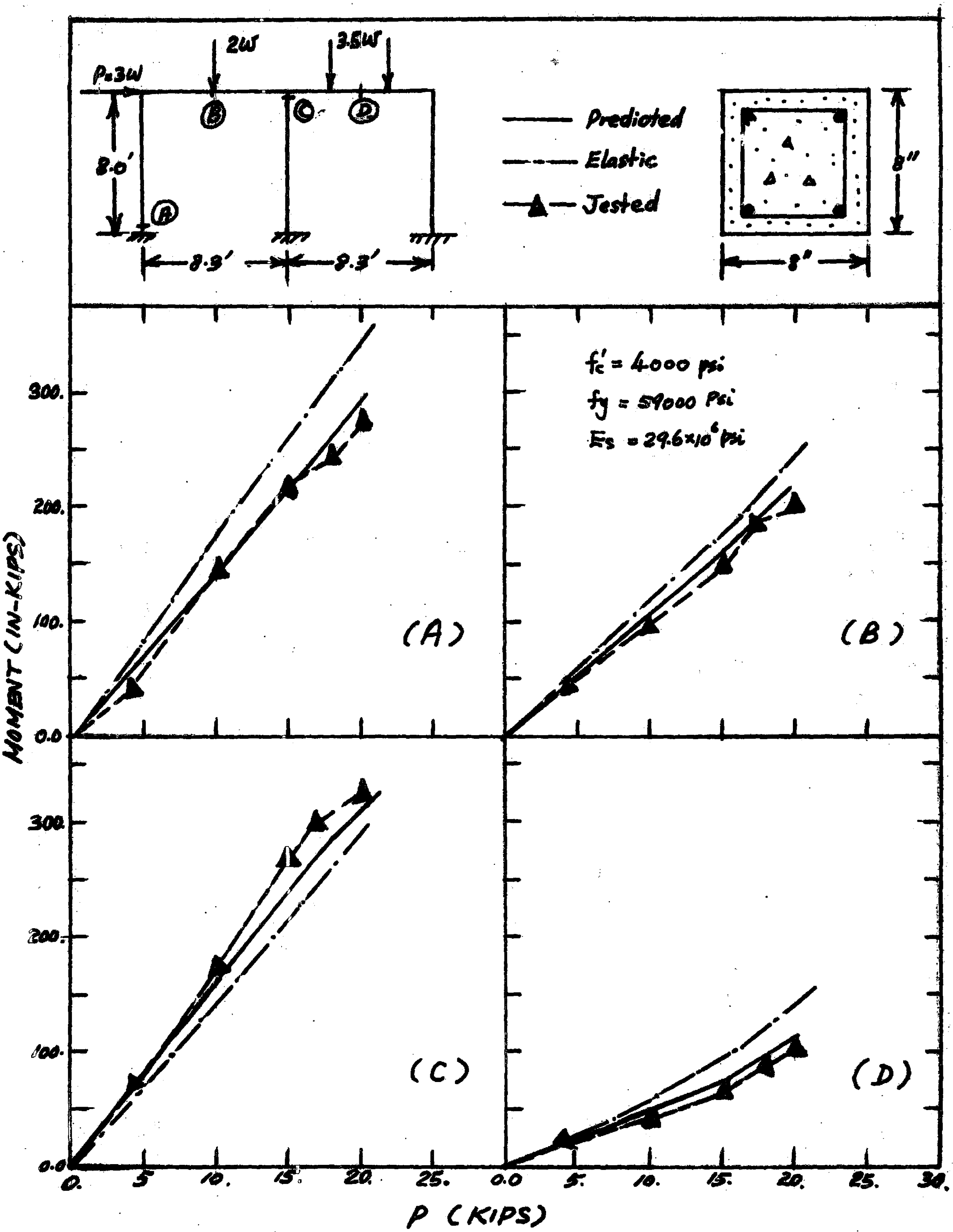

Figure 6.5

Comparison of Bending Moment for Svihra's Frame BF-4

(6.2.c) Danielson's Frames (19) :

The results of one of the three one bay single storey frames tested by Danielsen at McMaster University are shown in Figure 6.6. The frames had the same dimension as Svihra's Frame.

Frame R2 provided results for a short-term proportional load test. As can be seen in Figure 6.6, the non-linear analysis provide a reasonable prediction of the sidesway deflection and the midspan deflection whereas the elastic analysis did not. Even though an attempt was made to stiffen the joints, considerable cracking was readily visible. Hence this feature can account for some of the difference between predicted and test values.

In Figure 6.7, the bending moment in various critical point of the frame has been drawn against increasing horizontal load and the above discussion also applied.

(6.2.d) Cranston's Frames (17) :

Cranston in 1969 presented a report to the Cement and Concrete Association of the United Kingdom , describing the design and testing of eight one-storey single bay fixed-base frames. The purpose of these tests was to prove that the Mechanism Method of Limit Design could be equally applicable to reinforced concrete structures.

The dimensions of all his frames were the same, with the center to center span of the beam being 120 inches long and the height of the column 60 inches as shown in Figure 6.8. The cross-sections of the frames were constant at 4 inches wide and

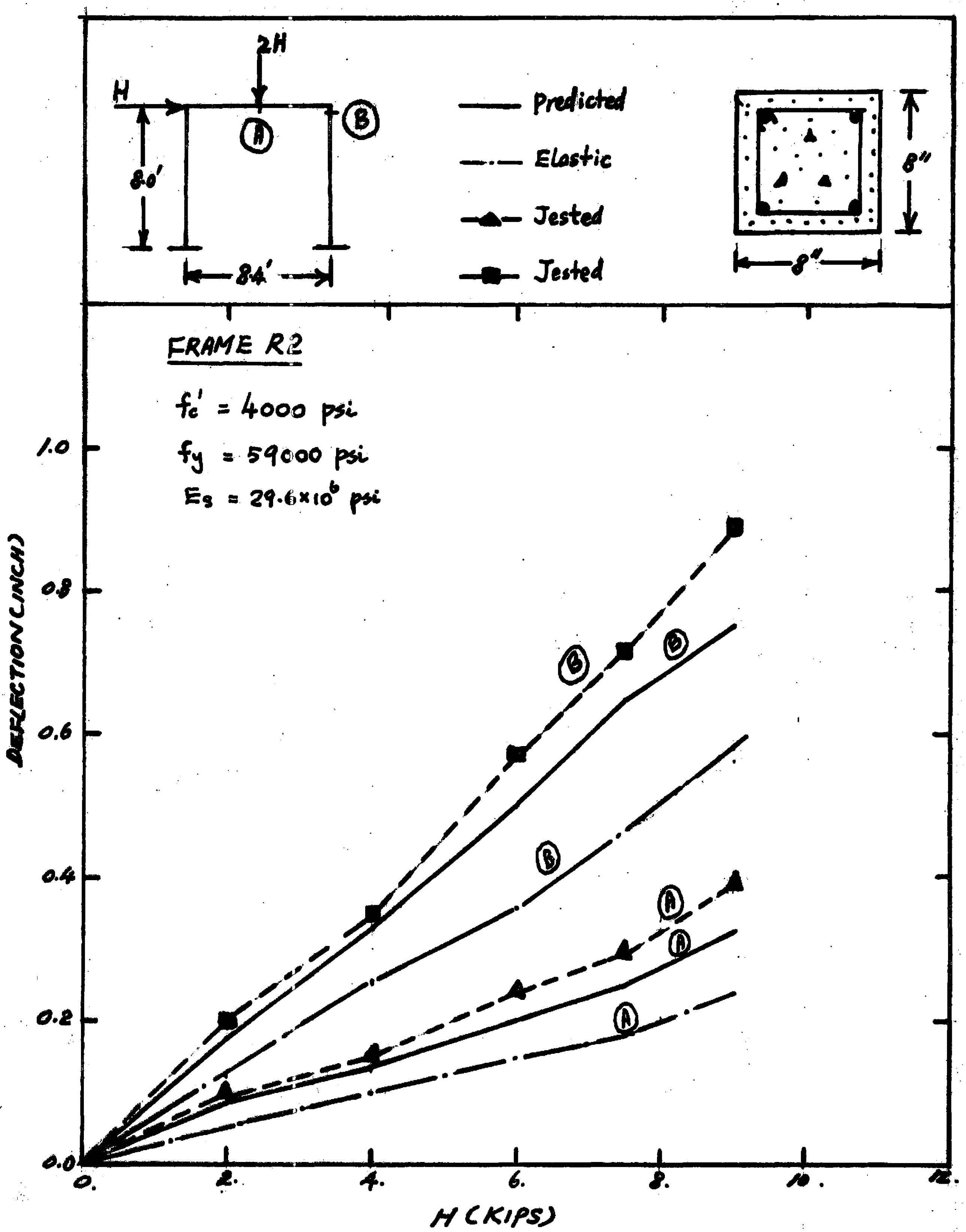

Figure 6.6

Comparison of Deflection for Danielson's Frame R2

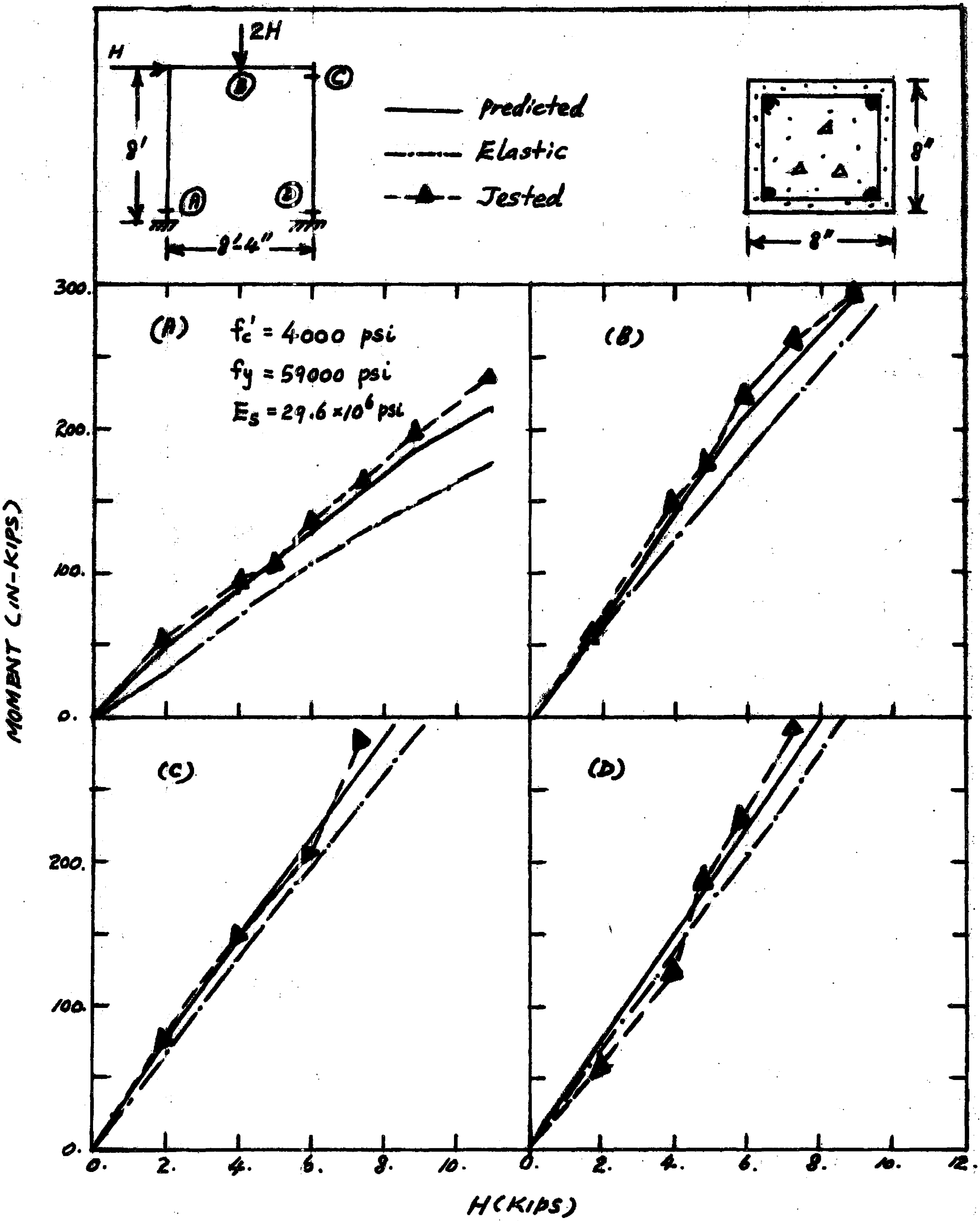

Figure 6.7

Comparison of Bending Moment for Danielson's Frame R2

6 inches deep. The reinforcing in the frame differed from cross-section to cross-section and from frame to frame. The vertical loads were not applied proportionally to the horizontal load. The magnitudes are included in Cranston's Report (17).

Six of the frames were analysed by the Matrix Stiffness-Modification method and by the elastic analysis. Both methods take into account the variation of distribution of reinforcement in the frames. The results of the predicted and tested deflections under increasing horizontal load are shown in Figure 6.8.

It is observed that both the stiffness modification method and the elastic analysis underestimate the experimental deflection. The discrepancy between test and elastic analysis was approximately double that between non-linear analysis and test. The unaccounted for effects of rotation in the joints and visible diagonal cracking may be identified as partially responsible for the larger measured deflections especially at high loads.

In Figure 6.9, the bending moment vs. horizontal load curves were drawn for the points F1 and K1 in the frames as shown in Figure 6.8 for four of the six frames selected. The same observation as discussed above is applicable to this Figure.

(6.2.e) Sader's Frames (51) :

In 1967, Sader tested 20 single storey one-bay frames with fixed bases at McGill University. The dimension of these frames were approximately at a one to six scale. The purpose of these experiments was to investigate the ultimate strength of concrete

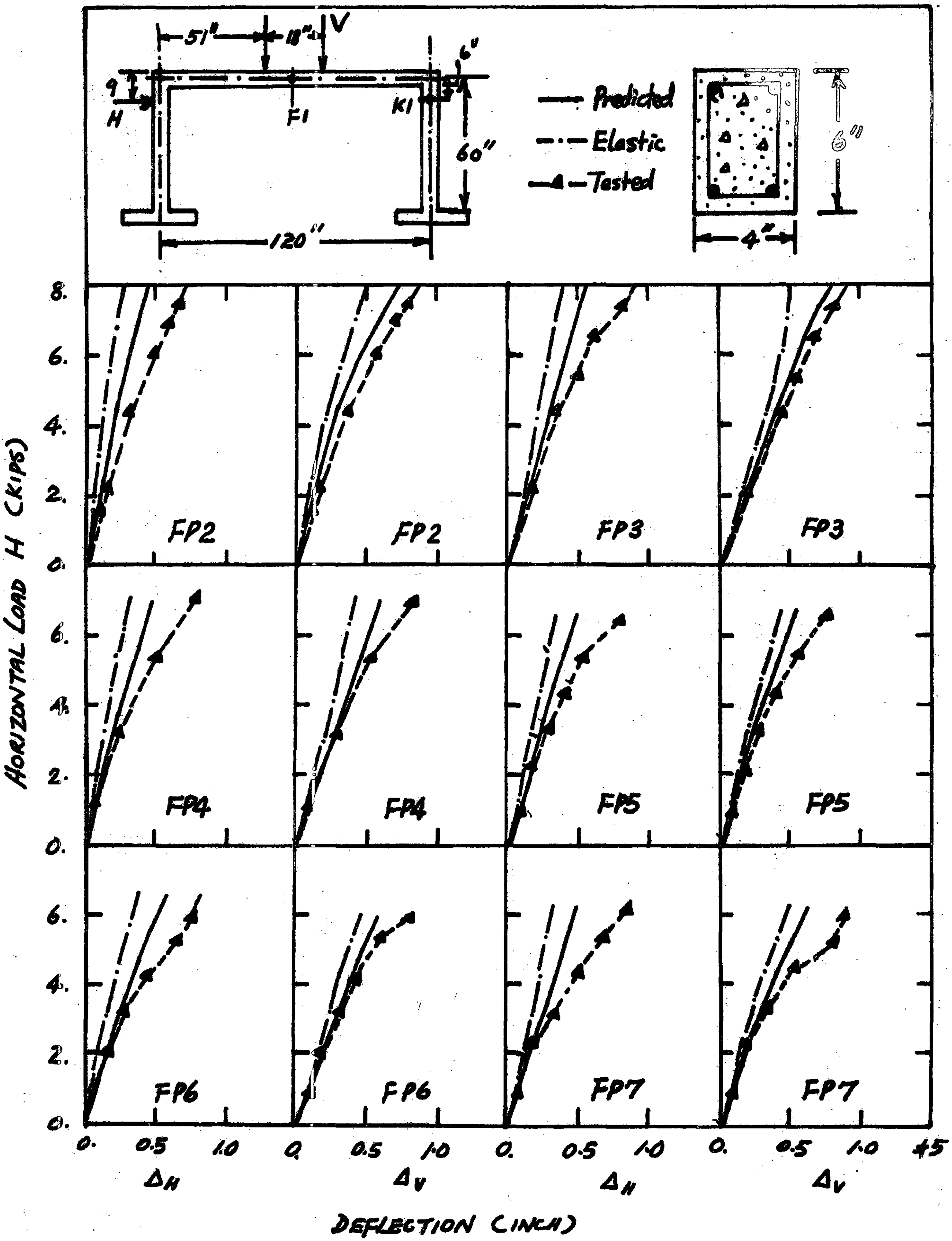

Figure 6.8

Comparison of Deflection for Cranston's Frames

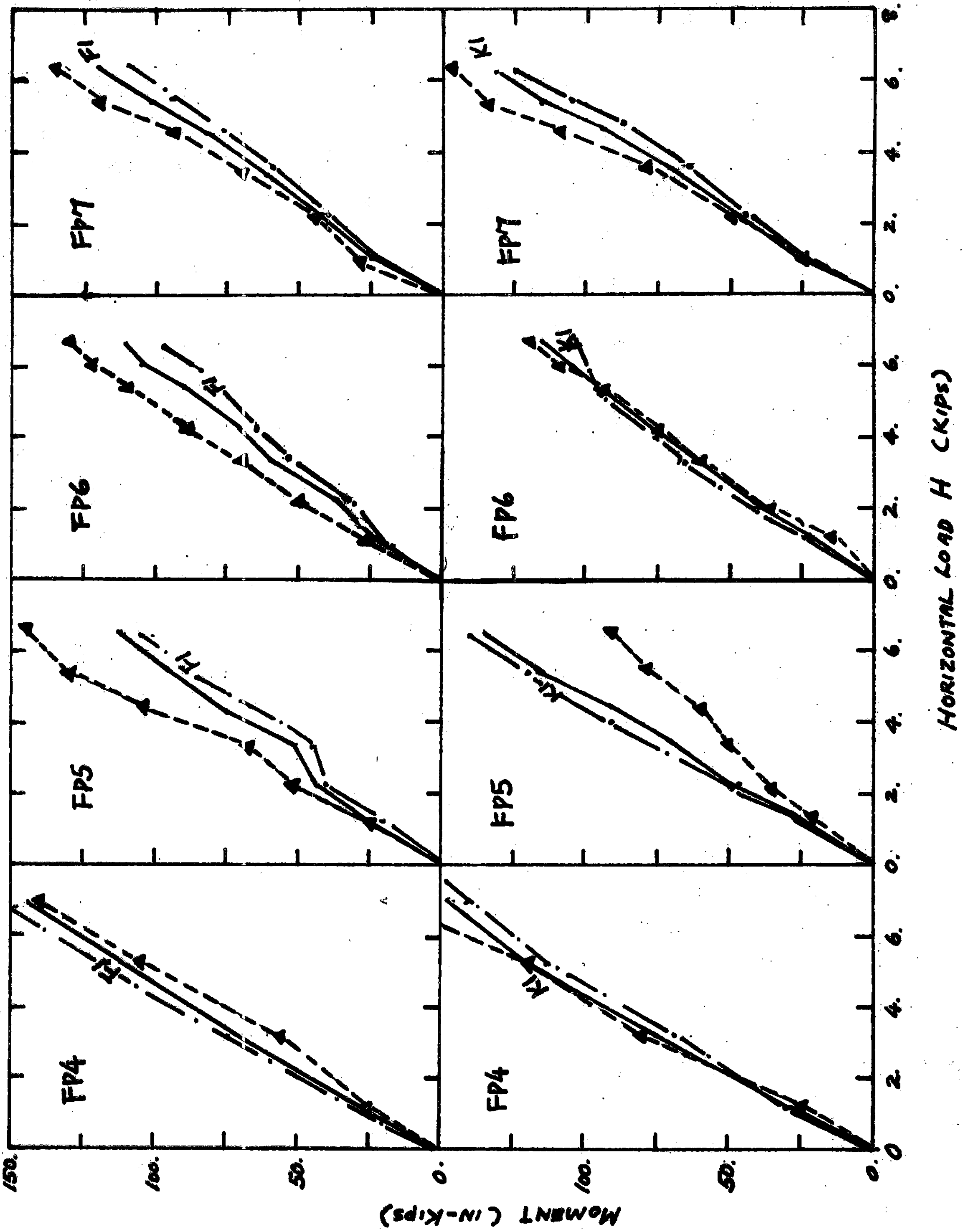

Figure 6.9

Comparison of Bending Moment for Cranston's Frames

frames, the mode of failure, and the moment rotation characteristics of a critical joint in the frames.

The results of four of these frames are presented in Figure 6.10. The four frames had different percentages of reinforcement and different loading configurations. In all but a few cases at very low loads, the nonlinear analysis predicted sidesways and midspan beam deflections fairly accurately. The deflections from elastic calculations exhibit much larger error. Except for Frame No. 1 , the experimental deflections were larger than the predicted values. The effect of joint rotation is thought to be the main reason for the difference between the tested and nonlinear predicted value.

(6.2.f) Adenoit's Frames (4) :

In 1970, Adenoit at McGill University tested 11 double-bay single-storey fixed end concrete frame models with the same scale as used by Sader. These frames were subjected to a constant double point vertical load and an increasing horizontal load. The experimental specimens include two set of concrete frames using plain and deformed reinforcing bars respectively. The varying parameter in this study was the percentage of reinforcement in the column cross-section.

Six of the eleven frames having a wide range of percentage of reinforcement were chosen for comparison. The sidesway deflection and the midspan deflection of the beams were predicted by the stiffness modification method and by the elastic method. The results are plotted in Figure 6.11. The comparison of this Figure is apparent and the same discussion as given for Sader's Frames applies.

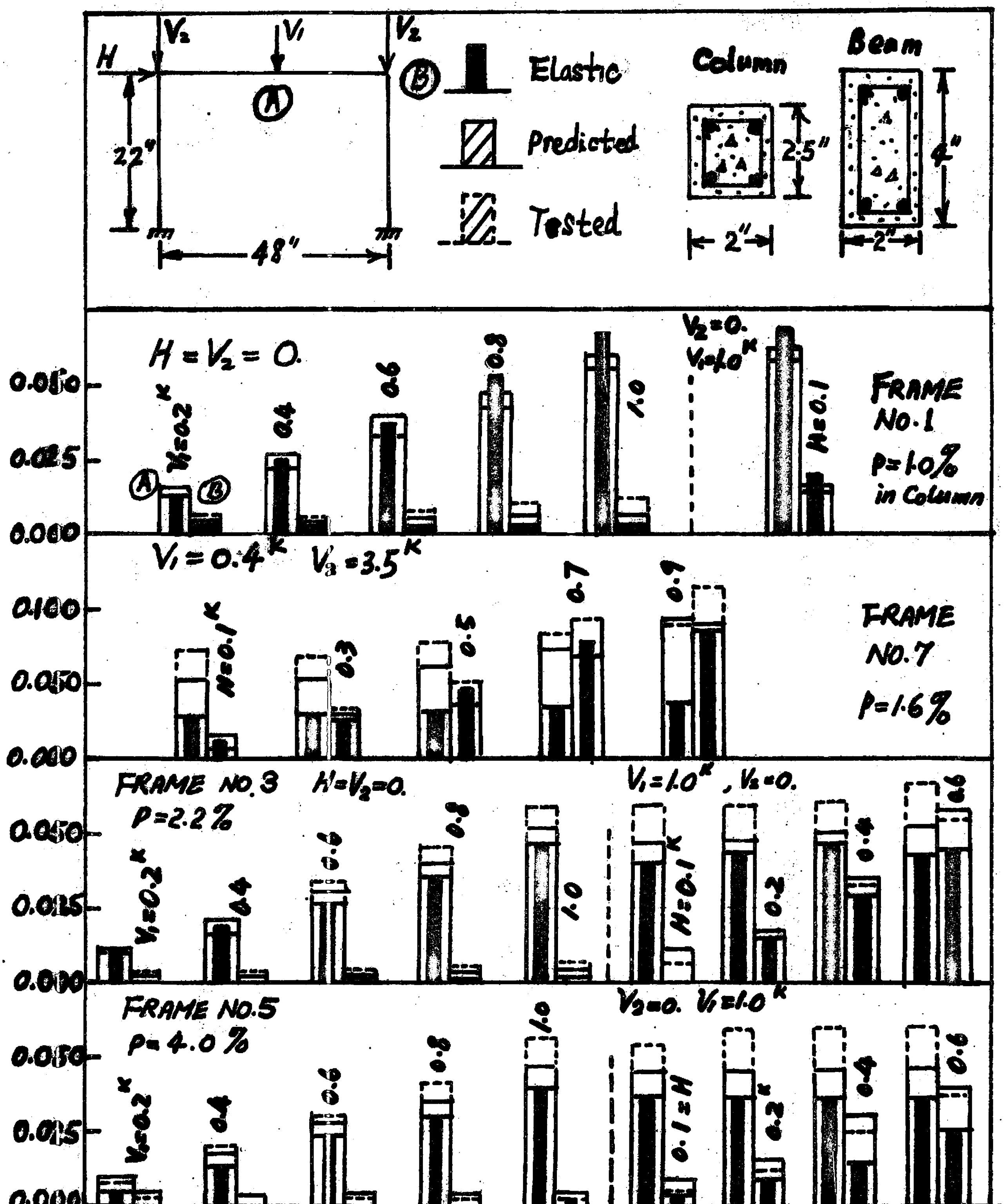

Figure 6.10

Comparison of Deflection for Sader's Frames

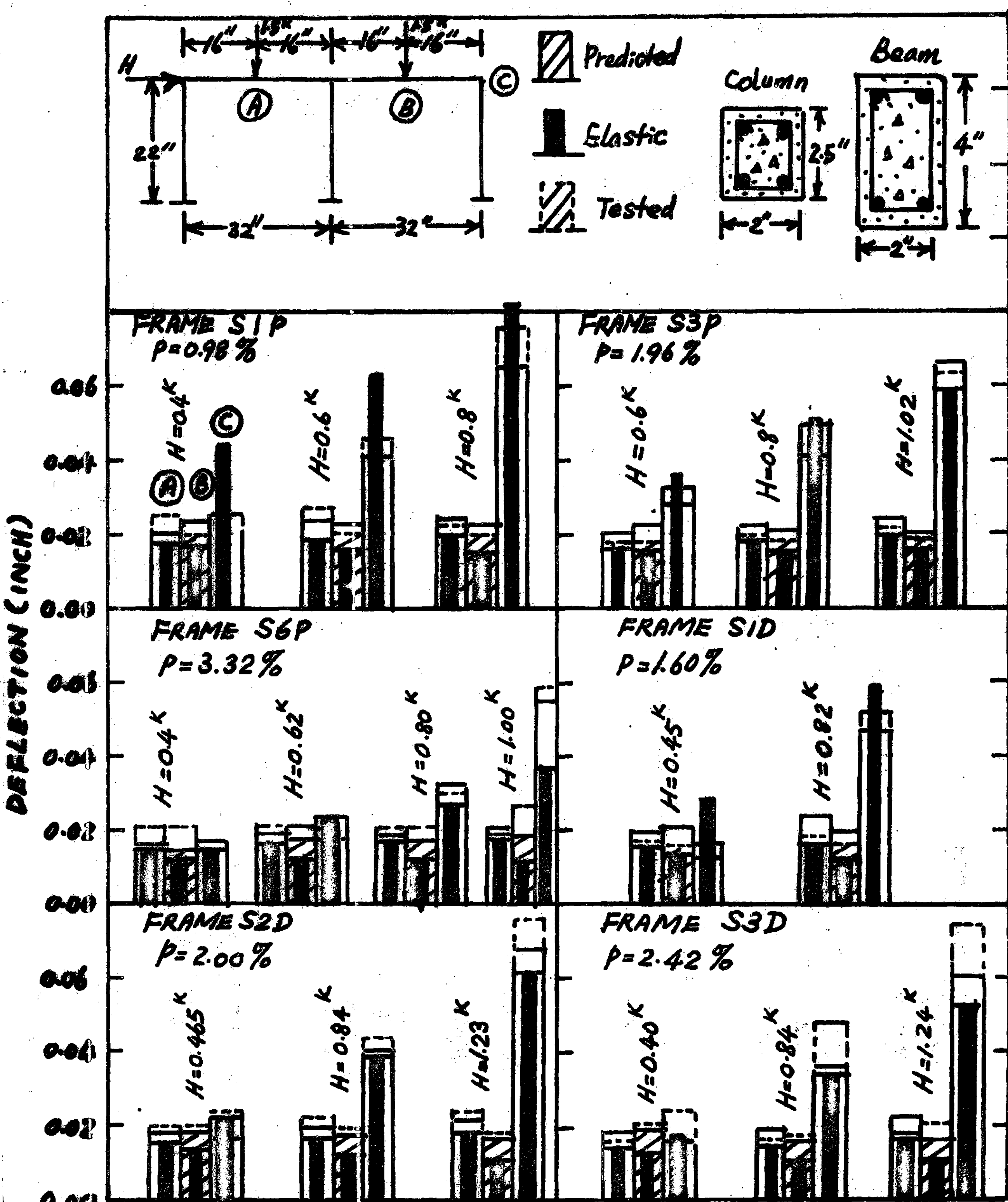

Figure 6.11

Comparison of Deflection for Adenoit's Frames

(6.3) Comparison of Sustained Load Test Results :

In this section, the sustained-load test results of three frames tested at McMaster University have been presented.

In Figure 6.12, the experimental deflections of Frame FS1, tested by the author have been plotted. The frame was loaded with a high column load of 46 kips and with a beam load of 10 kips. This loading was sustained for 80 days. The testing and observation of this frame is given in detail in section 2.9.b.

It is observed that the nonlinear predictions do not differ much from the test values whereas the elastic analysis obviously gives an erroneous constant deflection with time.

In Figure 6.13, the experimental result of Frame FG2 were presented. The details of this frame were given in section 6.2.a.

In Figure 6.14, the test results of Frame L1 tested by Danielson (19) were given. The dimension and cross-section of this frame were the same as Frame R2 as described in section 6.2.c.

From a study of Figure 6.13 and 6.14 , the same discussion as given for Frame FS1 applies to comparison of the results for these two frames.

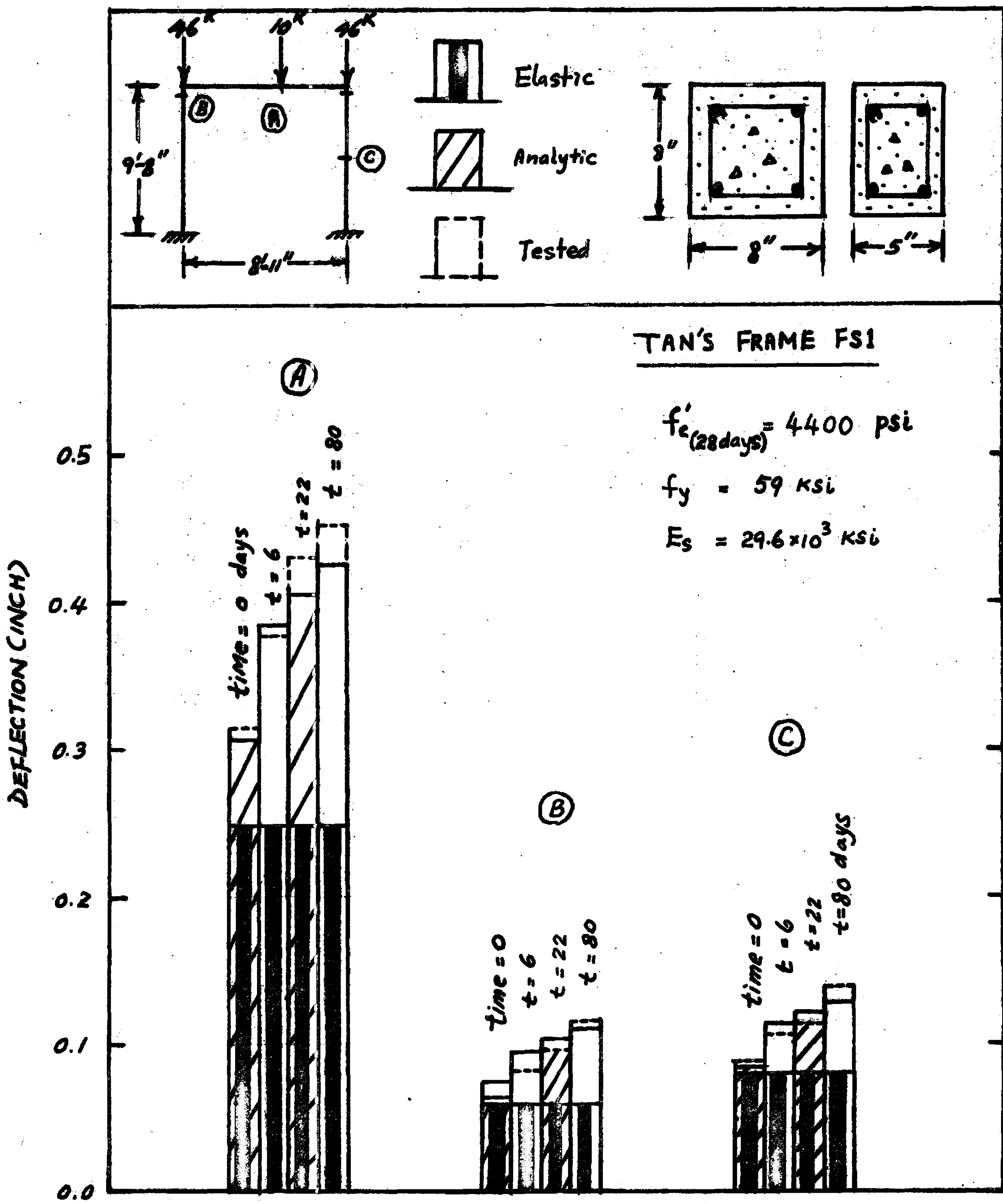

Figure 6.12

Comparison of Deflection for Tan's Frame FS1, Sustained-load Test

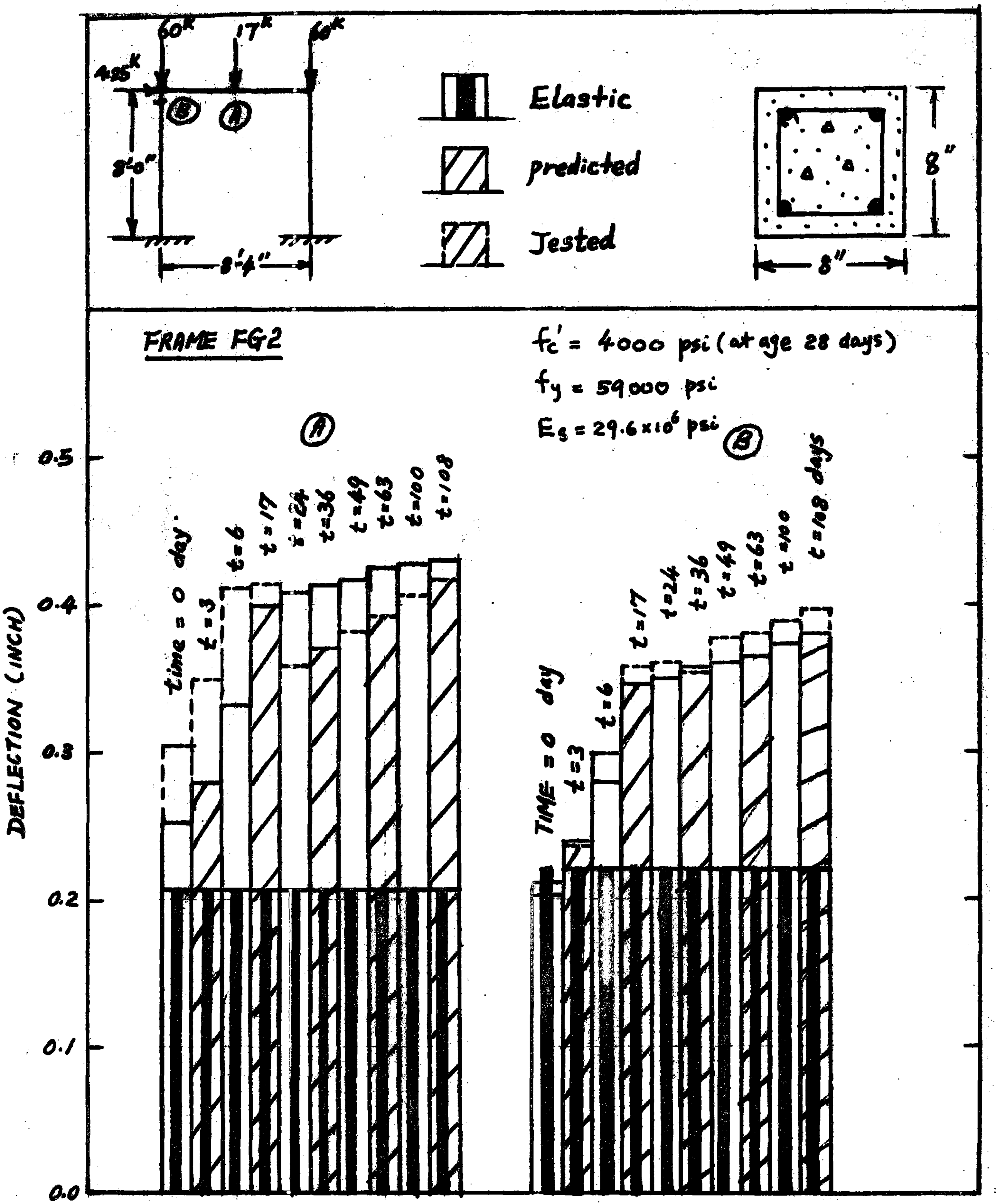

Figure 6.13

Comparison of Deflection for Tan's Frame FG2, Sustained-load Test

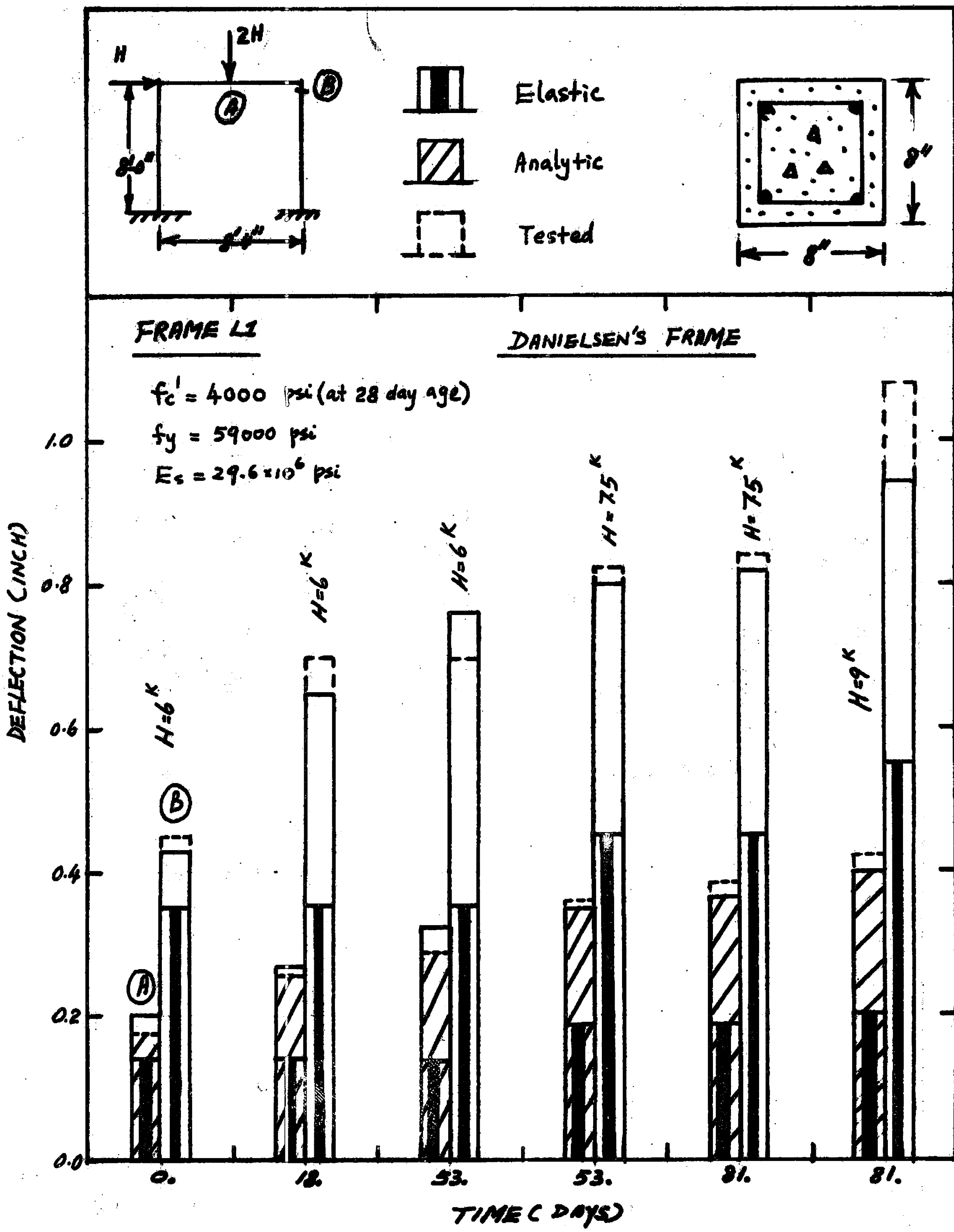

Figure 6.14

Comparison of Deflection for Danielson's Frame L1, Sustained-load Test

(6.4) Conclusion :

A representative sample of the test results reported from the Cement & Concrete Association, McGill University, and McMaster University has been chosen as a basis for evaluating the proposed Matrix Stiffness-Modification Technique. It can be concluded by comparison of the analytical and test results for a total of twenty four large scale and reduced scale frames, that the Matrix Stiffness-Modification method yields accurate results in predicting realistic behavior of actual structures. On the other hand, the elastic method which is based on a constant cracked transformed section of concrete, always gives inadequate prediction of the behavior of real structures, especially when time-dependent creep deformation or high loads are considered.

Chapter 7

DISCUSSIONS AND CONCLUSIONS

(7.1) Introduction :

The purpose of this research was to propose a method using a matrix approach for an efficient nonlinear analysis of reinforced concrete structures. The Matrix Stiffness-Modification Method was developed and its validity checked by comparison with the results of several experimental frame tests. The modification is in the evaluation of a set of equivalent stiffnesses EI and EA for each element of a structure which has been subjected to a particular loading and stress history. From comparisons with experimental data, it is concluded that the procedure for computation of the equivalent stiffnesses in this analysis yields realistic prediction of the deformations of a concrete structure. The discussion in this chapter is devoted to the following two sections which relate in the first case to the major work involved and in the second case to the major application of this research:

(1) Matrix Stiffness-Modification Technique

(2) Present Column Design Practice.

(7.2) Discussion of the Matrix Stiffness-Modification Method :

This section discusses the difference between the elastic matrix method of structural analysis and the stiffness modification method, the difficulties and experience found in developing the computer program, and the possibility of partial non-linear analysis for prediction of the effects of inelastic behavior on components of a multistorey rigid frame building.

(7.2.a) Elastic Matrix Method vs. Matrix Stiffness-Modification Method:

It is concluded, from the comparison of the analytical and experimental frame test results, presented in Chapter 6, that the Matrix Stiffness-Modification Technique predicts accurately the inelastic behavior of concrete frames provided that the mathematical model of the frame is adequately described. On the other hand, the elastic method using stiffnesses based on a cracked transformed section of concrete is seen to be inaccurate especially for sustained loads and high levels of load. This is due to the fact that the elastic method does not take into account the variation of stiffnesses due to the effect of the nonlinearity in the concrete stress-strain relationship, the effect of different load and moment combinations, the effect of secondary bending moments, and the effect of creep and shrinkage in concrete. However, the Matrix Stiffness-Modification method is based on a concept that equivalent stiffnesses of a structure can be obtained using a modification procedure which takes into account the aforementioned factors. Hence the non-linear short-term and sustained-load behavior of structure can be accurately predicted.

(7.2.b) Discussion on Convergence Control for the Computer Program:

In the early stage of developing the computer program for the Matrix Stiffness-Modification method, several difficulties were encountered. Of these, the convergence control of the iterative process for the main program and for the subroutine "MPHI" which are described in sections 5.5 and 5.6.c respectively, was the most difficult. It is thought to be worthwhile to contribute the experience accumulated in this research for future reference.

For the main program, it was discovered that in the process of iteration, which is described in section 5.5 , the stiffnesses for each element of the structure may occassionally exhibited periodic oscillation. This problem occured when a set of equivalent stiffnesses were used to generate a set of applied load which were used to yield new stiffnesses which inturn were used to calculate new loads which were used to generate new stiffnesses which changed very little from the first set of stiffnesses. This difficulty was overcome by introducing an averaging process for each iteration. The effective stiffnesses EI and EA were averaged with the corresponding stiffnesses from the previous two cycle after the comparison step described in section 5.5 was completed. These averaged stiffnesses were used as new stiffnesses to obtain the new displacement and force vectors for subsequent generation of another set of new equivalent stiffnesses. From a physical point of view, the averaging calculation serves as a dashpot to damp the oscillation of the stiffness to convergence.

In the subroutine "MPHI" as described in section 5.6.c, the Newton-Raphson method was used to determine the strain distribution for a cross-section of concrete subjected to known applied load and bending moment. This method required an initially assumed strain distribution to obtain a final strain distribution compatible to the applied loads. After several trials of the nonlinear frame program, it was concluded that the assumption of an initially elastic strain distribution would lead to satisfactory convergence in the subroutine.

(7.2.c) <u>Discussion on Partial Nonlinear Analysis</u> :

Most research done on the behaviorial study of the inelastic response of a beam column in multi-storey buildings has been restricted to an idealized member separated from the structure. The member is loaded with constant axial force and end eccentricity. However, the behavior of real beam-columns in a multistorey building subjected to constant externally applied loading, is actually influenced by the variation of the stiffnesses of the member itself, and of the other members in the structure. A rational analysis for this type of behavior has been missing. For this reason, the possibility of the application of the Matrix Stiffness-Modification Technique to a partial non-linear analysis of realistic inelastic reinforced concrete structure was studied.

The idea was that a localized portion of the structure would be studied for inelastic behavior. The reason for introducing partial non-linear analysis is also due to the limitation of the computer storage capacity and the computing time required. In addition, for a rational investigation of the behavior of a beam-column in a multistorey building, it is realized that those members which are far away from the localized inelastic column do not produce significant effect on the distribution and redistribution of bending moment in the beam-column. Therefore, it is justificable to apply partial nonlinear analysis to the behaviorial study of localized inelastic members in a multistorey structure. The selection of the partial inelastic portion of a multi-storey building is in turn limited by the computer storage capacity, the computing time required, and the error associated with the effect of using elastic elements for the remainder of the structure.

To illustrate this method, a four storey concrete frame has been analysed. The details of the location and amount of reinforcing steel in the frame are shown in Figure 7.1. The frame was subjected to a proportional loading for the short-term analysis. As indicated in Figure 7.2, the members AB, BC and CD of the frame were designed to exhibit nonlinear behavior while the other members remained essentially elastic with a cracked transformed section of concrete. The Matrix Stiffness-Modification method is then applied to the analysis of the whole structural system using constant stiffnesses for all members except members AB, BC and CD. Figure 7.2 and Figure 7.3 show the performance of the substructure under short-term and sustained load respectively.

From the above discussion, it is concluded that the Matrix Stiffness-Modification Technique is not only effective in system analysis but is also applicable for the analysis of substructures.

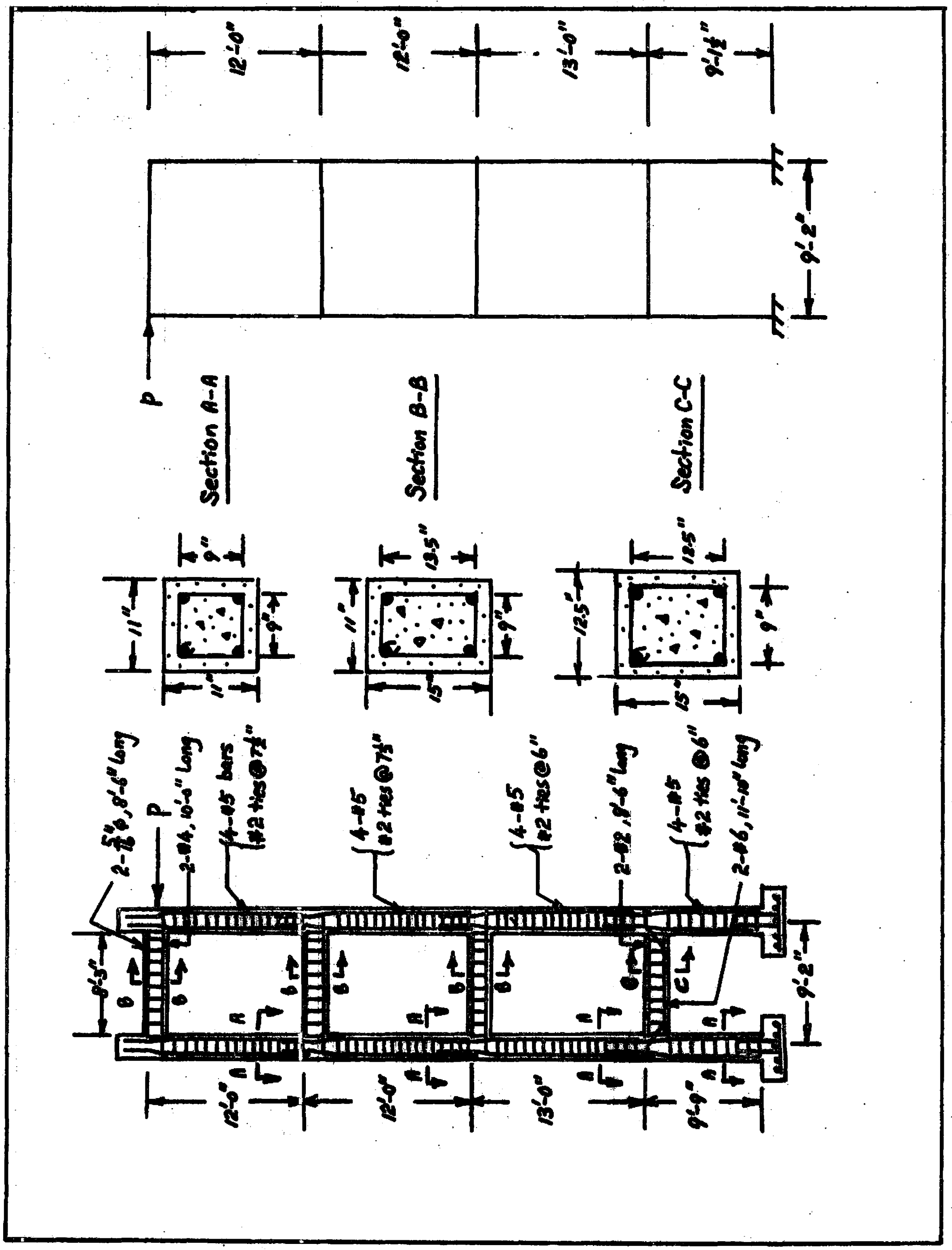

Figure 7.1

Partial Nonlinear Analysis, the Frame

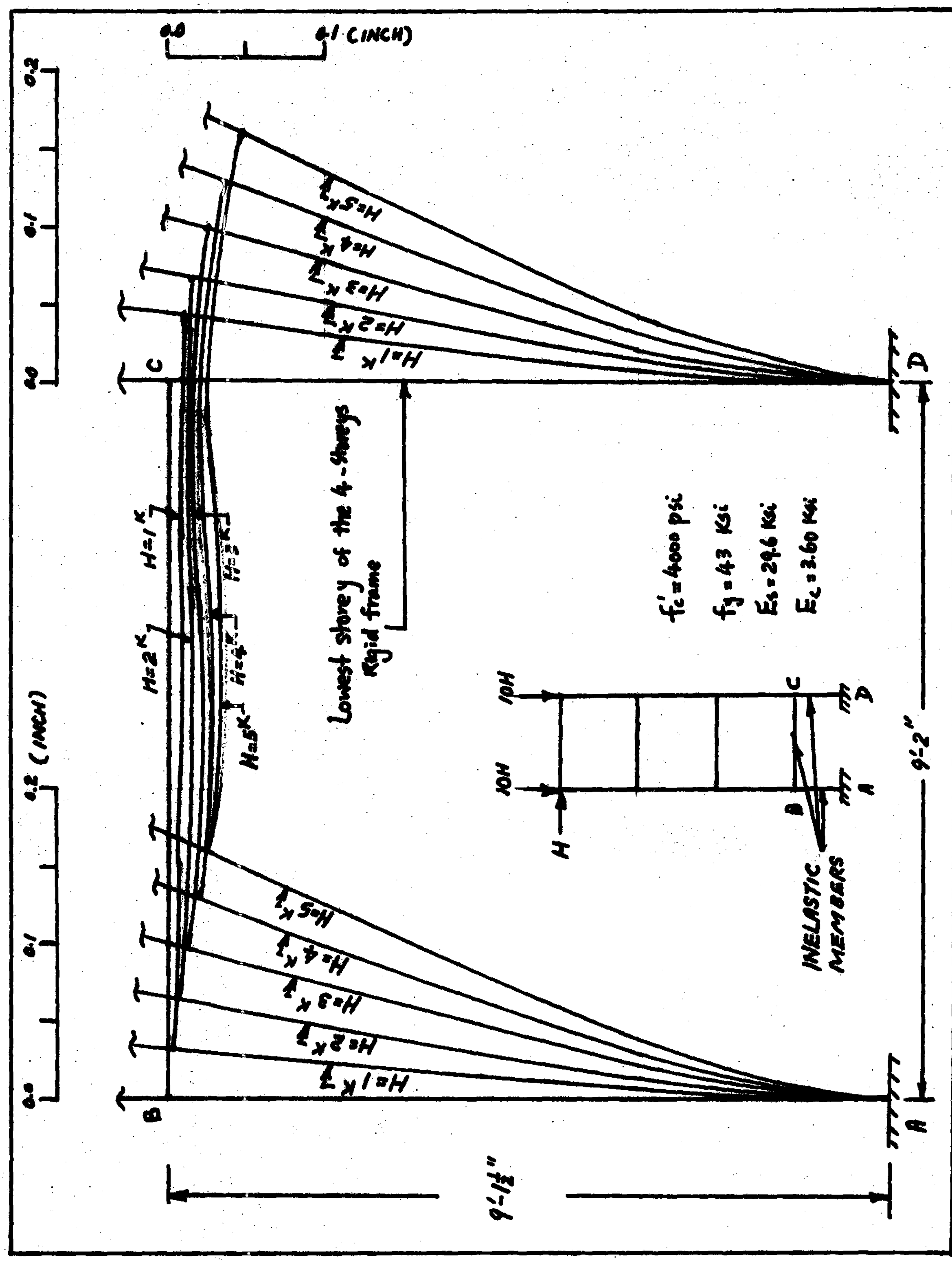

Figure 7.2

Short-term Partial Nonlinear Analysis

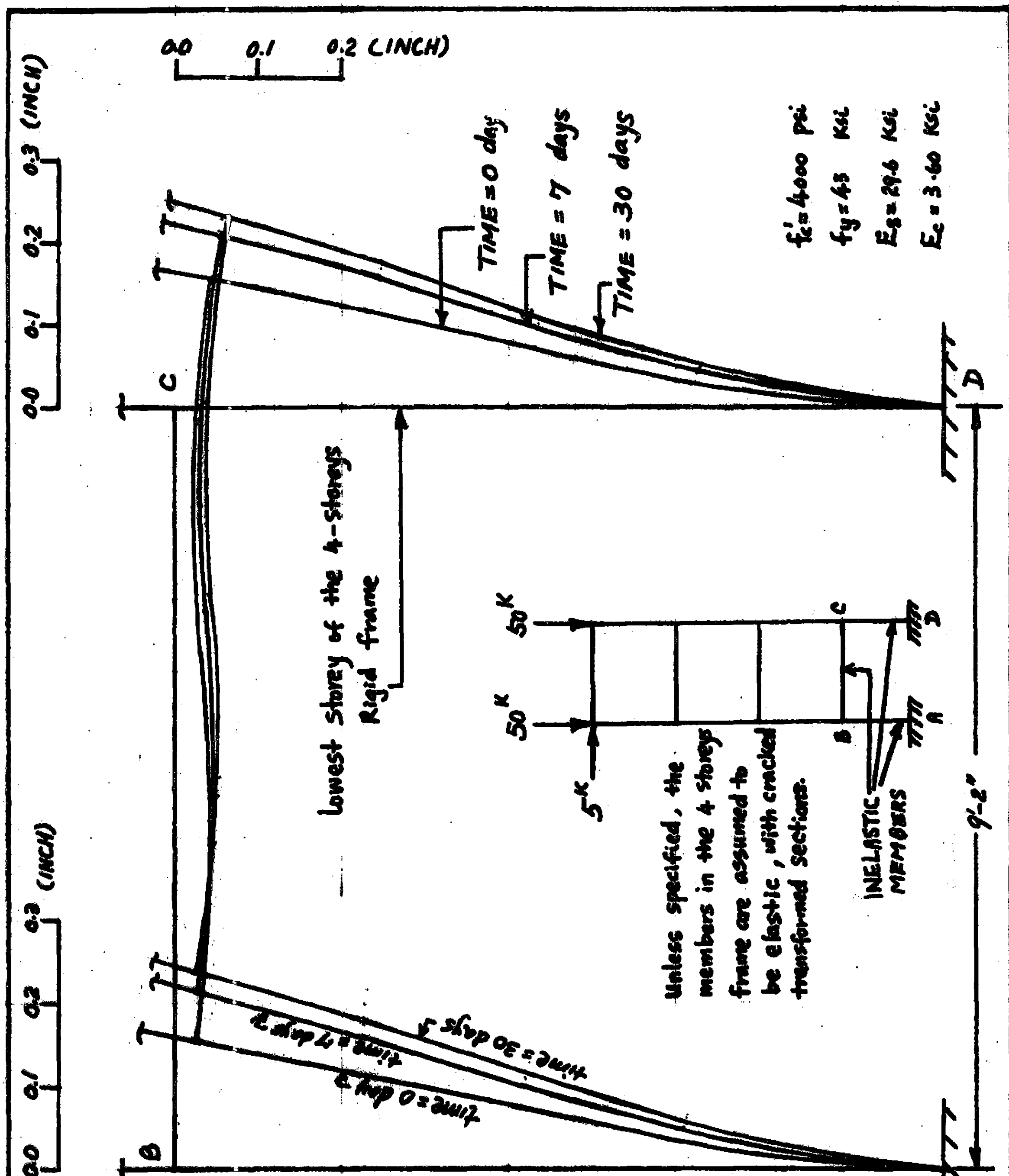

Figure 7.3

Sustained-load Partial Nonlinear Analysis

(7.3) Discussion on present Column Design Practice ::

From a study of the deformation characteristics of concrete sections given in Chapter 4, some comments can be made regarding present column design methods. The Reduction Factor Method (2) and the Moment Magnifier Method (37) are discussed in this section.

(7.3.a) 1963 ACI "Reduction Factor Method" (2) :

The 1963 ACI code (2) specified the use of a reduction factor for design of slender columns taking into account the length effects. This reduction factor was based directly on the slenderness ratio, l/r , of the columns. Different formula for the reduction factor provided for different ranges of slenderness and different modes of deformation.

It is observed that the reduction factor R is a function of the radius of gyration r of the structure. However, the ACI code specified that r is a constant regardless of the effect of the axial load versus bending moment relationship. In this regard, the investigation of the unit slenderness curves plotted in Figures 4.8 and 4.9 demonstrated that the radius of gyration of a concrete cross-section is not constant but is a function of the loading condition. Therefore, the reduction factor is concluded to be unrealistic and according to several researchers (24) may be unsafe.

(7.3.b) 1971 ACI"Moment Magnifier Method" :

Recently the Reduction Factor Method has been replaced by a Moment Magnifier Method in ACI Code 318-71 for design of slender columns (37). The Moment Magnifier Method requires the determination of the critical load, P_{cr} , which is given by,

$$P_{cr} = \frac{\pi^2 EI}{(Kh)^2}$$

The flexural stiffness EI can be taken either as,

$$EI = \frac{\left(\frac{E_c I_g}{5} + E_s I_s \right)}{(1 + R_m)}$$

or,

$$EI = \frac{E_c I_g}{2.5\,(1 + R_m)}$$

where,

Kh = effective height of column

$E_c = 33\, W^{1.5}\, f_c'^{1/2}$

E_s = modulus of elasticity of steel

I_g = moment of inertia of gross-section of concrete

I_s = moment of inertia of reinforcing steel about the column centroid.

The ratio R_m is the ratio of the dead load moment to the total moment and therefore is intended to take into account the effect of creep by reducing the effective stiffness in proportion to the amount of load which is sustained for a long period of time.

The Moment Magnifier, F, is given by,

$$F = \frac{C_m}{(1 - P_u/P_{cr})} \geq 1.0$$

where,

P_u = Ultimate axial force for which the column is designed

C_m = Coefficient reflecting ratio of end moments.

Now it is quite obvious that the moment magnifier method no longer relies directly on the slenderness ratio, l/r, of the member but it uses a stiffness EI which is modified to account for the cracking of concrete, the creep associated with the applied load and bending moment, and the load vs moment relationship.

The effective EI given by the moment magnifier method is evaluated by using some abstraction of the subroutine from the Matrix Stiffness-Modification method. In Figure 7.4, the analytical results of flexural stiffness EI were plotted for different values of constant reinforcement ratio, p, in the concrete section. The EI given by the moment magnifier method are shown by the bound lines as indicated. The ratio for dead load moment to total moment for this nonlinear analysis gives a R_m value of 1.0 . In Figures 7.5 through 7.8, the parameters d', f_y, f'_c and shrinkage strain are varied and compared to the EI value given by the Moment Magnifier Method. It is then concluded that the stiffness EI recommended by the Moment Magnifier Method provides a safe estimate of the effective stiffness EI.

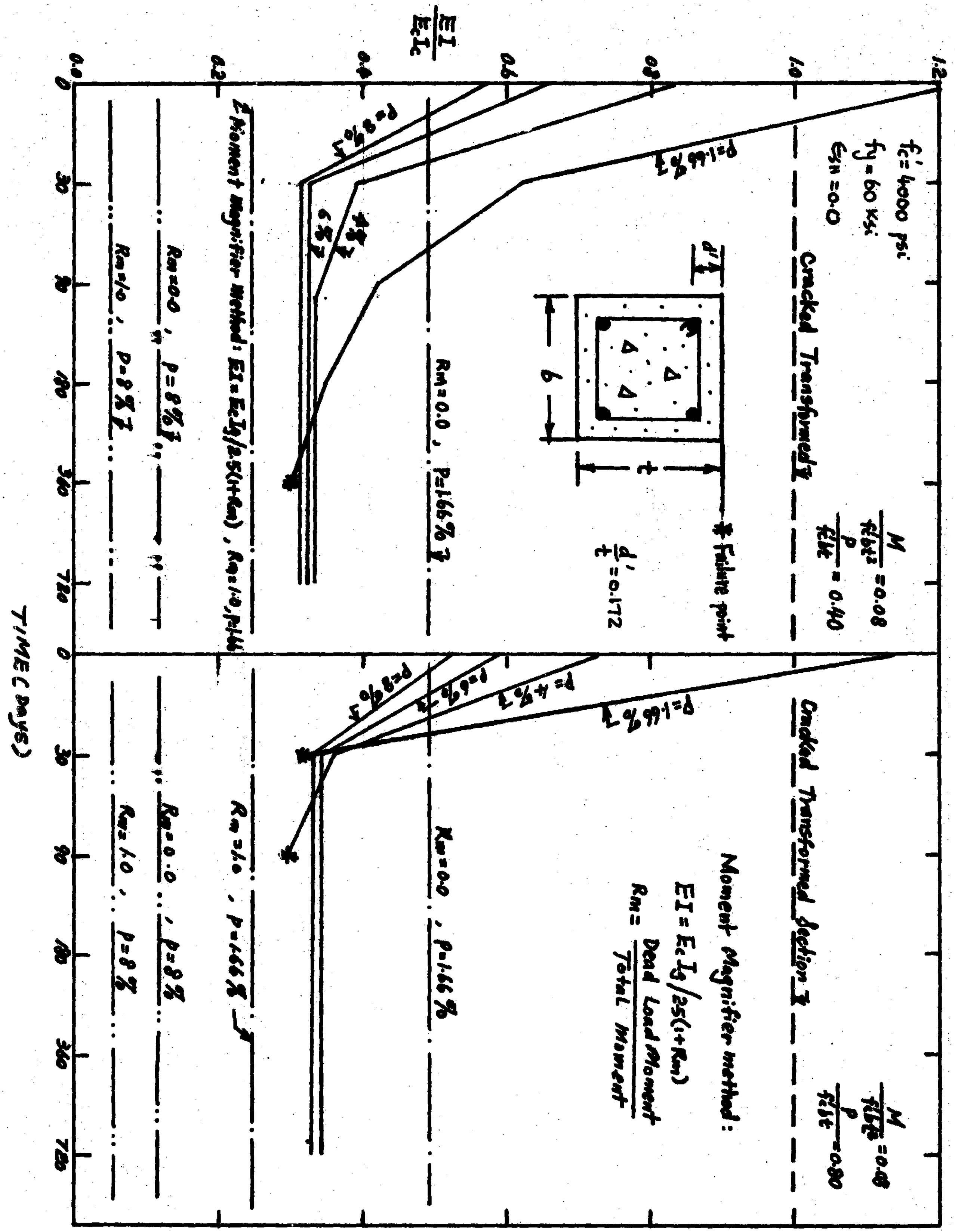

Figure 7.4

Comparison of EI with Varying p

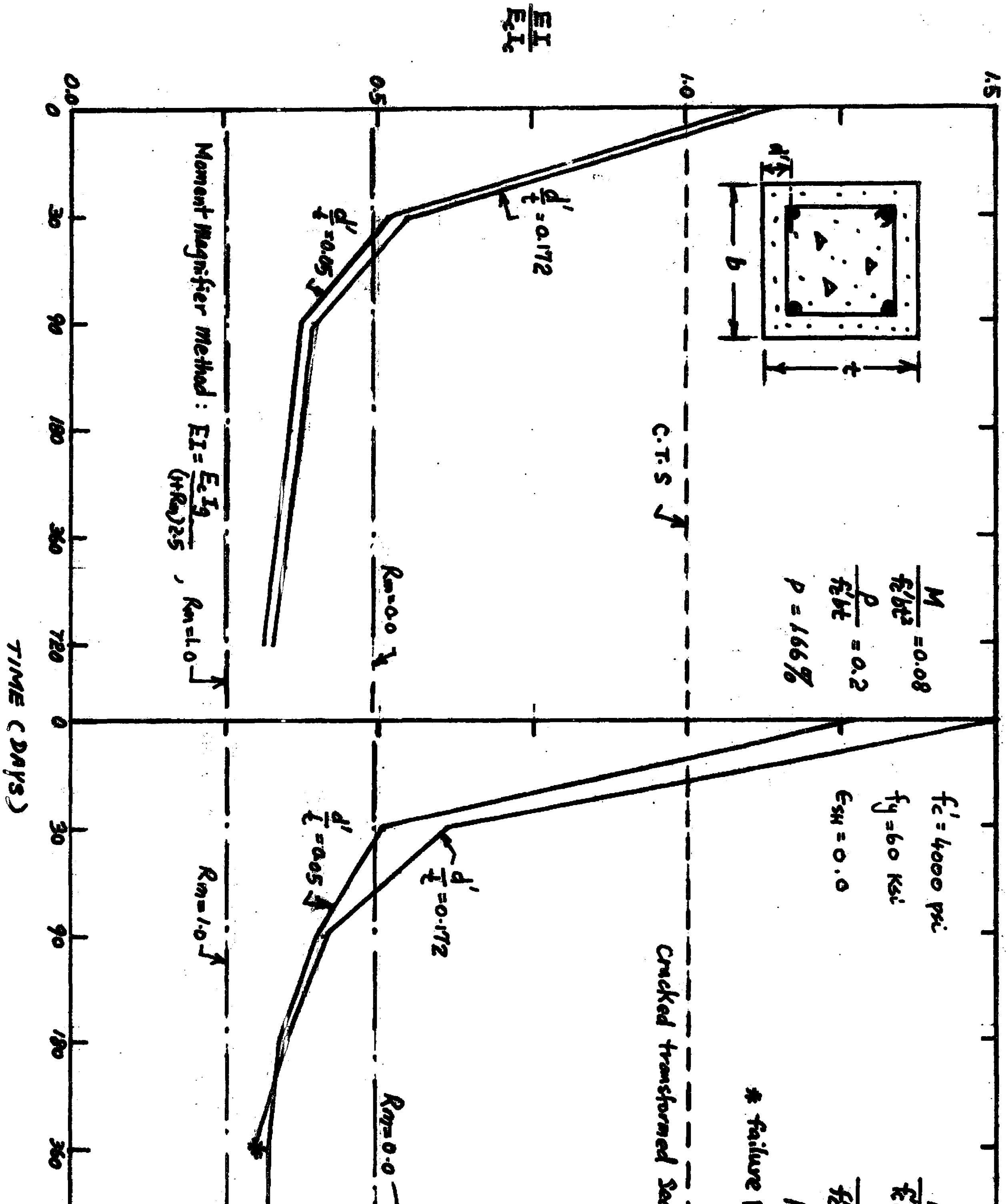

Figure 7.5

Comparison of EI with Varying d'/t

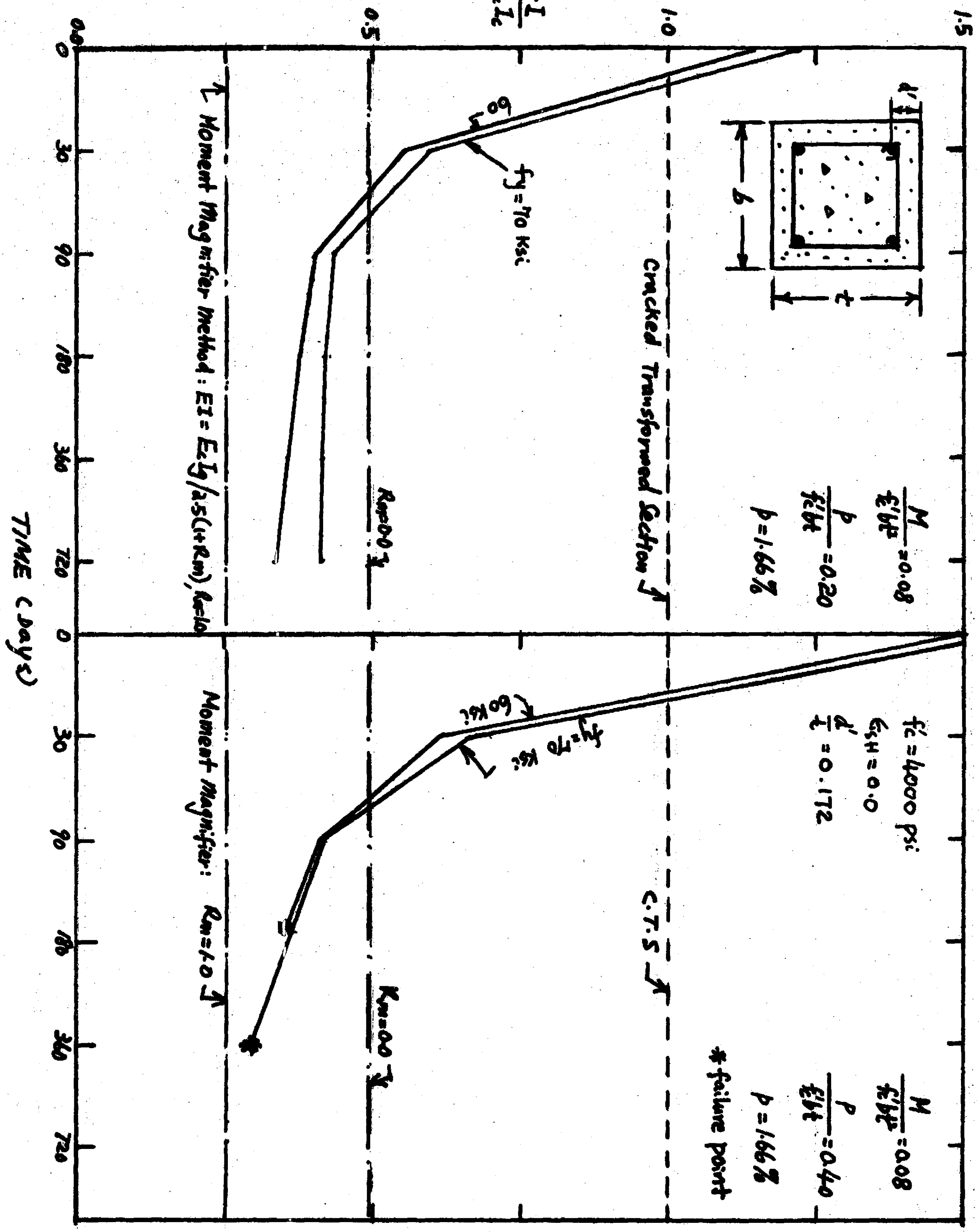

Figure 7.6

Comparison of EI with Varying f_y

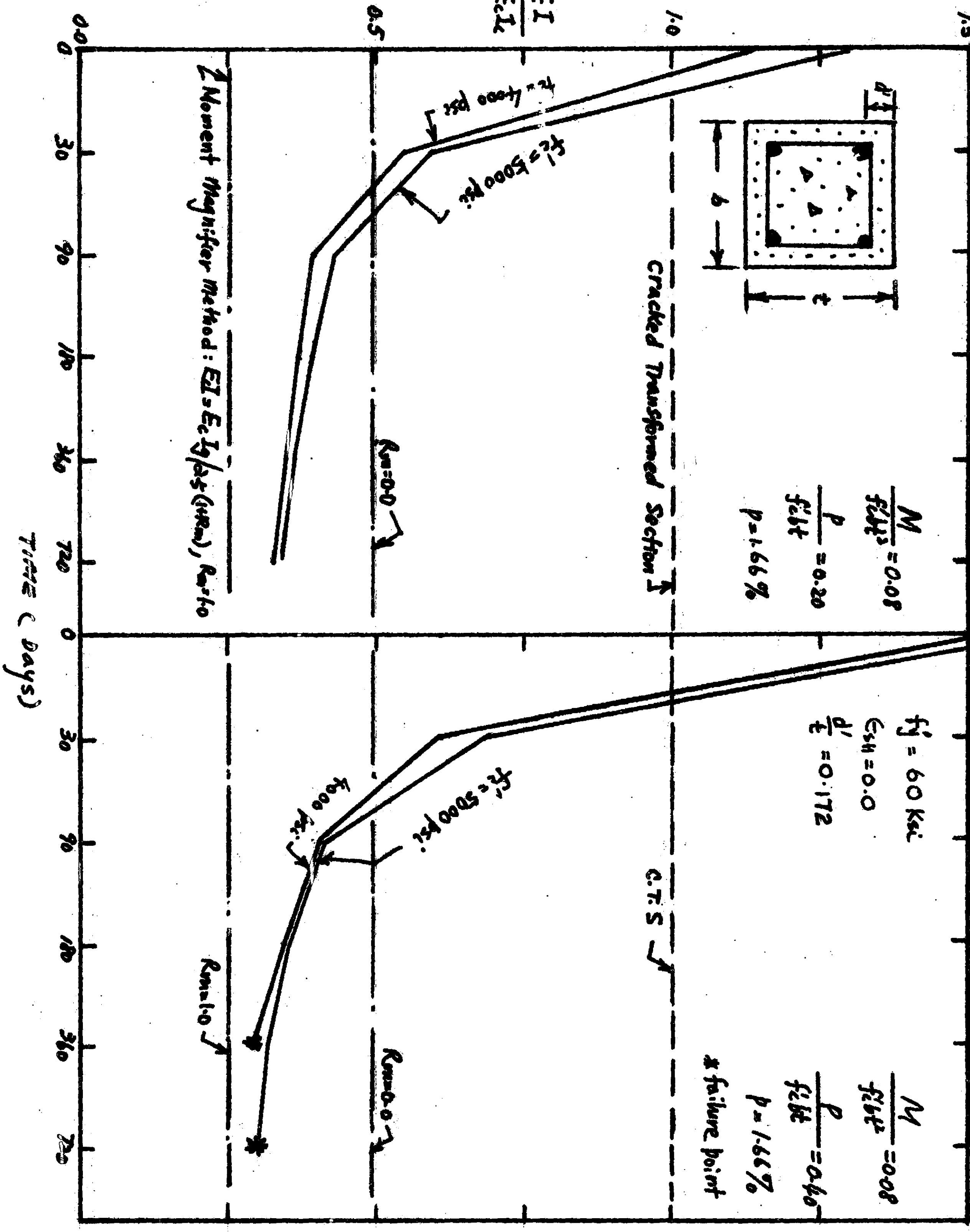

Figure 7.7

Comparison of EI with varying f'_c

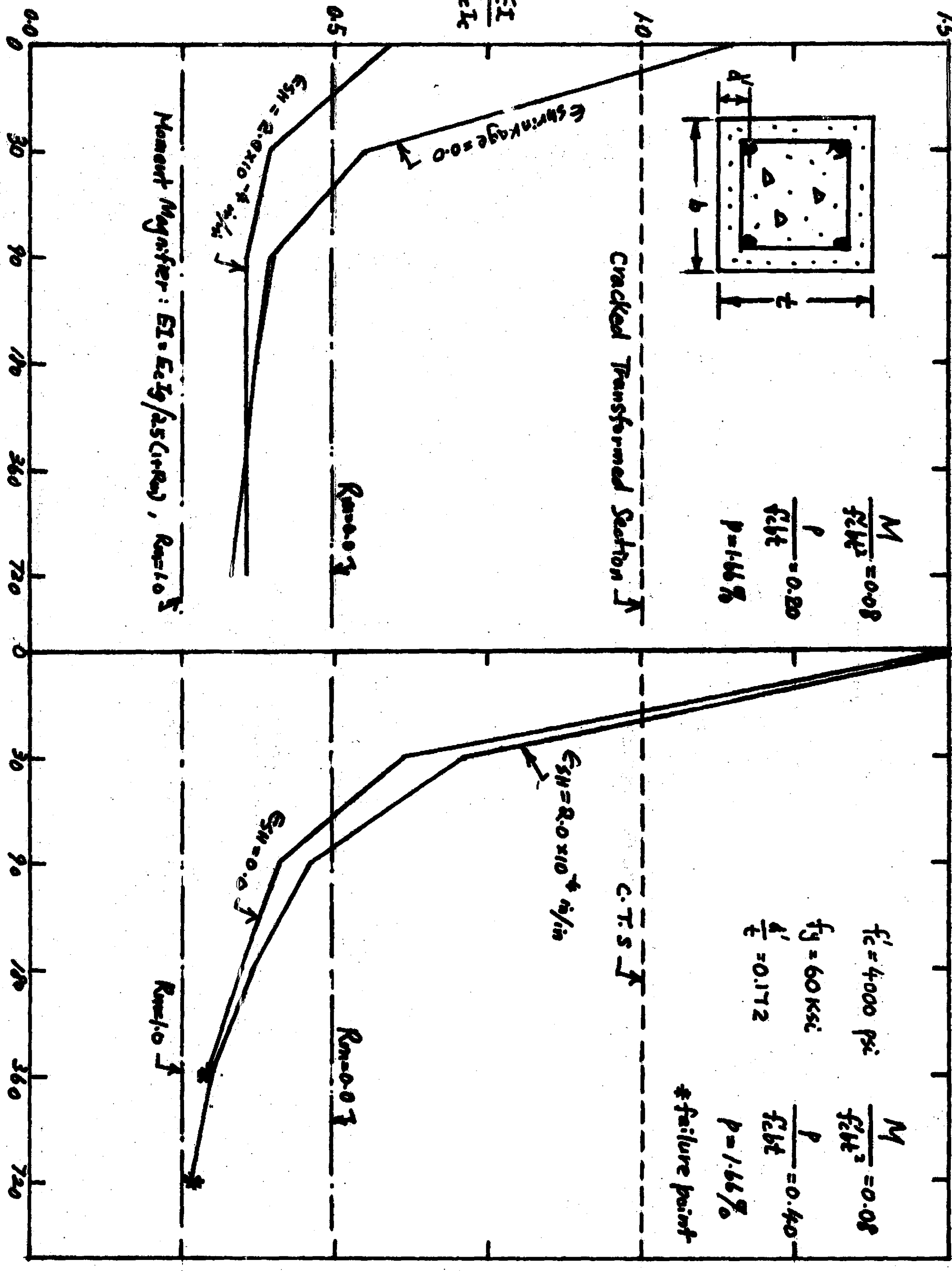

Figure 7.8

Comparison of EI with varying Shrinkage Strain

(7.4) Final Conclusion :

The following conclusions are made based on results reported in this research :

(1) The Matrix Stiffness-Modification Method which has been developed accurately predicts the behavior of real structures subjected to short-term and sustained loading with the provision that elastic and inelastic deformation characteristics of the concrete are properly modeled mathematically.

(2) The elastic matrix method using stiffnesses based on the cracked transformed section of concrete will give inadequated prediction of behavior of real structures especially when sustained loads or high levels of loading occur.

(3) The Moment Magnifier Method as recommended by the 1971 ACI Code gives a safe and realistic estimate of flexural stiffness EI for design of slender columns. It was also concluded that the Reduction Factor Method is unrealistic and may be unsafe (24).

(4) Additional studies have indicated that the Matrix Stiffness-Modification Technique can be easily modified to accomodate the analysis of prestressed concrete structures, composite structures and structures with variable cross-sections.

(5) For a realistic analysis of the behavior of single beam-column members in multistorey buildings, the partial nonlinear analysis using the Matrix Stiffness-Modification Method can be applied. It is intended that the development of this analytical technique will lead to a comprehensive evaluation of current column design procedure.

APPENDIX A

MATRIX STIFFNESS-MODIFICATION TECHNIQUE

COMPUTER PROGRAM

FOR

NONLINEAR ANALYSIS OF CONCRETE FRAMES

APPENDIX A

FORTRAN PROGRAM

Nomenclature :

The meanings of the important variables used in this program are listed below:

AASC(I)	Area of compression reinforcing steel
AAST(I)	Area of tensile reinforcing steel
CF	Length conversion factor
CYL	Concrete cylinder strength at 28 days
DDB(I)	Width of cross-section of element i
DDSC(I)	Distance from the centroid of the compression steel to the extreme compressive fibre of section
DDST(I)	Distance from the centroid of the tensile steel to the extreme compressive fibre of section
DDTH(I)	Total depth of cross-section of element i
EA(I)	Axial stiffness EA for element i
EI(I)	Flexural stiffness EI for element i
ES	Modulus of elasticity of reinforcing steel
FSY	Yield strength of steel
IIFROM(I)	Coordinate of end 1 of member i
IITO(I)	Coordinate of end 2 of member i
KJOIN	Joint number of which load is applied
NALLOW	Allowable cycle of iteration for subroutine "MPHI"
NELEM	Total number of elements in frame
NPLAST	Total number of inelastic element in frame
NSTRIP	Number of element strips in concrete cross-section

NJOIN	Total number of joints in frame
NCYCL	Number of iterative cycle in the main program
PHI, PHITRI	Curvature
PX	X-component of applied load
PY	Y-component of applied load
PMZ	Z-component of applied load
PCAL, BMCAL	Calculated axial force and bending moment acting at the centroid of a concrete cross-section.
T1, T2	Time increment , from time 1 to time 2
WEEP	Creep strain
WSHRINC	Shrinkage of concrete
WTENSIL	Allowable tensile strain of concrete
WU(L,I)	Effective or elastic strain of concrete
XP1(I)	X-coordinate of element i , end 1
XP2(I)	X-coordinate of element i, end 2
YP1(I)	Y-coordinate of element i, end 1
YP2(I)	Y-coordinate of element i, end 2

APPENDIX A

MATRIX STIFFNESS-MODIFICATION TECHNIQUE
FORTRAN PROGRAM FOR THE INELASTIC ANALYSIS OF CONCRETE FRAMES

BY K. B. TAN
GRADUATE STUDENT
DEPARTMENT OF CIVIL ENGINEERING
MCMASTER UNIVERSITY
HAMILTON , ONTARIO
CANADA

```
HRDC,CM100000,T400.
RUN(S)
SETINDF.
REDUCE.
LGO,LC,40000.
'         6400 END OF RECORD
      PROGRAM TST  (INPUT,OUTPUT,TAPE5=INPUT,TAPE6=OUTPUT)
      DIMENSION SAM(75,75),PD(75),IGLORP(1,2,30),D1(3),D2(3)
      DIMENSION GD1(3),GD2(3),FORC1(3),FORC2(3)  ,PDD(96)
      DIMENSION XA(3,3),XB(3,3),XE(3,3),XF(3,3),XINT1(5,5),XINT2(5,5)
      DIMENSION DD1(30),DD2(30),BBL(30),EI(30),EA(30)
      DIMENSION STIF1(5,5),STIF2(5,5),STIF3(5,5),STIF4(4,4)
      DIMENSION DDTH(30),DDB(30),AAST(30),AASC(30),DDST(30),DDSC(30)
      DIMENSION MEMBER(30),IIFROM(30),IITO(30),XP1(30),YP1(30),XP2(30)
      DIMENSION WU2(30,20),SEEP2(30,20),UUF1(30,20),UUF2(30,20).
      DIMENSION WEEP(30,20),WU1(30,20),SEEP1(30,20),CEEP(30,20)
      DIMENSION BMC(30),GDD(30),PAXIAL2(30),BMOM2(30),V2(30)
      DIMENSION YP2(30),NNR(30),IIR(30,4),EEII(20,30),EEAA(20,30)
      COMMON/BLOCK1/DTH,DB,AST,ASC,DST,DSC
      COMMON/BLOCK2/NSTRIP,KONT,T1,T2
      COMMON/BLOCK3/WSHRINS, WSHRINC
      COMMON/BLOCK4/WTENSIL, WY,FSY, CYL, TCF, NALLOW, ES
      COMMON/BLOCK5/PHITRI,WTRIAL
      COMMON/BLOCK7/XXP1,XXP2,YYP1,YYP2,EEI,EEA,KOUNT,CF
      COMMON/BLOK1/T(3,3)/BLOK2/TT(3,3)/BLOK3/SF(6,6)
      COMMON/BLOK4/RESTIF(5,5)/BLOK5/NR,IR(4)
      COMMON/BLOK6/STF11(3,3,30),STF12(3,3,30),STF21(3,3,30),
     1STF22(3,3,30),TTT(3,3,30)
      READ(5,7772)NA1,NA2,NA3,NA4,NA5,NA6,NA7,NA8,NA9,NA10,NA11,NA12,NB1
 7772 FORMAT(13A6)
      READ(5,15) MCYCL,CF
 15   FORMAT(I5,F10.3)
      READ(5,2)NJOIN,NELEM,NPLAST
 2    FORMAT(3I5)
      READ(5,1444)NSTRIP, NALLOW,WTENSIL,WSHRINC
 1444 FORMAT(2I5, 2E10.2)
      READ(5,1445)  CYL, FSY, ES
 1445 FORMAT(2F10.3, E10.3)
      DO 1004  I = 1, NELEM
      READ(5,5)MEMBER(I),IIFROM(I),IITO(I),NNR(I),XP1(I),YP1(I),XP2(I),
     1 YP2(I)
 5    FORMAT(4I5,4F10.3)
      IF(NNR(I))1008,1004,1008
 1008 NR = NNR(I)
      READ(5,20) (IIR(I,J), J = 1,NR)
 20   FORMAT(4I5)
 1004 CONTINUE
      DO 1007  I = 1, NELEM
      READ(5,1447)DDTH(I),DDB(I),AAST(I),AASC(I),DDST(I),DDSC(I)
 1447 FORMAT(6F10.3)
 1007 CONTINUE
      WCON= 145.00
      ECON=(33.0*(WCON)**1.5*(CYL*1000.)**0.5)/1000.
      WTRIAL = 1.00E-04
      PHITRI = WTRIAL/3.0
      TCF = 0.0
      NEC= ES/ECON
      ECS= NEC
      WY = FSY/ES
      WRITE(6,772)NA1,NA2,NA3,NA4,NA5,NA6,NA7,NA8,NA9,NA10,NA11,NA12,NB1
```

```
772  FORMAT(///35X,13A6///)
     WRITE(6,1001)
1001 FORMAT(1H0,30X,*COMPUTER ANALYSIS OF INELASTIC REINFORCED CONCRETE
    1 FRAME*/1H0,40X,*MATRIX METHOD OF STRUCTURAL ANALYSIS*/1H0,
    2 45X, *THESIS PROJECT,  BY K.B. TAN*/1H0,45X,*DEPARTMENT OF CIVIL
    3 ENGINEERING*/1H0,45X,*MCMASTER UNIVERSITY*///)
     WRITE(6,1002) MCYCL
1002 FORMAT(1H0, 40X,*ALLOWABLE MAXIMUM NO. OF ITERATION = *,I5)
     WRITE(6,1003) NJOIN, NELEM
1003 FORMAT(1H0,40X,*NUMBER OF DISCRETE JOINT = *,9X,I5/1H0,40X,
    1 *NUMBER OF FINITE ELEMENTS = * , 8X, I5)
     WRITE(6,8230) NSTRIP , NALLOW, WTENSIL
8230 FORMAT(1H0,40X,*NO. OF ELEMENT STRIP IN EACH CROSS-SECTION =*,I5/1
    11H0,40X,*PERMISSIBLE NO. OF CYCLE FOR MOMENT-CURVATURE ITERATION=*,
    2 I5/1H0,40X,*MAXIMUM CONCRETE TENSILE STRAIN =*,E12.5/)
     WRITE(6,2459)CYL,FSY,ES,WY
2459 FORMAT(1H0,40X,*CONCRETE CYLINDER STRENGTH AT AGE 28 DAYS =*,F15.5
    1/1H0,40X,*YIELD STRENGTH OF STEEL REINFORCEMENT =*,E15.5/1H0,40X,*
    2MODULUS OF ELASTICITY OF STEEL =*,E15.5/1H0,40X,*ULTIMATE STRAIN
    3OF STEEL =*, E15.5////)
     WRITE(6,1453)
1453 FORMAT(1H0,30X,*GEOMETRIC PROPERTIES OF CONCRETE ELEMENT CROSS-SEC
    1TION*//20X,12HELEMENT NO.    ,5X,5HTHICK,10X,5HWIDTH,5X,10HCOMP. AS
    2    5X,10HTENSION AS   ,5X,10HDIST. AST    ,5X,10HDIST. ASC     /)
     DO 1454 I = 1, NELEM
     WRITE(6,1457)I,DDTH(I),DDB(I),AAST(I),AASC(I),DDST(I),DDSC(I)
1457 FORMAT(1H,18X,I3,5X,6(5X,F10.3))
1454 CONTINUE
     WRITE(6,7696)
7696 FORMAT(1H0,15X,12HELEMENT NO.     ,10X,5HEND 1 ,5X,5HEND 2 ,5X,2HX1
   1,8X,2HY1,8X,2HX2,8X,2HY2,10X,5H EA   ,13X,3HEI  /)
     DO 1013  I = 1, NELEM
     DTH1=DDTH(I)
     DB1=DDB(I)
     AST1=AAST(I)
     ASC1=AASC(I)
     DST1=DDST(I)
     DSC1=DDSC(I)
     AA=DB1*0.50
     BB=ASC1*(2.0*ECS-1.0)+ECS*AST1
     CC=-ASC1*(2.0*ECS-1.0)*DST1-ECS*AST1*DST1
     XW=(-BB+(BB**2-4.0*AA*CC)**0.50)/(2.0*AA)
     EA(I)=ECON*DB1*DTH1
     EI(I)=ECON*(DB1*XW**3/3.0+ASC1*(2.0*ECS-1.)*(XW-DSC1)**2+ECS*AST1*
    1 (DST1 - XW)**2)
     WRITE(6,1006)MEMBER(I),IIFROM(I),IITO(I),XP1(I),YP1(I),XP2(I),
    1 YP2(I),  EA(I),EI(I)
1006 FORMAT(1H ,18X,I5,7X,2I10,4F10.3,E15.5,E18.5)
1013 CONTINUE
     JOINT=3*NJOIN
8147 READ(5,8148)IDEX
8148 FORMAT(I5)
     NM1=0
     NM2 = 0
     IF(IDEX.EQ.1) GO TO 9373
     DO 904 I=1,JOINT
904  PDD(I) = 0.0
 114 READ(5,3)KJOIN,INDEX,PX,PY,PMZ
3    FORMAT(2I5,3F10.3)
     JIND = 3*KJOIN -2
     JINE = JIND + 1
     JINF = JIND + 2
     PDD(JIND) = PX
     PDD(JINE) = PY
     PDD(JINF ) = PMZ
     IF(INDEX.EQ.0) GO TO 114
     WRITE(6,905)
905  FORMAT(1H1,35X,*APPLIED LOAD VECTORS*///1H0,16X,8HPX(KIPS),17X,
    1 8HPY(KIPS)    , 17X,10HMX(FT-KIP)     //)
     WRITE(6,903)(PDD(I),I = 1, JOINT)
903  FORMAT(3F25.5)
     IF( IDEX.GT.1) GO TO 1199
     DO 1977  J = 1, NELEM
     DO 1977  I = 1,NSTRIP
     CEEP(J,I) = 0.0
```

```
      SEEP1(J,I) = 0.0
      SEEP2(J,I) = 0.0
 1977 WEEP(J,I) = 0.0
 1199 CONTINUE
 9111 READ(5,9996) INDEXX, T1, T2
 9996 FORMAT(I5,2F10.3)
      IF(INDEXX.GT.0) GO TO 8147
      IF(NM1.GT.0.OR.NM2.GT.0) GO TO 9111
      NCYCL = 0
 16   NCYCL = NCYCL + 1
      WRITE(6,1010) NCYCL
 1010 FORMAT(1H0//1H0,80X,*ITERATION NO.*,2X,I3//)
      WRITE(6,9172)T1,T2
 9172 FORMAT(1H0,20X,8HTIME 1 =   ,F10.3,5X,8HTIME 2 =   ,F10.3/)
      DO 3773  I = 1, JOINT
      PD(I) = PDD(I)
 3773 CONTINUE
      DO 7 I=1,NJOIN
      IIIJ=3*I
      PD(IIIJ)=12.0*PD(IIIJ)
    7 CONTINUE
      DO 2008 I = 1, NELEM
      EEAA(NCYCL,I) = EA(I)
 2008 EEII(NCYCL,I) = EI(I)
      IF(NCYCL.LE.1) GO TO 2001
      DO 2002  I = 1, NELEM
      GDD(I) = DD2(I)
      EI(I) =(EEII(NCYCL,I)+EEII(NCYCL-1,I))*0.50
 2002 EA(I) =(EEAA(NCYCL,I)+EEAA(NCYCL-1,I))*0.50
      IF(NCYCL-5)2001,2003,2003
 2003 DO 2005 I = 1, NELEM
      EI(I)=(EEII(NCYCL,I)+EEII(NCYCL-1,I)+EEII(NCYCL-2,I))/3.0
 2005 EA(I)=(EEAA(NCYCL,I)+EEAA(NCYCL-1,I)+EEAA(NCYCL-2,I))/3.0
      IF(NCYCL-8)2001,2006,2006
 2006 DO 2007  I = 1, NELEM
      EI(I)=(EEII(NCYCL,I)+EEII(NCYCL-1,I)+EEII(NCYCL-2,I)+EEII(NCYCL-3,
     1 I))/4.0
 2007 EA(I)=(EEAA(NCYCL,I)+EEAA(NCYCL-1,I)+EEAA(NCYCL-2,I)+EEAA(NCYCL-3,
     1 I))/4.0
 2001 DO 5000 II = 1, NELEM
      KOUNT = II
      XXP1 = XP1(II)
      YYP1 = YP1(II)
      XXP2 = XP2(II)
      YYP2 = YP2(II)
      BBL(II)= (  ((XXP2-XXP1)**2 +(YYP2-YYP1)**2)**0.5   )*CF
      EEI = EI(II)
      EEA = EA(II)
      IFROM = IIFROM(II)
      ITO = IITO(II)
      IF(NNR(II) .EQ.0)GO TO 100
      NR = NNR(II)
      DO 1009 I = 1, NR
 1009 IR(I)  = IIR(II,I)
C     CHECK EQUILIBRIUM CONDITIONS IN MEMBER CONTAINING RELEASES
      CALL BALANCE
      IF(NR.GE.5)GO TO 124
C     FORMULATE MEMBER STIFFNESS MATRIX IN MEMBER COORDINATES
      CALL STIFFN
C     ARRANGE THE ELEMENTS OF STIFFNESS MATRIX FOR PARTITIONING
      CALL ARRANGE
C     PARTITION OF STIFFNESS MATRIX
      N=6-NR
      DO 25 I=1,N
      DO 25 J=1,N
      STIF1(I,J)=SF(I,J)
   25 CONTINUE
C     IF K1 ONLY IS NONSINGULAR, DELETE CALCULATION OF K2, K3, K4
      IF(NR.EQ.4)GO TO 81
      DO 30 J=1,NR
      NM=J+N
      DO 30 I=1,N
      STIF2(I,J)=SF(I,NM)
   30 CONTINUE
```

```
      DO 40 I=1,NR
      NI=I+N
      DO*40 J=1,N
      STIF3(I,J)=SF(NI,J)
   40 CONTINUE
      DO 50 I=1,NR
      NNI=I+N
      DO 50 J=1,NR
      NNJ=J+N
      STIF4(I,J)=SF(NNI,NNJ)
   50 CONTINUE
C     INVERT K4 TO OBTAIN K4-INVERSE
      CALL INVMAT(STIF4,4,NR,1E-07,IERR,N1)
      IF(IERR.NE.0)GO TO 126
      DO 60 I=1,5
      DO 60 J=1,5
      XINT1(I,J)=0.0
      XINT2(I,J)=0.0
   60 CONTINUE
      DO 70 I=1,NR
      DO 70 J=1,N
      DO 70 K=1,NR
      XINT1(I,J)=XINT1(I,J)+STIF4(I,K)*STIF3(K,J)
   70 CONTINUE
      DO 75 I=1,N
      DO 75 J=1,N
      DO 75 K=1,NR
      XINT2(I,J)=XINT2(I,J)+STIF2(I,K)*XINT1(K,J)
   75 CONTINUE
C     CALCULATE REDUCED STIFFNESS MATRIX, OF SIZE N X N
      DO 80 I=1,N
      DO 80 J=1,N
      RESTIF(I,J)=STIF1(I,J)-XINT2(I,J)
   80 CONTINUE
      GO TO 83
C     CALCULATE REDUCED STIFFNESS MATRIX, OF SIZE N X N (FOR 4 RELEASES)
   81 DO 82 I=1,N
      DO 82 J=1,N
      RESTIF(I,J)=STIF1(I,J)
   82 CONTINUE
C     EXPAND REDUCED STIFFNESS MATRIX TO FULL 6 X 6 BY INTRODUCTION OF
C         APPROPRIATE NULL ELEMENTS
 83   CALL ENLARGE(N)
C     PARTITION AND STORE REDUCED MEMBER STIFFNESS MATRIX
      DO 400 I=1,3
      DO 400 J=1,3
      STF11(I,J,KOUNT)=SF(I,J)
      STF12(I,J,KOUNT)=SF(I,J+3)
      STF21(I,J,KOUNT)=SF(I+3,J)
      STF22(I,J,KOUNT)=SF(I+3,J+3)
 400  CONTINUE
      DO 85 I=1,3
      DO 85 J=1,3
      XA(I,J)=SF(I,J)
      XB(I,J)=SF(I,J+3)
      XE(I,J)=SF(I+3,J)
      XF(I,J)=SF(I+3,J+3)
   85 CONTINUE
C     TRANSFORM STIFFNESS MATRIX TO GLOBAL COORDINATES
      CALL TRANSF(XA,1,1)
      CALL TRANSF(XB,1,4)
      CALL TRANSF(XE,4,1)
      CALL TRANSF(XF,4,4)
      GO TO 110
 100  CALL STIFFN
  110 IF(KOUNT.GE.2)GO TO 134
      DO 130 I=1,JOINT
      DO 130 J=1,JOINT
      SAM(I,J)=0.0
  130 CONTINUE
  134 IF(IFROM.EQ.0)GO TO 501
C     ADD K11, K12, K21, K22 TO ASSEMBLY MATRIX AT CORRECT LOCATION.
      DO 135 I=1,3
      DO 135 J=1,3
```

```
      IFROG = I + 3*(IFROM - 1)
      JFROG=J+3*(IFROM-1)
      ITOAD=I+3*(ITO-1)
      JTOAD=J+3*(ITO-1)
      SAM(IFROG,JFROG)=SAM(IFROG,JFROG)+SF(I,J)
      SAM(IFROG,JTOAD)=SAM(IFROG,JTOAD)+SF(I,J+3)
      SAM(ITOAD,JFROG)=SAM(ITOAD,JFROG)+SF(I+3,J)
      SAM(ITOAD,JTOAD)=SAM(ITOAD,JTOAD)+SF(I+3,J+3)
  135 CONTINUE
      GO TO 505
C     ADD K22 TO ASSEMBLY MATRIX FOR MEMBERS CONNECTING TO BASE JOINTS
  501 DO 502 I=1,3
      DO 502 J=1,3
      ITOAD=I+3*(ITO-1)
      JTOAD=J+3*(ITO-1)
      SAM(ITOAD,JTOAD)=SAM(ITOAD,JTOAD)+SF(I+3,J+3)
  502 CONTINUE
C     STORE JOINT NUMBERS CORRESPONDING TO MEMBER NUMBER
  505 IGLORP(1,1,KOUNT)=IFROM
      IGLORP(1,2,KOUNT)=ITO
C     WHEN ALL MEMBERS HAVE BEEN PROCESSED, PROCEED WITH SOLUTION
 5000 CONTINUE
C     SOLVE FOR JOINT DISPLACEMENTS USING LIBRARY SUBROUTINE 'SOLVE'
  160 CALL SOLVE(SAM,PD,ID,JOINT,75)
      WRITE(6,165)
 165  FORMAT(1H0,/ 15X     ,*MEMBER DISPLACEMENT (INCH) IN GLOBAL COORDI
     1NATE AND MEMBER FORCE(KIP AND IN-K) IN MEMBER COORDINATE */)
      WRITE(6,1666)
 1666 FORMAT(1H0       ,49X,12HX-DIRECTION   ,18X,12HY-DIRECTION     18X,
     1 12HZ-DIRECTION        )
      DO 250 K=1,NELEM
      JNO1=IGLORP(1,1,K)
      JNO2=IGLORP(1,2,K)
      IF(JNO1.EQ.0)GO TO 510
      NOPD1=3*(JNO1-1)
      NOPD2=3*(JNO2-1)
C     OBTAIN GLOBAL DISPLACEMENTS FROM SOLUTION VECTOR.  WRITE VA
      DO 200 I=1,3
      IPD1 = I + NOPD1
      IPD2=I+NOPD2
      GD1(I)=PD(IPD1)
      GD2(I)=PD(IPD2)
  200 CONTINUE
      WRITE(6,190) K ,(GD1(I),I = 1,3)
 190  FORMAT(1H0,         10X,11HMEMBER NO.   ,I3/1H ,10X,13HDISPL-END 1   ,
     1 7X,3E30.5)
      WRITE(6,191)(GD2(I),I=1,3)
 191  FORMAT(1H ,10X,13HDISPL-END 2    ,7X,3E30.5)
      DO 205 I= 1,3
      D1(I)=0.0
      D2(I)=0.0
      FORC1(I) = 0.0
      FORC2(I) = 0.0
  205 CONTINUE
      DO 405 L=1,3
      DO 405 M=1,3
      D1(L)=D1(L)+OTT(L,M,K)*GD1(M)
      D2(L)=D2(L)+TTT(L,M,K)*GD2(M)
  405 CONTINUE
C     CALCULATE MEMBER FORCES IN MEMBER COORDINATES
      DO 210 I=1,3
      DO 210 J=1,3
      FORC1(I)=FORC1(I)+STF11(I,J,K)*D1(J)+STF12(I,J,K)*D2(J)
      FORC2(I)=FORC2(I)+STF21(I,J,K)*D1(J)+STF22(I,J,K)*D2(J)
  210 CONTINUE
      WRITE(6,215)(FORC1(I),I=1,3)
 215  FORMAT(1H ,10X,13HFORCE-END 1    ,7X,3E30.5)
      WRITE(6,216)(FORC2(I),I=1,3)
 216  FORMAT(1H ,10X,13HFORCE-END 2    ,7X,3E30.5)
      GO TO 259
  510 NOPD2=3*(JNO2-1)
      DO 515 I=1,3
      IPD2=I+NOPD2
      GD2(I)=PD(IPD2)
```

```
 515 CONTINUE
     WRITE(6,516) K,(GD2(I),I = 1,3)
516  FORMAT(1H0,          10X,11HMEMBER NO.  ,I3/1H ,10X,13HDISPL-END 2   ,
    1 7X,3E30.5)
     DO 520 I=1,3
     D2(I)=0.0
     FORC1(I)=0.0
     FORC2(I)=0.0
 520 CONTINUE
     DO 525 L=1,3
     DO 525 M=1,3
     D2(L)=D2(L)+TTT(L,M,K)*GD2(M)
     D1(L) = 0.0
 525 CONTINUE
     DO 530 I=1,3
     DO 530 J=1,3
     FORC1(I)=FORC1(I)+STF12(I,J,K)*D2(J)
     FORC2(I)=FORC2(I)+STF22(I,J,K)*D2(J)
 530 CONTINUE
     WRITE(6,535)(FORC1(I),I=1,3)
535  FORMAT(1H ,10X,13HFORCE-END 1    ,7X,3E30.5)
     WRITE(6,536)(FORC2(I),I=1,3)
536  FORMAT(1H ,10X,13HFORCE-END 2    ,7X,3E30.5)
259  PAXIAL2(K) = -FORC2(1)
     V2(K) =-FORC2(2)
     BMOM2(K) =-FORC2(3)
     DD1(K) = D1(2)
     DD2 (K) =-D2(2)
 250 CONTINUE
     IF(NCYCL.LE.1) GO TO 9573
     KADD2 = 0
     KADD= 0
     DO 7379  I = 1, NELEM
     RATIO1= ( EEII(NCYCL,I)-EEII(NCYCL-1,I))/EEII(NCYCL,I)
     RATIO2= ( EEAA(NCYCL,I)-EEAA(NCYCL-1,I))/EEAA(NCYCL,I)
     RATIO3=(GDD(I)-DD2(I))/DD2(I)
     IF(ABS(RATIO1).LE.0.01.AND.ABS(RATIO2).LE.0.01) KADD2= KADD2+ 1
     IF(ABS(RATIO3).LE.0.01) KADD=KADD+1
7379 CONTINUE
     IF(KADD.EQ.NELEM.OR.KADD2.EQ.NELEM)GO TO 5555
     GO TO 9573
5555 WRITE(6,9273)
9273 FORMAT(1H0,40X,*- - - - - - CORRECT ANSWER - - - - - - -*/1H1)
     GO TO 9111
9573  DO 733  JJ= 1, NELEM
     BMC(JJ)=BMOM2(JJ)+V2(JJ)*BBL(JJ)*0.50+PAXIAL2(JJ)*(DD2(JJ)+DD1(JJ)
    1 )*0.50
733  CONTINUE
     WRITE(6,610)
610  FORMAT(///1H0,13X,5HWCONC , 8X, 5HWTENS         ,7X,12H  CURVATURE
    1,6X,10HAXIAL P    ,2X,10HAPPLIED M ,5X,10H    EI          ,4X, 5H  EA ,
    2 10X,5H R     /)
     DO 9991 I = 1, NELEM
     IF(I.GT.NPLAST) GO TO 126
     KONT = I
     ASC = AASC(I)
     AST = AAST(I)
     DB = DDB(I)
     DTH = DDTH(I)
     DST = DDST(I)
     DSC = DDSC(I)
     PAX1 = PAXIAL2(I)
     BMCL= ABS(BMC(I))
     DCGC = (DB*DTH**2*0.5+AST*DST+ASC*DSC)/(DB*DTH + ASC + AST)
     WTRIAL = (BMCL*DCGC)/EI(I) + PAX1/EA(I)
     WBOT = (BMCL*DCGC)/EI(I) - PAX1/EA(I)
     PHITRI =(WTRIAL + WBOT)/ DTH
     CALL MPHI(PAX1,BMCL,WW1,PHI1,WEEP,WU1,SEEP1,NM1,UUF1,WTN)
     IF(NM1.GT.0) GO TO 9111
     WTRIAL = (BMCL*DCGC)/EI(I)
     PHITRI = WTRIAL / DCGC
     CALL MPHI(0.0,BMCL,WP1,PHIP1,CEEP,WU2,SEEP2,NM2,UUF2,W9)
     IF(NM2.GT.0) GO TO 9111
     IF(KADD2.EQ.NELEM.OR.KADD.EQ.NELEM ) GO TO 1279
```

```
      DO 1239  L2 = 1, NSTRIP
      WEEP(I,L2)=WEEP(I,L2)-SEEP1(I,L2)
 1239 CEEP(I,L2)=CEEP(I,L2)-SEEP2(I,L2)
 1279 CONTINUE
      DNAX3 = WP1/PHIP1
      DNAX1 = WW1/PHI1
      WCGC1 = PHI1*(DNAX1-DCGC)
      WCGCP1 = PHIP1*(DNAX3-DCGC)
      WAXIAL1 = WCGC1-WCGCP1
      IF(WAXIAL1.EQ.0.)WAXIAL1=WCGC1
      EI(I) = ABS(BMCL/PHI1)
      EA(I) = ABS(PAX1/WAXIAL1)
      RC =(EI(I)/EA(I))**0.50
      WRITE(6,613) WW1,WTN,PHI1,PAX1,BMCL,EI(I),EA(I) ,RC
 613  FORMAT(1H ,5X,3E15.5,5E14.5)
 9991 CONTINUE
      GO TO 126
  124 WRITE(6,125) KOUNT
  125 FORMAT(45H SYSTEM UNSTABLE. TOO MANY RELEASES IN MEMBER,I3)
      WRITE(6,127) IFROM,ITO
  127 FORMAT((33H REPLACE BY FORCE ACTING AT JOINT,I3),(9H OR JOINT,I3))
      CALL EXIT
 126  IF(NCYCL.LT.MCYCL)GO TO 16
      WRITE(6,8127)
 8127 FORMAT(///40X,*- - - - - -  NO CONVERGENCE - - - - - - - -- - - -*/)
      GO TO 9111
 9373 WRITE(6,8012)
 8012 FORMAT(1H0,////1H0,50X,*END OF PROGRAM*)
      CALL EXIT
      END
```

```
      SUBROUTINE ARRANGE
C     THIS SUBROUTINE REPOSITIONS THE COLUMNS OF THE STIFFNESS MATRIX,
C     IN PREPARATION FOR THE PARTITIONING OF SF, AND THE SUBSEQUENT
C     MULTIPLICATION OF THE PARTITIONED SUBMATRICES.
      COMMON/BLOK3/SF(6,6)
      COMMON/BLOK5/NR,IR(4)
      DIMENSION WMAT(7,7)
C     TRANSFER STIFFNESS MATRIX (MEMBER COORD'S) TO WORKING MATRIX WMAT
      DO 3 I=1,6
      DO 3 J=1,6
      WMAT(I,J)=SF(I,J)
    3 CONTINUE
C     TRANSFER COLUMNS CONTAINING RELEASES FROM PRESENT POSITIONS IN
C        WMAT TO EXTREME RIGHT-HAND SIDE OF MATRIX.  INTERMEDIATE STEP
C        CONSISTS OF TRANSFER FROM PRESENT POSITION TO COLUMN 7, THEN
C        MOVING ALL COLUMNS ONE POSITION TO THE LEFT.
      DO 7 K=1,NR
      KRAP=IR(K)-K+1
      DO 4 I=1,6
      WMAT(I,7)=WMAT(I,KRAP)
    4 CONTINUE
      DO 6 J=KRAP,6
      DO 6 I=1,6
      WMAT(I,J)=WMAT(I,J+1)
    6 CONTINUE
    7 CONTINUE
C     TRANSFER ALL ROWS CONTAINING RELEASES FROM PRESENT POSITIONS TO
C        BY PREVIOUS COLUMN SHIFT).
      DO 12 K=1,NR
      KRR=IR(K)-K+1
      DO 11 J=1,7
      WMAT(7,J)=WMAT(KRR,J)
   11 CONTINUE
      DO*10 I=KRR,6
      DO*10 J=1,7
      WMAT(I,J)=WMAT(I+1,J)
   10 CONTINUE
   12 CONTINUE
C     TRANSFER RE-ARRANGED STIFFNESS MATRIX (WMAT) BACK TO SF AND
C        RETURN TO MAIN PROGRAM.
      DO 8 I=1,6
      DO 8 J=1,6
      SF(I,J)=WMAT(I,J)
    8 CONTINUE
      RETURN
      END
```

```
      SUBROUTINE BALANCE
C     THIS SUBROUTINE CHECKS THE EQUILIBRIUM CONDITIONS FOR POSSIBLE
C     ERRONEOUS SPECIFICATION OF MEMBER RELEASES.
      COMMON/BLOK5/NR,IR(4)
      DIMENSION IP(6)
C     GENERATE INTEGER ARRAY OF 6 ELEMENTS, SUCH THAT ELEMENT VALUE IS
C         IDENTICAL WITH SUBSCRIPT VALUE.  CALL THIS ARRAY 'IP'.
      DO 5 K=1,6
      IP(K)=K
    5 CONTINUE
      DO 10 L=1,NR
      KK=IR(L)
      IP(KK)=0
   10 CONTINUE
C     CHECK AXIAL AND SHEAR FORCE EQUILIBRIUM.  IF EITHER P1X OR P2X
C         IS ZERO, SET BOTH EQUAL TO ZERO.  (SIMILARLY FOR P1Y, P2Y)
      ICHEK1=IP(1)*IP(4)
      ICHEK2=IP(2)*IP(5)
      IF(ICHEK1.EQ.0)GO TO 30
   15 IF(ICHEK2.EQ.0)GO TO 35
      GO TO 50
   30 IP(1)=0
      IP(4)=0
      GO TO 15
   35 IP(2)=0
      IP(5)=0
C     CHECK MOMENT EQUILIBRIUM FOR ALL 3 POSSIBILITIES OF NON-RESTRAINT
C         AND ADJUST ACCORDINGLY.
   50 ICHEK3=IP(3)+IP(6)+10*IP(2)
      IF(ICHEK3.EQ.20)GO TO 60
      IF(ICHEK3.EQ.6) GO TO 65
      IF(ICHEK3.EQ.3)GO TO 70
      GO TO 90
   60 IP(2)=0
      IP(5)=0
      GO TO 90
   65 IP(6)=0
      GO TO 90
   70 IP(3)=0
C     SPECIFY ACTUAL NUMBER OF RELEASES IN SYSTEM FOR EQUILIBRIUM (WITH
   90 KOUNT=0
      DO 95 I=1,6
      ISNIK=IP(I)
      IF(ISNIK.NE.0)GO TO 95
      KOUNT=KOUNT+1
      IR(KOUNT)=I
      NR=KOUNT
   95 CONTINUE
      RETURN
      END
```

```
      SUBROUTINE BMPCAL(W,PHI,PCAL,BMCAL,WU,WEEP,CYL,W4)
      COMMON/BLOCK1/DTH,DB,AST,ASC,DST,DSC
      COMMON/BLOCK2/NSTRIP,L,T1,T2
      COMMON/BLOCK3/WSHRINS, WSHRINC
      COMMON/BLOCK4/WTENSIL, WY,FSY,FCYL, TCF, NALLOW, ES
      DIMENSION WEEP(30,20), WU(30,20)
      DL = DTH/NSTRIP
      DCGC = (DB*DTH**2*0.5+AST*DST+ASC*DSC)/(DB*DTH + ASC + AST)
      W1 = W
      DNAXIS = W1/PHI
      W2 =(DNAXIS - DSC)*PHI  + WSHRINS
      W3 =(DNAXIS - DST)*PHI  + WSHRINS
      W4 = PHI*(DNAXIS-DTH)
      DX = DCGC + 0.5*DL
      PCON = 0.0
      BMCON = 0.0
      DO 100  I = 1, NSTRIP
      DX = DX - DL
      WU(L,I)=PHI*(DNAXIS+DL*0.50-DL*FLOAT(I)) -WEEP(L,I) - WSHRINC
      WX = WU(L,I)
      IF(WX+WTENSIL)10,20,20
10    STRESS = 0.0
      GO TO 30
20    STRESS=CYL*(-4.5005079E+09*WX**4+7.6164509E+07*WX**3-4.8022754E+05
     1 *WX**2 +1.1902628E+03*WX)
30    PCONCR = STRESS*DB*DL
      BMCONC = PCONCR *DX
      PCON = PCON + PCONCR
      BMCON = BMCON + BMCONC
100   CONTINUE
      IF(W2.EQ.0.) W2 = 1.0
      IF(W3.EQ.0.0) W3 = 1.0
      WA= ABS(W2)
      WB= ABS(W3)
      STEEL2= FSY*W2*(WA+WY-ABS(WA-WY))/(2.0*WY*WA)
      STEEL3= FSY*W3*(WB+WY-ABS(WB-WY))/(2.0*WY*WB)
      IF(W2.EQ.0.) STEEL2= 0.0
      IF(W3.EQ.0.) STEEL3=0.0
      PS2 = ASC*STEEL2
      PS3= AST*STEEL3
      BMS2 = PS2*(DCGC-DSC)
      BMS3 = PS3*(DCGC -DST)
      PCAL = PCON +PS2+PS3
      BMCAL = BMCON + BMS2+BMS3
      RETURN
      END
```

```
      SUBROUTINE CREEP(WEEP,WU,SEEP,UUF1)
      COMMON/BLOCK2/NSTRIP,KONT,T1,T2
      DIMENSION WEEP(30,20),WU(30,20),SEEP(30,20),UUF1(30,20)
      A1 = -1.03050E+06
      A2 = 5.748870E+02
      A3 = - 3.776740E-01
      A4 = - 3.072250E-06
      B1 = 1.858390E+06
      B2 = -1.012295E+03
      B3=1.5215225E+00
      B4 = -7.9862500E-06
      L = KONT
      IF(T1.GT.0.0) GO TO 87
      SHRINK=-0.000111+0.000224*ALOG10(T2)
      GO TO 88
   87 IF(T2.GT.700.)  GO TO 129
      SHRINK=0.000224*(ALOG10(T2)-ALOG10(T1))
      GO TO 88
  129 SHRINK = 0.000224*(ALOG10(700.) - ALOG10(T1))
   88 SSRR= SHRINK
      IF(T1.GT.700.) SSRR = 0.
      IF(T1.GT.0.0) GO TO 67
      DO 69  I = 1,NSTRIP
      CLU=WU(L,I)
      X= CLU
      IF( X )124,124,125
  125 WEEP(L,I)=(A1*X**3+A2*X**2+A3*X+A4)+(B1*X**3+B2*X**2+B3*X+B4)*
     1 ALOG10(T2)+ SSRR
      UUF1(L,I)= X
      GO TO 96
  124 WEEP(L,I) = SSRR
      UUF1(L,I) = 0.0
   96 SEEP(L,I) = WEEP(L,I)
   69 CONTINUE
      RETURN
   67 DO 75  I = 1, NSTRIP
      CLU = WU(L,I)
      X = CLU
      IF( X )988,988,987
  987 OLDU=ABS( X -UUF1(L,I))
      Y = OLDU
      SOLD=(A1*Y**3+A2*Y**2+A3*Y+A4)+(B1*Y**3+B2*Y**2+B3*Y+B4)*ALOG10(T2
     1  - T1)
      SEEP(L,I)=(B1*X**3+B2*X**2+B3*X+B4)*(ALOG10(T2)-ALOG10(T1))+SSRR+
     1 SOLD
      WEEP(L,I)=WEEP(L,I)+SEEP(L,I)
      UUF1(L,I)= CLU
      GO TO 75
  988 WEEP(L,I)=WEEP(L,I)+SSRR
      UUF1(L,I) = 0.
      SEEP(L,I) = SSRR
   75 CONTINUE
      RETURN
      END
```

```
      SUBROUTINE ENLARGE(N)
C     TO ENLARGE THE REDUCED STIFFNESS MATRIX TO THE ORIGINAL SIZE(6X6)
      COMMON/BLOK3/SF(6,6)/BLOK4/R(5,5)/BLOK5/NR,IR(4)
      DIMENSION RINT1(6,6),RINT2(6,6)
C     TRANSFER REDUCED STIFFNESS MATRIX, R, TO WORKING MATRIX RINT1
      DO 5 I=1,N
      DO 5 J=1,N
      RINT1(I,J)=R(I,J)
    5 CONTINUE
C     TRANSFER ALL COLUMNS, WHICH HAVE NUMBERS EQUAL TO OR GREATER THAN
C        THE RELEASE CODE NUMBERS, ONE POSITION TO THE RIGHT.
C        POPULATE THE COLUMNS HAVING NUMBERS EQUAL TO RELEASE CODE
C        NUMBERS WITH ZERO ELEMENTS.
      DO 10 K=1,NR
      KRAP=IR(K)-K+1
      IF(KRAP.LE.N)GO TO 6
      KKRAP=IR(K)
      DO 40 I=1,N
      RINT1(I,KKRAP)=0.0
   40 CONTINUE
      GO TO 10
    6 DO 10 J=KRAP,N
      JJ=J+K
      DO 10 I=1,N
      RINT1(I,JJ)=R(I,J)
   10 CONTINUE
C     TRANSFER RINT1 TO WORKING MATRIX RINT2
      DO 50 I=1,N
      DO 50 J=1,6
      RINT2(I,J)=RINT1(I,J)
   50 CONTINUE
C     EXPAND ROW POSITIONS FOR ROWS HAVING NUMBERS EQUAL TO OR GREATER
C        THAN RELEASE CODE NUMBERS (AS FOR COLUMNS, ABOVE).
      DO 15 K=1,NR
      KRUD=IR(K)-K+1
      IF(KRUD.LE.N)GO TO 11
      KKRUD=IR(K)
      DO 35 J=1,6
      RINT2(KKRUD,J)=0.0
   35 CONTINUE
      GO TO 15
   11 DO 15 I=KRUD,N
      II=I+K
      DO 15 J = 1,6
      RINT2(II,J) = RINT1(I,J)
 15   CONTINUE
C     ZERO ROWS AND COLUMNS OF RINT2 CORRESPONDING TO RELEASE CODES
      DO 55 K=1,NR
      DO 55 I = 1, 6
      KOUT=IR(K)
      RINT2(I,KOUT)=0.0
      RINT2(KOUT,I)=0.0
   55 CONTINUE
C     TRANSFER EXPANDED (6 X 6) MODIFIED STIFFNESS MATRIX BACK TO SF
C     AND RETURN TO MAIN PROGRAM
      DO 60 I=1,6
      DO 60 J=1,6
      SF(I,J)=RINT2(I,J)
   60 CONTINUE
      RETURN
      END
```

```
      SUBROUTINE MPHI(PAXIAL,BMOM,STRAIN,CURVA,WEEP,WU,SEEP,NM,UUF1,WTE)
      COMMON/BLOCK1/DTH,DB,AST,ASC,DST,DSC
      COMMON/BLOCK2/NSTRIP,KONT,T1,T2
      COMMON/BLOCK3/WSHRS, WSHRC
      COMMON/BLOCK4/WTENSIL, WY,FSY,FCYL, TCF, NALLOW, ES
      COMMON/BLOCK5/PHITRI,WTRIAL
      DIMENSION WG(30,20),WH(30,20)
      DIMENSION WEEP(30,20),WU(30,20),SEEP(30,20),UUF1(30,20)
      KADD= 0
      CCA=5.0E-04
      CCB = 1.0E-10
      EROR = 0.01
      KDD= 0
      P = PAXIAL
      BM = BMOM
      TDEL= T2 - T1
      W*= WTRIAL
      PHI = PHITRI
      WCF = 145.0
      EC = 33.*WCF**1.5*( FCYL*1000.)**0.50/1000.
      WSHRS =  (DB*DTH-AST-ASC)*EC*WSHRC/((AST+ASC)*ES)
      KOUNT = 0
      LM = KONT
      IF(T2)2388,2388,3377
 2388 CYL = FCYL
      DO 3388 LN= 1, NSTRIP
      SEEP(LM,LN)= 0.0
 3388 WEEP(LM,LN)= 0.0
      GO TO 444
 3377 FCI= FCYL
      IF(T2.LE.0.0.OR.TDEL.EQ.0.) GO TO  444
      CALL CREEP(WEEP,WU,SEEP,UUF1)
      IF(T2.LE.120.) CYL = (1.0+TCF*T2/120.)*FCI
      CYL =(1.0+TCF)*FCI
 444  CONTINUE
 436  CALL BMPCAL(W,PHI,PCAL1,BMCAL1,WU,WEEP,CYL,W4)
      KOUNT = KOUNT + 1
      IF(P.EQ.0.) P= 1.0
      IF(BM.EQ.0.)BM= 1.0
      ERR1 = ABS((P-PCAL1)/P)
      ERR2 = ABS((BM-BMCAL1)/BM)
      IF(P.EQ.0.0) ERR1 = ABS(PCAL1)
      IF(BM.EQ.0.)ERR2 = ABS(BMCAL1)
      IF(ERR1.LE.EROR.AND.ERR2.LE.EROR) GO TO 600
      IF(ABS(BM).LE.10.0)  GO TO 7712
      GO TO 3012
 7712 IF(BMCAL1.LE.10.0.AND.ERR1.LE.EROR) GO TO 600
 3012 CONTINUE
      WINC = CCA*W + CCB
      PHINC = CCA*PHI+CCB
      IF(WINC.EQ.0.0.OR.PHINC.EQ.0.0) GO TO 608
      WNEW = W + WINC
      PHINEW = PHI + PHINC
      CALL BMPCAL(W,PHINEW,PCAL2,BMCAL2,WG,WEEP,CYL,W7)
      CALL BMPCAL(WNEW,PHI,PCAL3,BMCAL3,WH,WEEP,CYL,W8)
      A11 =(PCAL2-PCAL1)/PHINC
      A12 = (PCAL3-PCAL1)/WINC
      A13 = P - PCAL1
      A21 = (BMCAL2 - BMCAL1)/PHINC
      A22 = ( BMCAL3-BMCAL1)/WINC
      A23 = BM - BMCAL1
      RR = A11*A22-A21*A12
      IF(RR.EQ.0.) GO TO 608
      WDEL = (A11*A23-A13*A21)/RR
      PHIDEL = (A13*A22 - A23*A12)/RR
      PHI = PHI + PHIDEL
      W = W + WDEL
      IF(KOUNT-NALLOW)436,436,608
 600  STRAIN = W
      CURVA = PHI
      WTE= W4
      NM= 0
      IF(CURVA.LE.0.) GO TO 608
      RETURN
 608  KOUNT= 0
      KADD= KADD + 1
```

```
      GG = KADD
      W = WTRIAL*GG*0.25
      PHI = PHITRI*GG*0.20
      IF(KADD- 20)436,123,123
123   WRITE(6,198)
198   FORMAT(1H ,40X,*- - - - - - - - - - - - - - - - - - - - - - - - - - - - -*)
      NM= 1
      STRAIN = 0.0015
      CURVA=0.0002
      RETURN
      END
```

```
      SUBROUTINE STIFFN
C     THIS SUBROUTINE CALCULATES THE  6X6  STIFFNESS MATRIX, EITHER IN
C     MEMBER COORDINATES OR GLOBAL COORDINATES, DEPENDING UPON WHETHER
C     THE MEMBER HAS REDUCED OR FULL STIFFNESS (RESPECTIVELY).
      COMMON/BLOCK7/X1,X2,Y1,Y2,EI,EA,KNT,CF
      COMMON/BLOK5/NR,IR(4)
      COMMON/BLOK1/T(3,3)/BLOK2/TT(3,3)/BLOK3/SF(6,6)
      COMMON/BLOK6/STF11(3,3,30),STF12(3,3,30),STF21(3,3,30),
     1STF22(3,3,30),TTT(3,3,30)
      DIMENSION RK(3,3),SK(3,3),QK(3,3),UK(3,3)
C     CALCULATE MEMBER LENGTH FROM COORDINATES
      AL=((X2-X1)**2+(Y2-Y1)**2)**0.5
C     POPULATE TRANSFORMATION MATRIX
      T(1,1)=(X2-X1)/AL
      T(1,2)=(Y2-Y1)/AL
      T(1,3)=0.0
      T(2,1)=-T(1,2)
      T(2,2)=T(1,1)
      T(2,3)=0.0
      T(3,1)=0.0
      T(3,2)=0.0
      T(3,3)=1.0
      DO 3  I=1,3
      DO 3  J=1,3
      TTT(I,J,KNT)=T(I,J)
    3 CONTINUE
    4 DO 7  I=1,3
      DO 7  J=1,3
      RK(I,J)=0.0
      SK(I,J)=0.0
      QK(I,J)=0.0
      UK(I,J)=0.0
    7 CONTINUE
      BL = AL * CF
      RK(1,1)= EA/BL
      RK(2,2) = 12.*EI/BL**3
      RK(2,3)=6.0*EI/BL**2
      RK(3,2) = 6.0 * EI/BL**2
      RK(3,3) = 4.0*EI/BL
      SK(1,1)=-RK(1,1)
      SK(2,2)=-RK(2,2)
      SK(2,3)=RK(2,3)
      SK(3,2)=-RK(3,2)
      SK(3,3)=0.5*RK(3,3)
      QK(1,1)=-RK(1,1)
      QK(2,2)=-RK(2,2)
      QK(2,3)=-RK(2,3)
      QK(3,2)=RK(3,2)
      QK(3,3)=SK(3,3)
      UK(1,1)=RK(1,1)
      UK(2,2)=RK(2,2)
      UK(2,3)=-RK(2,3)
      UK(3,2)=-RK(3,2)
      UK(3,3)=RK(3,3)
C     CALCULATE TRANSPOSE OF TRANSFORMATION MATRIX
      DO 8  I=1,3
      DO 8  J = 1, 3
      TT(J,I) = T(I,J)
    8 CONTINUE
C     STORE MEMBER STIFFNESS MATRIX (MEMBER COORD'S) IN 3-DIMENSIONAL
C         ARRAY.  THIRD SUBSCRIPT DEFINES MEMBER NUMBER.
      DO 30  I=1,3
      DO 30  J=1,3
      STF11(I,J,KNT)=RK(I,J)
      STF12(I,J,KNT)=SK(I,J)
      STF21(I,J,KNT)=QK(I,J)
      STF22(I,J,KNT)=UK(I,J)
   30 CONTINUE
C     IF MEMBER HAS NO RELEASES, TRANSFORM MEMBER STIFFNESS TO GLOBAL CORD.
      IF(NR.GE.1)GO TO 15
      CALL TRANSF(RK, 1,1)
      CALL TRANSF(SK,1,4)
      CALL TRANSF(QK,4,1)
      CALL TRANSF(UK,4,4)
      GO TO 25
C     IF MEMBER HAS RELEASES, RETAIN MEMBER STIFFNESS MATRIX IN MEMBER
```

```
C         COORDINATES FOR SUBSEQUENT CALCULATION OF REDUCED STIFFNESS
C         MATRIX IN MAIN PROGRAM.
   15 DO 35 I=1,3
      DO 35 J=1,3
      SF(I,J)=STF11(I,J,KNT)
      SF(I,J+3)=STF12(I,J,KNT)
      SF(I+3,J)=STF21(I,J,KNT)
      SF(I+3,J+3)=STF22(I,J,KNT)
   35 CONTINUE
 25   RETURN
      END
```

```
      SUBROUTINE TRANSF ( A , I1, J1)
C     THIS SUBROUTINE ACTUATES A SIMILARITY TRANSFORM, OPERATING ON THE
C     PRIMARY 3X3 MATRICES.  THESE ARE SUBSEQUENTLY PLACED IN THE PROPER
C     LOCATIONS IN THE STIFFNESS MATRIX, SF.
      COMMON/BLOK1/T(3,3)/BLOK2/TT(3,3)/BLOK3/SF(6,6)
      DIMENSION A(3,3),B(3,3),D(3,3)
C     ZERO WORKING MATRICES B AND D
      DO 12 I=1,3
      DO 12 J=1,3
      B(I,J)=0.0
      D(I,J)=0.0
   12 CONTINUE
      DO 14 I=1,3
      DO 14 J=1,3
      DO 14 K=1,3
      B(I,J)=B(I,J)+A(I,K)*T(K,J)
 14   CONTINUE
      DO 16 I=1,3
      DO 16 J=1,3
      DO 16 K=1,3
      D(I,J)=D(I,J)+TT(I,K)*B(K,J)
   16 CONTINUE
C     POPULATE STIFFNESS MATRIX WITH SUBMATRICES WHICH ARE NOW
C         EXPRESSED IN GLOBAL COORDINATES.  RESULT IS MEMBER STIFFNESS
C         MATRIX IN GLOBAL COORDINATES, READY FOR ADDITION TO SAM.
      SF(I1,J1)=D(1,1)
      SF(I1,J1+1)=D(1,2)
      SF(I1,J1+2)=D(1,3)
      SF(I1+1,J1)=D(2,1)
      SF(I1+1,J1+1)=D(2,2)
      SF(I1+1,J1+2)=D(2,3)
      SF(I1+2,J1)=D(3,1)
      SF(I1+2,J1+1)=D(3,2)
      SF(I1+2,J1+2)=D(3,3)
      RETURN
      END
```

APPENDIX B

FRAME	CYLINDER NO.	AGE (DAY)	STRENGTH (LB/IN^2)
FR1	K1	28	4380.
	K2	28	4420.
	K3	28	4425.
	K4	28	4360.
	K5	28	4400.
	K6	28	4470.
	Average		4408.
	Mean Deviation		23.
	Standard Deviation		17.
FS1	C1	28	4360.
	C2	28	4420.
	C3	28	4460.
	Average		4410.
	Mean Deviation		37.
	Standard Deviation		41.
FS1	C4	44	4620.
	C5	44	4600.
	Average		4610.
	Mean Deviation		10.
	Standard Deviation		10.

Mean Deviation $= \sum(|f'_c - \bar{f}'_c|) / N$

Standard Deviation $= ((f'_c - \bar{f}'_c)^2 / N)^{1/2}$

$\bar{f}'_c = \sum f'_c / N$

N = number of specimen

BIBLIOGRAPHY :

(1) ACI Symposium, "Reinforced Concrete Columns", Publication SP-13, ACI-ASCE Joint Committee 441, 1965.

(2) ACI Committee 318, "Building Code Requirements for Reinforced Concrete", Detroit , 1963.

(3) ASCE & ACI, "Flexural Mechanics of Reinforced Concrete", Proceedings of the International Symposium, Miami,1964.

(4) Adenoit, A., "Behavior of a Double-bay one-storey Reinforced Concrete Frame subjected to Horizontal and Vertical Loadings", Structural Concrete Series, No.70-4, September 1970, McGill University.

(5) Barnard, P. R., "Researches into the complete Stress-Strain Curve of Concrete", Magazine of Concrete Research, vol. 16, No. 49, Dec. 1964, pp.203 - 210.

(6) Bazant, Z.P., "Creep Stability and Buckling Strength of Concrete Columns", Magazine of Concrete Research, vol. 20, no.63, June 1968, pp. 85-94.

(7) Breen, J.E., "Restrained Long Concrete Columns as a part of a Rectangular Frame", ACI Journal, Vol.61, No.5, May 1964, pp. 563-588.

(8) Breen, J.E., Ferguson, P.M., "Long Cantilever Columns subjected to Lateral Forces", ACI Journal, November 1969,pp.884-893.

(9) Breen, J.E.," Computer use in studies of Frame with Long Columns", Proceedings of reference no.(3). pp. 535-556.

(10) Bresler, B., "Design Criteria for Reinforced Columns under Axial Load and Biaxial Bending", ACI Journal, Nov. 1960, pp. 481-490.

(11) Broms, B., Viest, M., "Ultimate Strength of Hinged Columns", Transaction ASCE vol.126, 1961, pp.309-397.

(12) Broms, B., Viest, M., "Ultimate Strength Analysis of Long Restrained Reinforced Concrete Columns", ASCE Structural Division, vol.84, No.ST-3, May 1958, paper 1635 , pp. 1-30.

(13) Broms, B., Viest., "Design of Long Reinforced Concrete Columns", Proceeding ASCE, vol.84, ST-4, July 1958,pp.1694:1-28.

(14) Chang, W.F., Ferguson, P.M., "Long Hinged Reinforced Concrete Columns", ACI Journal, vol.61,No.1, Jan. 1963, pp.1-25.

(15) Chang, W.F., Ferguson, P.M., "Critical Length of Long Hinged and Restrained Concrete Columns", Reference (3)

(16) Cranston, W.B., "A Computer Method for the Analysis of Restrained Columns", Technical Report, Cement and Concrete Association (U.K.), London, TRA-402, April 1967.

(17) Cranston, W.B., "Tests on Reinforced Concrete Frames in Portal Frames with Fixed Feet", Technical Report, Cement and Concrete Association, London, TRA-420, Sept.1969.

(18) Cranston, W.B., "A Computer Method for Inelastic Analysis of Plane Frames", Technical Report, Cement and Concrete Association, London, TRA-386, March 1965.

(19) Danielson, C.T., "Sustained Load Behavior of Reinforced Concrete Frames", M.Eng. Thesis, 1970, McMaster University.

(20) Drysdale, R.G., "The Behavior of Slender Reinforced Concrete Columns subjected to Sustained Biaxial Bending", Ph.D. Dissertation, 1967, University of Toronto, Department of Civil Engineering. Also, ASCE Journal, Structural Division, May 1971, pp.1423-1443.

(21) Drysdale, R.G., "Prediction of the Behavior of Concrete Frames", Symposium of the Design of Concrete Structures for Creep, Shrinkage and Temperature changes, International Association of Bridges and Structural Engineering, Madrid, 1970, pp.395-404.

(22) Eichler, G.J., "Creep of Plain Concrete and Prediction of Creep Behavior under variation of Stress", M.Eng. Thesis, McMaster University, 1971.

(23) Farah, A., Huggins, M.W., "Analysis of Reinforced Concrete Columns subjected to Longitudinal Load and Biaxial Bending", ACI Journal, July 1969, pp.569-575.

(24) Ferguson, P.M., "Computer Study of Long Columns in Frames", ACI Journal, Dec. 1970, pp. 955-958.

(25) Fluck, P.G., Washa, G.W., "Creep of Plain and Reinforced Concrete", ACI Journal, April 1958, pp.879-895.

(26) Freudenthal, A.M., Roll, F., "Creep and Creep-recovery of Concrete under high Compressive Stress", ACI Journal June 1958, pp. 1112-1142.

(27) Furlong, R.W., "Column Slenderness and Charts for Design", ACI Journal, January 1971.

(28) Furlong, R.W., "Long Columns in Single Curvature as a part of Concrete Frames", Ph.D. Dissertation, Department of Civil Engineering, University of Texas, Austin, 1963.

(29) Green, R., "Behavior of unrestrained Reinforced Concrete Columns under Sustained Load", Ph.D. Dissertation Department of Civil Engineering, University of Texas, Austin , 1966.

(30) Gray, D.C., "Prediction of the effects of Creep of Concrete under non-uniform stress", M.Eng. Thesis, McMaster University, 1968.

(31) Gopa, A.K.S., Neville, A.M., "A Hypothesis on Mechanism of Creep of Concrete with reference to Multi-axial Compression", ACI Journal, January 1970.

(32) Hognestad, E., Hanson, N.W., McHenry, D., "Concrete Stress Distribution in Ultimate Strength Design", ACI Journal, Proceedings vol.52, no.4, Dec. 1955.

(33) Illston, J.M., England, L., "Creep and Shrinkage of Concrete and their Influence on Structural Behavior - A review of method of analysis", Journal of the Structural Engineers (U.K.), July 1970, No.7, vol. 48.

(34) Johnson, R.P., "Structural Concrete", McGraw-Hill Publishing Company , 1967.

(35) Karman, Von, "The Theory of Buckling and Compression Tests on Long Slender Columns", Translation, Journal of the Society of Hungarian Engineers and Architects 1906.

(36) Livesley, R.K., "Matrix Methods of Structural Analysis", Pergamon Press, London, 1969.

(37) MacGregor, J.G., Breen, J.E., Pfrang, E.O., "Design of Slender Concrete Columns", American Concrete Institute Journal, January 1970, pp.6-28.

(38) Manuel, R.F., MacGregor, J.G., "Analysis of Restrained Reinforced Concrete Columns under Sustained Loads", Ph.D. Dissertation, Department of Civil Engineering, University of Alberta, Edmonton, Alberta, Canada.

(39) Miller, C.A., Guralnick, S.G., "Creep Deflection of Reinforced Concrete Beam", Proceedings ASCE, ST-12, Dec. 1970, pp. 2625-2678.

(40) Neville, A.M., "Properties of Concrete", Sir Issac Pitman & Son Publishing Company, London, U.K., 1963.

(41) Neville, A.M., "Theories of Creep in Concrete", ACI Journal, Proceedings vol.52, No.1, Sept. 1955, pp.47-60.

(42) Parme, A.L.," Capacity of Reinforced Rectangular Column subjected to Biaxial Bending", ACI Journal, vol. 93 September 1966, pp. 911-922.

(43) Popovics, S., "A review of Stress-Strain Relationships for Concrete", ACI Journal, March 1970, pp. 243-248.

(44) Przemieniecki, J.S., "Theory of Matrix Structural Analysis", McGraw-Hill Book Co., 1968.

(45) Pfrang, E.O., Siess, C.P., "Analytical study of the behavior of Long Restrained Reinforced Concrete Columns subjected to Eccentric Loads", Civil Engineering Studies, Structural Research Series, No. 214, University of Illinois, Urbana, June 1961.

(46) Pfrang, E.O., "A study of the influence of Creep on the behavior and capacity of reinforced concrete Columns", Department of Civil Engineering, University of Delaware, 1964.

(47) Pagay, S.N., Ferguson, P.M., Breen, J.E., "Importance of Beam Properties on Concrete Column Behaviors", ACI Journal no. 10, Proceedings vol. 67, Oct. 1970, pp. 808-815.

(48) Rusch, H., "Researches towards a general flexural theory for Structural Concrete", ACI Journal, vol.57, no.1, July 1960, pp. 1-28.

(49) Robinson, A., Gurfinkel, G., "Determination of Strain-distribution and Curvature in a reinforced concrete section subjected to bending moment and longitudinal load", ACI Journal, July 1967, pp. 398-402.

(50) Ross, A.D., "Creep of Concrete under variable stress", ACI Journal, March 1958, pp.739-758.

(51) Sader, W.H., "Ultimate Strength of Single Bay One Storey Reinforced Concrete Frame subjected to horizontal and vertical loadings", Structural Concrete Series, No. 16, Aug., 1967, McGill University, Canada.

(52) Svihra, J., "Incremental Collapse of Reinforced Concrete Frames", M.Eng. Thesis, McMaster University, 1970.

(53) Zienkiewicz, O.C., Cheung, Y.K., "The Finite Element Method in Structural and Continuum Mechanics", McGraw-Hill Publishing Company Limited., 1967.